

LINEAR AND NONLINEAR PROGRESSIVE FAILURE ANALYSIS OF
LAMINATED COMPOSITE AEROSPACE STRUCTURES

A THESIS SUBMITTED TO
THE GRADUATE SCHOOL OF NATURAL AND APPLIED SCIENCES
OF
MIDDLE EAST TECHNICAL UNIVERSITY

BY

MURAT GÜNEL

IN PARTIAL FULFILLMENT OF THE REQUIREMENTS
FOR
THE DEGREE OF MASTER OF SCIENCE
IN
AEROSPACE ENGINEERING

JANUARY 2012

Approval of the thesis:

**LINEAR AND NONLINEAR PROGRESSIVE FAILURE ANALYSIS OF
LAMINATED COMPOSITE AEROSPACE STRUCTURES**

submitted by **MURAT GÜNEL** in partial fulfillment of the requirements for the degree of **Master of Science in Aerospace Engineering Department, Middle East Technical University** by,

Prof. Dr. Canan Özgen
Dean, Graduate School of **Natural and Applied Sciences**

Prof. Dr. Ozan Tekinalp
Head of Department, **Aerospace Engineering**

Prof. Dr. Altan Kayran
Supervisor, **Aerospace Engineering Department, METU**

Examining Committee Members:

Asst. Prof. Dr. Melin Şahin
Aerospace Engineering Department, METU

Prof. Dr. Altan Kayran
Aerospace Engineering Department, METU

Asst. Prof. Dr. Demirkan Çöker
Aerospace Engineering Department, METU

Asst. Prof. Dr. Ercan Gürses
Aerospace Engineering Department, METU

Dr. Muvaffak Hasan
Chief Engineer, TAI

Date: 19.01.2012

I hereby declare that all information in this document has been obtained and presented in accordance with academic rules and ethical conduct. I also declare that, as required by these rules and conduct, I have fully cited and referenced all material and results that are not original to this work.

Name, Last name: Murat GÜNEL

Signature:

ABSTRACT

LINEAR AND NONLINEAR PROGRESSIVE FAILURE ANALYSIS OF LAMINATED COMPOSITE AEROSPACE STRUCTURES

Günel, Murat

M.Sc., Department of Aerospace Engineering

Supervisor: Prof. Dr. Altan Kayran

January 2012, 129 pages

This thesis presents a finite element method based comparative study of linear and geometrically non-linear progressive failure analysis of thin walled composite aerospace structures, which are typically subjected to combined in-plane and out-of-plane loadings. Different ply and constituent based failure criteria and material property degradation schemes have been included in a PCL code to be executed in MSC Nastran. As case studies, progressive failure analyses of sample composite laminates with cut-outs under combined loading are executed to study the effect of geometric non-linearity on the first ply failure and progression of failure. Ply and constituent based failure criteria and different material property degradation schemes are also compared in terms of predicting the first ply failure and failure progression. For mode independent failure criteria, a method is proposed for the determination of separate material property degradation factors for fiber and matrix failures which are assumed to occur simultaneously. The results of the present study show that under combined out-of-plane and in-plane loading, linear analysis can significantly underestimate or overestimate the failure progression compared to geometrically non-linear analysis even at low levels of out-of-plane loading.

Keywords: Progressive Failure Analysis, Composite Aerospace Structures, Non-linear Deformation, Material Property Degradation, Nastran PCL Code

ÖZ

LAMİNAT KOMPOZİT HAVACILIK YAPILARINDA DOĞRUSAL VE DOĞRUSAL OLMAYAN İLERLEYEN HATA ANALİZİ

Günel, Murat

Yüksek Lisans, Havacılık ve Uzay Mühendisliği Bölümü

Tez Yöneticisi: Prof. Dr. Altan Kayran

Ocak 2012, 129 sayfa

Bu tez ince cidarlı havacılık yapılarında genel olarak maruz kalınan düzlem içi ve düzlem dışı kombine yüklemeler için, sonlu eleman metodu kullanılarak yapılan bir doğrusal ve geometrik olarak doğrusal olmayan hata analizi karşılaştırmasını sunmaktadır. Farklı katman ve bileşen temelli hata kriterleri ve hasara bağlı olarak malzeme özelliklerini indirme metodları MSC Nastran'da çalıştırmak üzere bir PCL koduna dahil edilmiştir. Örnek çalışmalar olarak, geometrik olarak doğrusal olmayan hasar analizinin ilk katman hasarında ve hasar ilerlemesindeki etkilerini inceleme amaçlı delikli kompozit laminatların kombine yükler altında ilerleyen hasar analizleri yapılmıştır. Katman ve bileşen temelli hasar kriterleri ve malzeme özelliklerini indirme metodları ilk katman hasarı ve hasar ilerleyişini tahmin etmeleri açısından kıyaslanmıştır. Bileşenden bağımsız hasar kriteri olarak, eş zamanlı gerçekleşen lif ve matris hasarları için ayrı malzeme özelliği indirme faktörleri elde etmeye yarayan bir method önerilmiştir. Sunulan çalışmanın sonuçları göstermektedir ki, kombine düzlem içi ve düzlem dışı yükler altında doğrusal analiz düzlem dışı yüklemenin çok alt seviyelerinde bile hata ilerlemesini geometrik olarak doğrusal olmayan analizin tahmin ettiğinin önemli ölçüde altında veya üzerinde tahmin edebilmektedir.

Anahtar Kelimeler: Hata İlerleme Analizi, Kompozit Havacılık Yapıları, Doğrusal Olmayan Deformasyon, Malzeme Özelliđi Düşürme, Nastran PCL Kodu.

ACKNOWLEDGMENTS

The author would like to express sincere appreciation to his supervisor Prof. Dr. Altan KAYRAN; for his guidance, advice, motivation, continuous support and encouragements throughout this study.

The author also wishes to express his love and gratitude to his wife Elvan ZEYBEK GÜNEL; for her understanding and endless love through the duration of his studies.

TABLE OF CONTENT

| | |
|--|------|
| ABSTRACT | iv |
| ÖZ | vi |
| ACKNOWLEDGMENTS..... | viii |
| TABLE OF CONTENT | ix |
| LIST OF TABLES..... | xi |
| LIST OF FIGURES | xii |
| CHAPTERS | |
| 1. INTRODUCTION | 1 |
| 2. FAILURE THEORIES | 5 |
| 2.2 Mode-Dependent Failure Theory..... | 8 |
| 2.1 Mode-Independent Failure Theory | 9 |
| 3. DESCRIPTION OF PCL | 12 |
| 4. PROGRESSIVE FAILURE ANALYSIS | 15 |
| 4.1 Methodology..... | 15 |
| 4.2 Material Degradation | 18 |
| 4.2.1 Material Property Degradation Method for Mode Dependent Failure Theory..... | 24 |
| 4.2.2 Material Property Degradation Method for Mode Independent Failure Theory..... | 26 |
| 4.3 Linear and Nonlinear Analysis | 31 |

| | |
|---|-----|
| 5. RESULTS AND DISCUSSIONS | 37 |
| 5.1 Verification of PCL Code by Hand Calculation..... | 37 |
| 5.2 Verification of PCL Code by Test Results | 44 |
| 5.3 Description of the Model and Laminate Definition | 52 |
| 5.4 Mesh Sensitivity Study | 54 |
| 5.5 Pure Tensile Loading (Load Case 1)..... | 58 |
| 5.6 Pure Pressure Loading (Load Case 2)..... | 59 |
| 5.7 Gradual Tensile Loading under Constant Pressure (Load Case 3)..... | 62 |
| 5.8 Gradual Compressive Loading under Constant Pressure (Load Case 4) | 68 |
| 5.9 Effect of Degradation Factor on the Failure Progression..... | 74 |
| 6. CONCLUSIONS AND FUTURE WORKS | 80 |
| REFERENCES | 85 |
| APPENDICES | |
| A. PCL CODE | 88 |
| B. NONLINEAR SOLUTION PARAMETERS..... | 116 |
| C. MESH SENSITIVITY STUDY..... | 126 |
| CURRICULUM VITAE | 128 |

LIST OF TABLES

TABLES

| | |
|--|----|
| Table 1: Material properties for E-glass/epoxy material | 38 |
| Table 2: Reduced stiffness's for plies | 40 |
| Table 3: Ply stresses in material coordinate system | 41 |
| Table 4: Material properties for T300/1034-C carbon/epoxy | 45 |
| Table 5: Comparison of failure loads based on the failure criterion of Hashin | 47 |
| Table 6: Stress results of Gauss points and centroid for the most critical element | 49 |
| Table 7: Material properties for T300/N5208 [22] | 53 |
| Table 8: Load cases and boundary conditions | 54 |
| Table 9: Basic operators used in PCL | 91 |

LIST OF FIGURES

FIGURES

| | |
|--|----|
| Figure 1: Comparison of the most common failure theories [16] | 7 |
| Figure 2: Comparison between the predicted and measured biaxial ‘initial’ failure stresses of E-glass/MY750 laminates for current failure theories [1] | 7 |
| Figure 3: Distinct ply, laminate and element property generation sequence implemented in PCL code | 13 |
| Figure 4: Color coding used for ply failures in a finite element | 14 |
| Figure 5: Progressive failure analysis methodology [17] | 16 |
| Figure 6: Post-failure degradation behavior in composite laminates [7] | 20 |
| Figure 7: Post-failure degradation behavior in composite laminates [6] | 23 |
| Figure 8: Load-displacement curve for Lamination, L1 [6]..... | 23 |
| Figure 9: Schematic drawing of fiber failure of a representative element in unidirectional composite | 26 |
| Figure 10: Exponential decay function used to determine separate degradation factors for $R=0.001$ | 31 |
| Figure 11: Follower force effect | 34 |
| Figure 12: Examples of (a) large displacement, small strain (b) large displacement, large strain [21] | 35 |
| Figure 13 : Follower Forces | 36 |
| Figure 14: Geometry and boundary conditions of box beam | 37 |

| | |
|---|----|
| Figure 15: Geometry and boundary conditions of the unwrapped box beam with an initial load of 45 lb/in..... | 43 |
| Figure 16: Tensile test specimen [7]..... | 44 |
| Figure 17: 2D Finite element model of test specimen..... | 45 |
| Figure 18: Comparison of load / displacement curves..... | 46 |
| Figure 19: 3D Finite element model prepared for Gauss stress check..... | 48 |
| Figure 20: Laminate geometry and boundary definitions..... | 52 |
| Figure 21: Finite element models for mesh sensitivity check..... | 55 |
| Figure 22: Load/displacement curves of different mesh sizes for the combined pressure and tension loads by using SOL600 nonlinear analysis..... | 56 |
| Figure 23: Comparison of failure progression plots (a) 340 elements (b) 700 elements..... | 57 |
| Figure 24: First ply failure; Load case: 1; T=14.52 kN; Failure Theory: Hashin; R=0.001..... | 59 |
| Figure 25: Failure progression; Load case: 1; T=29.04 kN; Failure Theory: Hashin; R=0.001..... | 59 |
| Figure 26: Failure progression; Load case: 2; Non-linear analysis; Failure Theory: Hashin; R=0.001..... | 60 |
| Figure 27: Comparison of transverse stresses in the 45° and -45° plies along the diagonal lines..... | 61 |
| Figure 28: Failure progression; Load case: 2; Nonlinear analysis; Failure Theory: | 62 |
| Figure 29: Failure progression; Load case: 3; Nonlinear analysis; Failure Theory: Hashin; R=0.001..... | 63 |

| | |
|---|----|
| Figure 30: Failure progression; Load case:3; Nonlinear anal.; Failure Crit.: Tsai-Wu-Classical; $R=0.001$ | 64 |
| Figure 31: Failure progression; Load case:3; Nonlinear anal.; Failure Crit.: Tsai-Wu-Modified; $R=0.001$ | 64 |
| Figure 32: First ply failures; Load case: 3; Failure Theory: Hashin; $R=0.001$ | 66 |
| Figure 33: Failure progression; Load case: 3; Failure Theory: Hashin; $R=0.001$ | 66 |
| Figure 34: First ply failures; Load case: 3; Failure Theory: Tsai-Wu-Classical; $R=0.001$ | 68 |
| Figure 35: Failure progression; Load case: 3; Failure Theory: Tsai-Wu-Classical; $R=0.001$ | 68 |
| Figure 36: First ply failures; Load case: 4; Failure Theory: Tsai-Wu-Classical; $R=0.001$ | 69 |
| Figure 37: Failure progression; Load case: 4; Failure Theory: Tsai-Wu-Classical; $R=0.001$ | 69 |
| Figure 38: Failure progression; Load case: 4; Failure Theory: Tsai-Wu-Modified; $R=0.001$ | 70 |
| Figure 39: Deformation Plots; Load case: 4; Failure Theory: Tsai-Wu-Classical; $R=0.001$ | 70 |
| Figure 40: Maximum σ_1 Stress (MPa); Load case : 4; Failure Theory: Tsai-Wu-Classical; $R=0.001$ | 71 |
| Figure 41: Maximum σ_2 Stress (MPa); Load case: 4; Failure Theory: Tsai-Wu-Classical; $R=0.001$ | 71 |

| | |
|---|----|
| Figure 42: Failure progression; Combined pressure and compression; Non-linear anal.; $R=0.001$ | 74 |
| Figure 43: Failure progression; Combined pressure and tension; Non-linear anal.; $R=0.001$ | 74 |
| Figure 44: Load/displacement curves of sudden and gradual degradation used linear/non-linear progressive failure analysis..... | 75 |
| Figure 45: Ultimate failure loads; Load case: 1; (a)Linear analysis (b) Non-linear analysis; Failure theory: Hashin | 77 |
| Figure 46: Load/displacement curves of sudden and gradual degradation used SOL600 non-linear progressive failure analysis | 78 |

CHAPTER 1

INTRODUCTION

The use of composite materials in primary aerospace structures is rapidly increasing. Composite laminates are the building blocks of composite aerospace sub-structures therefore understanding the failure characteristics of composite laminates is essential in order to exploit the full strength of composite materials in aerospace structures. Thin walled composite aerospace sub-structures, such as skin panels of lifting surfaces or pressurized fuselage sections, are commonly exposed to combined in-plane and out-of-plane loadings. Understanding the failure initiation and failure progression mechanisms of composite aerospace structures, which are subjected to common load cases encountered in flight, is very crucial to prevent premature failure and to design fault tolerant laminates. Fiber composite laminates can develop local damages such as matrix failure, fiber breakage, fiber matrix de-bonding and delaminations which eventually cause the ultimate failure of the laminate. However before the ultimate failure, composite laminates with local damages can sustain operating loads much better than their metallic counterparts. Especially, intra-laminar local failures such as matrix cracks, fiber breakage and fiber matrix de-bonding can be tolerated much better than inter-laminar failures such as delaminations. Progressive failure analysis of fiber reinforced composites is a powerful method to determine the capability of composite structures to sustain loads.

Over the last three decades many studies have been performed on the progressive failure analysis of composite laminates which are the major building blocks of composite

structures. In this section some of the research done on progressive failure analysis of composite laminates is summarized. In most of these studies, mode independent and mode dependent failure criteria are used during the failure progression. Mode dependent failure criteria consist of relations which define a particular failure mode such as fiber breakage or matrix cracking whereas mode independent failure criteria do not directly identify the failure mode or the nature of the damage. Therefore, when mode dependent failure criteria are used, direct relation between failure prediction and the failure mode facilitates the implementation of material property degradation (stiffness reduction) models during progressive failure analysis. Some key examples on the assessment of theories for predicting the failure of composite laminates include the studies of Hinton et.al [1] and Icardi et.al. [2]. Literature on the progressive failure analysis of composite laminates is vast. Therefore, only some selected examples are presented in this section. Chang and Chang [3] developed a progressive failure analysis method using non-linear finite element analysis using the modified Newton-Raphson scheme. Tolson and Zabaraz [4] used higher order shear deformation plate theory and performed progressive failure analysis using two dimensional finite element analysis. Reddy and Reddy [5] compared first ply failure loads obtained by using both linear and non-linear finite element analysis on composite plates subject to in-plane tensile loading and transverse loading. Reddy et.al [6] developed a progressive failure algorithm using the generalized layer wise plate theory of Reddy and geometric non-linearity is taken into account in the Von Karman sense. A gradual stiffness reduction scheme was proposed to study the failure of composite laminates under tensile or bending load. Sleight [7] developed a progressive failure analysis method under geometrically non-linear deformations and implemented the method in the Comet finite element analysis code. The implementation of progressive failure analysis in commercial FE software is often achieved through user defined subroutines. As an example study, Basu et.al [8] used Abaqus as the finite element software in the prediction of progressive failure in multidirectional composite

laminated panels. Recently, Tay et.al. [9] proposed an element failure method for the progressive failure analysis in composites as an alternative to the commonly used material property degradation methods in predicting failure progression. In the element failure method, the nodal forces of finite elements are manipulated to simulate the effect of damage while leaving the material stiffness values unchanged. In their article, Tay et.al. also presented a wide literature on the current strategies used in progressive failure analysis. In a recent article, Garnish and Akula [10] made a very comprehensive review of degradation models for progressive failure analysis of fiber reinforced polymer composites.

In this study, two dimensional finite element based progressive failure analysis method is used to study first ply failure and progression of failure of composite laminates with cut-outs under in-plane and out-of-plane loading and geometrically non-linear deformations. Presented study is restricted to intra-laminar failures and emphasis is given to the effect of non-linearity on the failure initiation and progression. In the progressive failure analysis of structures which are exposed to especially out-of-plane loads, geometric non-linear effects become prominent when the structure is subjected to large displacement and/or rotation. Follower force effect due to a change in load as a function of displacement and rotation is one aspect of geometric non-linearity that must also be taken into account especially when the structures are subjected to out-of-plane loads resulting in large deformation. One of the aims of the presented study is to perform a comparative study of linear and non-linear progressive failure analysis through case studies. In addition, in most of the previous studies on progressive failure analysis of composites single load case is used. Progressive failure analysis of composites under combined loads is particularly important for thin walled aerospace structures which are usually subjected to combined in-plane and out-of-plane loads. Therefore, a major objective of the present study is also to investigate the significance of geometrically non-

linear analysis on the progressive failure response of composite laminates under combined in-plane and out-of-plane loading. For this purpose different ply and constituent based failure criteria and material property degradation schemes have been coded into a PCL code in MSC Nastran. It should be noted that in the classical lamination theory that is implemented in MSC Nastran first order transverse shear deformation is also included. Currently, linear static, large displacement-small strain non-linear static (SOL 106) and large displacement-large strain non-linear static (SOL 600) solution types of MSC Nastran are implemented as the solution types which can be selected as the solver in the PCL code. During the progressive failure analysis of the sample cases, the effects of performing small strain/large strain non-linear solution on the failure initiation and progression is also studied. In the study it is also shown how the MSC Patran command language can be used effectively to exploit the capabilities of MSC Nastran solver in performing progressive failure analysis and to visualize failure progression at the ply level.

CHAPTER 2

FAILURE THEORIES

While designing a structure, it should be considered that whether the selected material strength can sustain the estimated load or not. If the applied load level is higher than the material load carrying capacity then failure occurs in the structure. Since it is a very expensive and complicated way to extract strength characteristics for all complex stress states, failure theories are defined. By using data obtained from uniaxial tests, failure theories predict the response of the structure under applied multi-axial stress states. The term failure criterion refers to mathematical equations that predict the states of stress and strain at the onset/progression of material damage.

In composite structures, ultimate laminate failure occurs due the propagation or accumulation of failure which initiated in a ply as first ply failure or in the form of delamination of two layers. The initiation of failure in ply level can be predicted by using a failure theory. Then a ply-by-ply basis progressive failure is considered for composite laminates [15]. The failure can be due to fiber breakage, matrix cracking, fiber-matrix debonding or delamination of layers in a laminate due to the loads applied. Boundary conditions, geometry and the laminate definition also play a key role on the initiation and progression of failure. Presented study is restricted to intra-laminar failures, and emphasis is given to the effect of non-linearity on the failure initiation and progression. Inter-laminar failure is not considered since most inter-laminar failures are modeled by fracture mechanics based approach. However, delaminations can also be predicted by using strength or strain based failure criteria. By employing inter-laminar

stresses in a failure criterion, such as a polynomial failure criterion, delamination can be predicted. For instance, Tolson and Zabaras [4] developed a two-dimensional finite element analysis for determining failures in composite plates. In their finite element formulations, they developed a seven degree-of-freedom plate element based on a higher-order shear-deformation plate theory. The in-plane stresses were calculated from the constitutive equations, but the transverse stresses were calculated from the three-dimensional equilibrium equations. The method gave accurate interlaminar shear stresses very similar to the three dimensional elasticity solution. The stress calculations were performed at the Gaussian integration points. Delamination was also predicted by examining the interlaminar stresses according to a polynomial failure equation. If delaminations occurred, then the stiffness matrix in both lamina adjacent to the delamination is degraded accordingly.

In the literature, there are various failure theories used to predict failure in composite materials and the list of most commonly used failure theories can be found in several papers such as the one by Nahas [16]. Moreover, a good assessment of predictive capabilities of the current failure theories in the literature has been performed by Hinton [1]. Figure 1 and Figure 2 present some examples of the comparison of different failure theories. In Figure 2, comparison between the predicted and measured biaxial ‘initial’ failure stresses of E-glass/MY750 laminates for current failure theories [1].

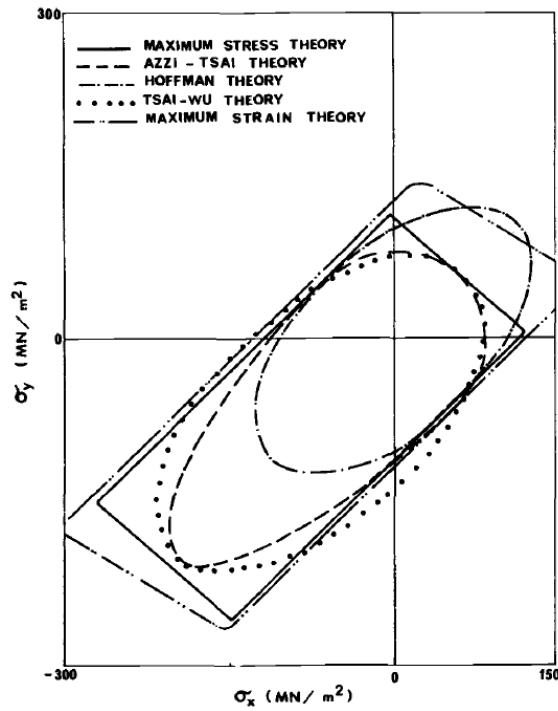


Figure 1: Comparison of the most common failure theories [16]

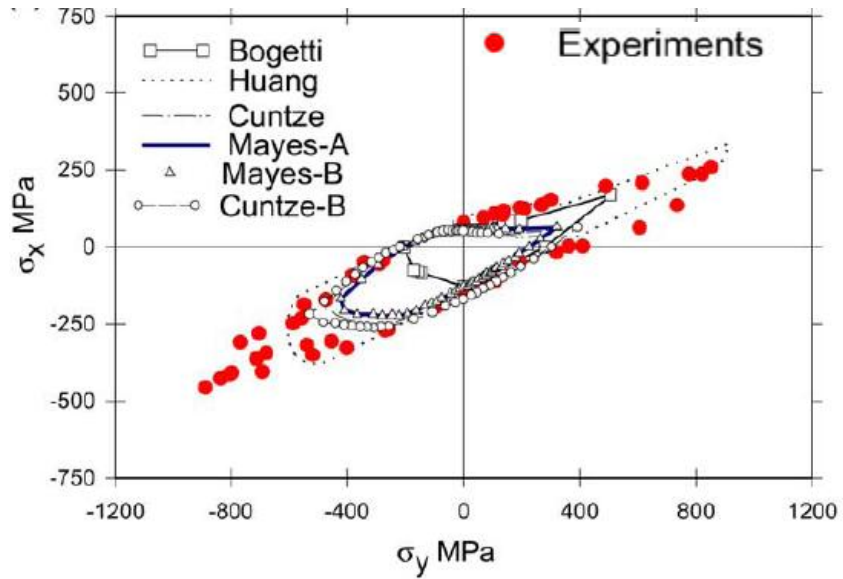


Figure 2: Comparison between the predicted and measured biaxial 'initial' failure stresses of E-glass/MY750 laminates for current failure theories [1]

Generally, the failure theories can be categorized into two groups: mode-dependent failure theories and mode-independent failure theories [10].

2.2 Mode-Dependent Failure Theory

Mode-dependent failure theories are sets of equations that each defines the event of a particular failure mode. Besides, the material degradation scheme is directly based on the failure mode extracted from failure prediction [10]. The Hashin [12], the Hashin-Rotem [27], criterion developed by Lee [29] and criterion developed by Christensen [28] are a few examples of mode dependent failure criteria. These criteria predict a variety of failure modes such as fiber tensile failure, fiber compressive failure, matrix tensile failure, matrix compressive failure, and delamination using stress-based equations.

Plane stress failure theory of Hashin [12] is an example of mode dependent failure theory. Failure modes of Hashin's failure theory are expressed in terms of fiber and matrix failures in tension and compression, and they are given by Equations (1) and (2).

Fiber failure modes: (tension: $\sigma_1 > 0$, compression: $\sigma_1 < 0$)

$$\text{in tension } \left(\frac{\sigma_1}{X_T} \right)^2 + \left(\frac{\tau_{12}}{S} \right)^2 \geq 1 \quad ; \quad \text{in compression } \left(\frac{\sigma_1}{X_C} \right)^2 \geq 1 \quad (1)$$

Matrix failure modes: (tension: $\sigma_2 > 0$, compression: $\sigma_2 < 0$)

$$\text{in tension } \left(\frac{\sigma_2}{Y_T} \right)^2 + \left(\frac{\tau_{12}}{S} \right)^2 \geq 1 \quad (2)$$

in compression
$$\frac{\sigma_2}{Y_c} \left[\left(\frac{Y_c}{2S} \right)^2 - 1 \right] + \left(\frac{\sigma_2}{2S} \right)^2 + \left(\frac{\tau_{12}}{S} \right)^2 \geq 1$$

In Equations (1) and (2) "1" and "2" directions are the fiber and transverse directions, respectively. Composite material allowables in the fiber and the transverse directions are denoted by "X" and "Y" with subscripts "T" and "C" representing tension and compression respectively, and "S" denotes the in-plane shear allowable.

2.1 Mode-Independent Failure Theory

Mode-independent failure theories predict the failure without defining the mode of failure such as fiber or matrix failure. Failure theories are represented by linear, quadratic or cubic mathematical equations which describe a mathematical curve/surface in stress/strain space. The simplest mode-independent polynomial failure criteria are the maximum stress and maximum strain criteria. These theories are simple inequality conditions reflecting the experimental data obtained from uniaxial tests aligned with the principal material coordinates. Their simplicity, having just one stress or strain component in each equation, makes for trivial assumptions that associate the modes of failure. Due to the simple form of the equations, these criteria are sometimes referred to as “noninteractive criteria” since individual tensor components of stress or strain do not interact within the criteria. For example, failure prediction in transverse tension is not influenced by the presence of longitudinal shear [10].

Besides maximum stress and strain failure criteria, the most common mode-independent failure theories can be summarized as Tsai-Hill [30,31], Tsai-Wu [13] and Hoffman[32].

These theories are single polynomial stress-based equations that contain some or all the stress components. Due to the interaction of the terms in the polynomial equation, these criterias are sometimes referred to as the “interactive failure criteria” [10].

In this study, Tsai-Wu failure theory [13] is selected as the mode-independent failure theory which is widely used in progressive failure analysis. It should be noted that most of these theories can be viewed as different forms of the Tsai–Wu criterion. For the plane stress state, failure index of the Tsai-Wu ply failure theory, which is implemented in the current study, is calculated by Equation (3). In Equation (3), "FI" represents the failure index, and according to the failure theory, failure is predicted if the failure index is higher than one. In the mode independent failure criteria, ply failure is predicted but to identify a failure mode individual contributions of the stress terms to the failure prediction are considered. Identification of the failure modes is explained;

$$F_1 \sigma_1 + F_{11} \sigma_1^2 + F_2 \sigma_2 + F_{22} \sigma_2^2 + F_{66} \tau_{12}^2 + F_{12} \sigma_1 \sigma_2 = FI \quad (3)$$

where

$$F_1 = \frac{1}{X_T} - \frac{1}{X_C} \quad F_{11} = \frac{1}{X_T X_C} \quad F_2 = \frac{1}{Y_T} - \frac{1}{Y_C} \quad F_{22} = \frac{1}{Y_T Y_C} \quad F_{66} = \frac{1}{S^2} \quad (4)$$

and the interaction coefficient F_{12} is given by:

$$F_{12} = -\frac{1}{2} \frac{1}{\sqrt{X_T X_C Y_T Y_C}} \quad (5)$$

It should be noted that Tsai-Wu failure criterion is an extension of the maximum distortion energy theory which is also known as maximum von Mises failure theory. It

can be shown that if the tensile and compression strengths in the fiber and transverse directions are equal to each other, then Tsai-Wu theory transforms into maximum distortion energy theory.

CHAPTER 3

DESCRIPTION OF PCL

The Patran Command Language (PCL) is a programming language which is an integral part of the MSC Patran system. PCL can be used to write application or site specific commands and forms, create functions to be called from MSC Patran, create functions from all areas of MSC Patran including all applications, graphics, the user interface and the database and completely integrate commercial or in-house programs. The entire MSC Patran user interface is driven by PCL [11].

In this study, finite element based progressive failure analysis method is used to study the first ply failure and progression of failure of composite laminates under combined in-plane and out-of-plane loading and geometrically linear and non-linear deformations. For this purpose, different ply and constituent based failure criteria and material property degradation schemes have been coded into a PCL code which employs linear and non-linear solution types of MSC Nastran depending on the analysis type desired. In order to effectively allow material property degradation at the ply level, for each element in the finite element mesh, distinct composite laminate properties with distinct two dimensional orthotropic materials are generated for each ply via the PCL code that is developed. Thus, stiffness reduction scheme is implemented easily for the failed ply by referencing the element property identification and material identification numbers of the ply. In the PCL code ply thicknesses, ply orientations, ply material properties for each ply and their stacking sequences are identified as variables. By using the assigned variables, a new 2D orthotropic material is created for each ply and then according to the

pre-defined stacking sequence a new laminate is created for each element. Finally, for each element distinct element properties are created by referencing the laminates which are created for each element in the composite structure. The sequence of material and property generation steps are summarized schematically in Figure 3 for a composite laminate composed of four layers. For the example shown in Figure 3, finite element model has 4 elements and 4 plies per element. After the material and property generation operations inside the PCL code, 4 element properties, 4 composite laminates and 16 two dimensional orthotropic materials are created.

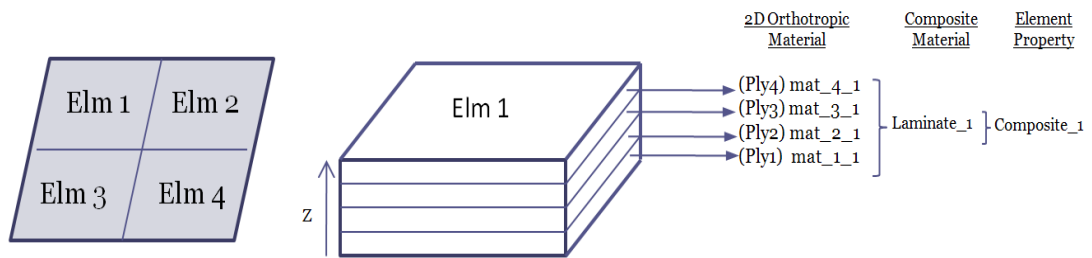


Figure 3: Distinct ply, laminate and element property generation sequence implemented in PCL code

In the current study to visualize failure progression at the ply level, a color code scheme is also designed and implemented in the PCL code. Failure progression at any load step is monitored between the first ply failure and ultimate failure at the ply level using the color coded elements. Currently in the PCL code, color coding used to visualize the failure progression does not distinguish the mode of failure and the failed ply. However, one can extract the mode of failure and ply number of the failed ply from the session files easily. During the color coding, depending on the number of failed plies, a different color is used. Thus, irrespective of the ply number of the failed ply in an element and the mode of failure, an element with one to eight failed plies is painted with different colors. The failure color coding is used for the sample application presented in this article is

shown in Figure 4. For instance, during the failure progression, if the element is painted with red color, it means that all 8 plies of the element are failed according to the pre-defined failure theory.



Figure 4: Color coding used for ply failures in a finite element

In the present study, strains and stresses, which are calculated by the desired solution type, are used in calculating the failure indices for the failure theory selected. Currently, plane stress failure theory of Hashin [12], Tsai-Wu [13] and modified Tsai-Wu, which is proposed in the thesis, failure theories are implemented in the PCL code.

In Appendix A, the PCL code developed in the thesis study is given. Inside the PCL code, descriptions are also made for the critical code segments to familiarize the reader to the Patran Command Language.

CHAPTER 4

PROGRESSIVE FAILURE ANALYSIS

4.1 Methodology

As it was stated before, progressive failure analysis is used for the simulation of the failure progression from the beginning of the failure (first ply failure) to the ultimate failure load level. In other words, by means of progressive failure analysis residual strength of the laminates can be determined. It is known that composite laminates with local damages can sustain operating loads much better than their metallic counterparts. Higher residual strength is a desirable property because especially in aerospace applications, the structure with local damage is expected to sustain the operating loads before the local damage is identified in a maintenance period. There are various methodologies used for progressive failure analysis in the literature but all of these examples are based on same procedure. A typical methodology for progressive failure analysis is shown in Figure 5.

As shown in Figure 5, for an initial state which is in equilibrium statically, load is incremented and finite element analysis is performed to calculate the displacements, strains and stresses in the composite structure. In general, one can perform geometrically linear or non-linear finite element analysis to determine the field quantities. Figure 5 shows a typical procedure in which geometrically non-linear finite element analysis is employed in the strain/stress recovery procedure.

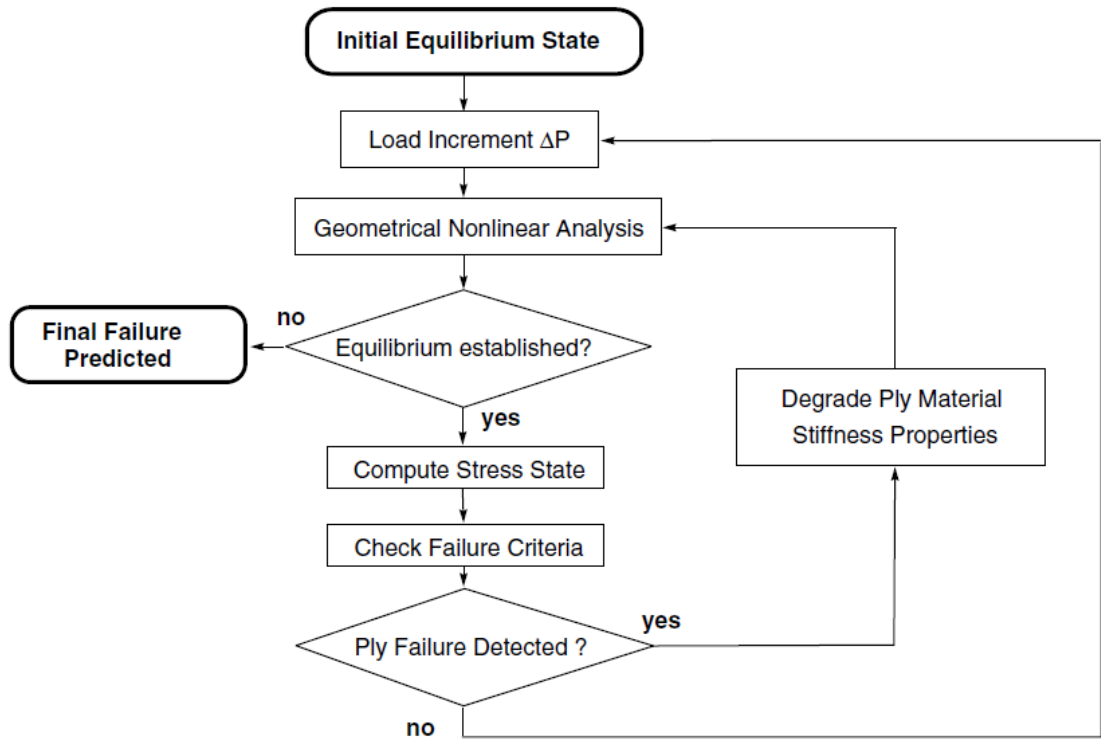


Figure 5: Progressive failure analysis methodology [17]

Most structural non-linear problems are solved in an incremental manner. An incremental load is applied and then iteration is undertaken until a converged solution has been achieved. Once the converged solution has been achieved, after the stress recovery a failure criterion is invoked to detect local lamina failure and determine the failure mode. If no failure is detected at the particular load level, the load is incremented again and the whole process of establishing the equilibrium, stress recovery and check of the failure criterion is repeated at the current load level. If failure is detected at a particular load level, then material degradation or damage models are needed in order to determine new estimates of the local material properties and propagate the failure. After the degradation of the material properties of the damaged layer, a finite element analysis

is conducted at the same load level without incrementing the load. Since the material properties are degraded locally due the failure induced, equilibrium must be re-established. Once the equilibrium is re-established, stress recovery and failure checks are performed as before. This loop continues until equilibrium can not be established in geometrically non-linear finite element analysis. Because of the stiffness loss due to the accumulation of the damages, it turns out that at a certain load level failure propagates without incrementing the load until equilibrium can not be established. Usually, this load level is referred to as ultimate load [17]. However, depending on the application, which involves a particular load and boundary condition case, one can come up with other definitions of ultimate load. For instance, ultimate load can also be defined as the load at which all elements along a line, which divides a structure into two pieces, fail. Or, as defined by Reddy [5] in case of tensile loading of a composite laminate, one may define the ultimate load as the load at which fiber failure takes place in the 0° plies. Such a definition of ultimate load implies that the load carrying capacity of plies with non-zero fiber orientation angles are ignored.

In the current study, in principle, progressive failure analysis procedure is similar to the one defined in Figure 5. At an initial equilibrium state, finite element model is automatically sent to analysis in MSC Nastran for the particular load and boundary condition case which is defined. Inside the PCL code, the analysis type can be selected easily as linear or non-linear analysis by the user. Since each load step takes a certain time, during the execution period PCL code is instructed to wait till the end of the analysis. After the completion of the analysis, the requested results are attached and depending on the failure criteria used, failure indices are calculated based on the strains or stresses at the pre-defined location within the element.

In the results presented in this study, failure indices are calculated based on the stresses at the center of shell elements, at the mid plane of plies. Similarly, Lee [18] used the stresses at the element centroid for the purpose of detecting matrix and fiber failures during progressive failure analysis. However, it should be noted that failure indices can also be calculated based on the stresses at the Gauss points. For instance, Tolson and Zabaras [4] performed failure check for the each Gauss point within element, and based on the number of failed Gauss points, they have extracted a degradation factor for the material degradation. For a 2D element which has four Gauss points, if one of the Gauss points has failed then degradation factor is taken as 0.75 and if all of the Gauss points have failed then degradation factor is taken as 0.0. In MSC Patran, for solid elements stress output at Gauss points is available but for shell elements stress output at Gauss points is not available. Therefore, in the current study, since stress result for the Gauss points of the 2D elements is not available in MSC Patran, the centroid stresses have been used to perform the progressive failure analysis. It should also be noted that in MSC Patran corner stress output can be requested. However, corner stress, which is the stress at the grid points, is not equivalent to Gauss point stress.

4.2 Material Degradation

Material degradation is the core of progressive failure analysis especially for the estimation of ultimate failure. If failure does not cause an ultimate failure, the load on the failed material should be redistributed to the remaining undamaged material in some manner. This can be done in several ways. For example, as mentioned by Tay et.al [9] in the element failure method that he has proposed, the nodal forces of finite elements are manipulated to simulate the effect of damage while leaving the material stiffness values unchanged. However, in the most of studies in the literature, material property degradation has been performed by the stiffness reduction method [10]. Material

property degradation proceeds throughout the structure according to the failure criterion implemented until no additional load can be sustained. However, material property degradation has some arbitrariness in its implementation, because multiple failure modes, directionality of failure, interaction of the failed and intact layers, and issues related to numerical implementation all are complex issues all of which cannot be handled accurately simultaneously with a material property degradation model.

The main idea in the stiffness reduction method is modeling post-initial failure of damaged material by reducing stiffness values. As an example, Tan et.al [19] has proposed a two-dimensional progressive failure method for a laminate with central hole under tensile/compressive loads. As shown in Equation (6), Tan used three internal state variables or in other words degradation factors to reduce stiffnesses. Here E_{11}^0 , E_{22}^0 , G_{12}^0 are undamaged material properties and E_{11} , E_{22} , G_{12} are damaged/degraded material properties.

$$\begin{aligned}
 E_{11} &= D_1 E_{11}^0 \\
 E_{22} &= D_2 E_{22}^0 \\
 G_{12} &= D_6 G_{12}^0
 \end{aligned} \tag{6}$$

As in the study of Tan, in the present study constant degradation factors have been preferred for convenience and also due to the ease of use constant degradation factors in progressive failure analysis. It should also be noted that in the implementation of the progressive failure analysis in finite element context, degradation factors must be different from “0”, otherwise convergence problems may occur during computation due to ill-conditioned stiffness matrices or sometimes due to encountering singularity [20].

The main challenge in material property degradation is to properly characterize the residual stiffness of the damaged material. At this point, material property degradation can be divided into three categories; sudden degradation, gradual degradation and constant stress at ply failure. As it is shown in Figure 6, in sudden degradation by using small degradation factors, associated material properties are dropped to small values instantaneously. In gradual degradation, associated material properties are degraded to zero gradually by using degradation factors between "0" and "1". Also, for constant stress type degradation, load carrying capacity of material is fixed at the point of failure [7].

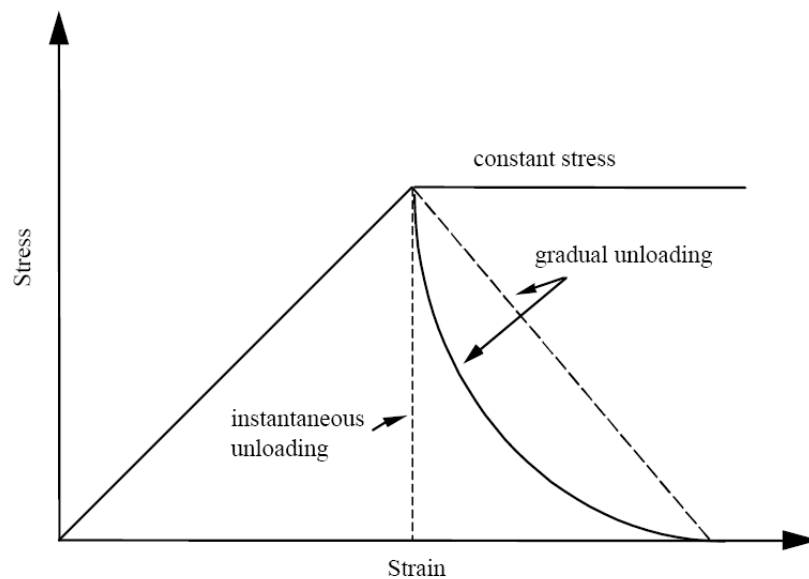


Figure 6: Post-failure degradation behavior in composite laminates [7]

While performing sudden degradation in a finite element based progressive failure analysis, after degrading associated material properties of an element according to a degradation model, compared to the intact element, the degraded element will take less

load in the following iterations. This can be only achieved by using degradation factors less than one. However, as mentioned before, selecting too small degradation factors like 10^{-20} causes computational problems during stiffness matrix evaluation as also experienced in this study. By taking these issues into consideration and also considering the degradation factors used in the literature, for sudden degradation of the material properties, degradation factor is selected as 0.001 in this study. It should be noted that when elements are degraded by this degradation factor for sudden degradation, in the next step of the progressive failure analysis degraded elements do not carry appreciable load compared to the intact elements. Moreover, a comparison has been performed by using different sudden degradation factors like 10^{-1} , 10^{-2} , 10^{-20} for a rail-shear specimen studied by Sleight [7], and it is concluded that the differences between final failure states reached by the analyses performed by using these factors, are negligible.

In gradual degradation, material properties are degraded gradually until zero, thus it is considered that, load carrying capacity of the material after failure, is simulated more accurately. It is shown by Reddy [6] that by using gradual degradation, final failure predictions agree with the experimental results much better than match obtained by using sudden degradation. Selecting appropriate degradation factor between "0" and "1", is the most critical part in gradual degradation. Because, selecting a factor too close to "0" can cause ignoring damage accumulation in the material. Likewise, selecting degradation factor too close to unity can cause unnecessary computational effort due to the repeated analysis. For this reason, an optimum value should be selected for gradual degradation. It is argued by Reddy [6] that the size of the actual damage in the form of micro or meso cracks is very small compared to the size of elements used in practice. Therefore, it appears that reducing the stiffness property of the whole element to zero is unjustified. Reddy [6], performed a comparison for the effects of different degradation factors on the ultimate failure for gradual degradation. The study is performed on a

laminate which is under uniform tensile loading. Figure 7 shows the effect of stiffness reduction coefficient on the ultimate failure load of the laminate. Reddy studied three different laminates and varied the stiffness reduction coefficient from very small values such as 10^{-6} to about "0.5", and plotted the ultimate load calculated in terms of percent of experimental value as a function of the stiffness reduction coefficient. As shown in Figure 7, according to the results of the study performed by Reddy, for small degradation factors there is a sharp decrease in ultimate failure load. Reddy [6] argues that such a reduction in ultimate failure load with the decrease of the stiffness reduction factor is anticipated, because the stiffness properties of the failed elements are reduced to very small values irrespective of the amount of damage the element accumulates. However, in case when large stiffness reduction coefficients are used, the property reduction is controlled by repeated failures of the element which implies damage accumulation. Thus, by using large degradation factors ultimate failure load can be predicted within $\pm 10\%$ [6]. As it can be seen from the Figure 7, ultimate load showed very small variation over a wide range of stiffness reduction factor, and it seems that "0.5" is an optimum value for predicting accurate ultimate failure loads in gradual degradation. A factor of "0.5" is also a reasonable value when one considers the computational effort. When large stiffness reduction factors are used, the computational effort increases dramatically especially for non-linear analysis. Based on the discussions presented in this section, in this study for gradual degradation "0.5" has been used as the degradation factor. Figure 8 shows the total load acting on the laminate versus average displacement at the free end of the laminate where the uniform load is applied. Load displacement curves are given for two different stiffness reduction factors "0.001" and "0.5". As it can be seen in Figure 8, load displacement curves are different for different stiffness reduction factors, indicating different progression of damage. It is also noted that the curves for small stiffness reduction factors are more stepped compared to that for large stiffness reduction factor. It is noted by Reddy that results from experiments on

similar laminates also indicate smooth curves, and in that respect the curves for larger stiffness reduction factors are closer to experimental observation.

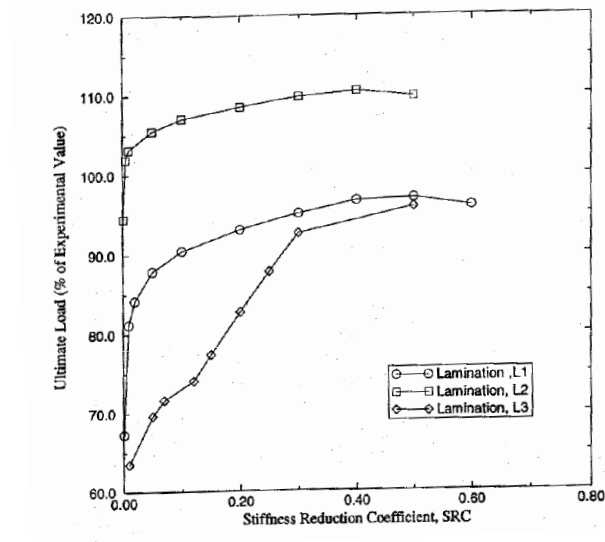


Figure 7: Post-failure degradation behavior in composite laminates [6]

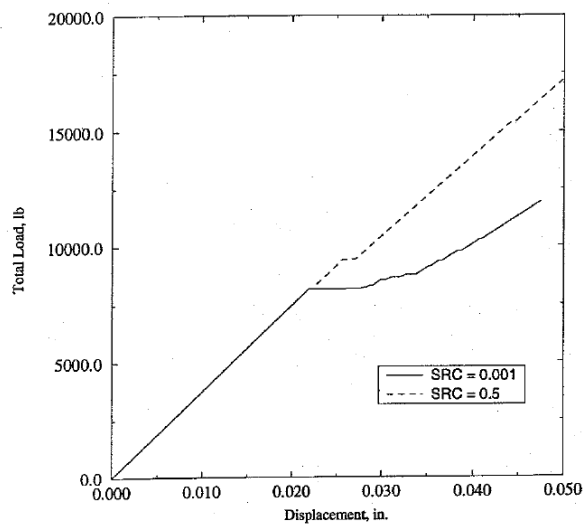


Figure 8: Load-displacement curve for Lamination, L1 [6]

4.2.1 Material Property Degradation Method for Mode Dependent Failure Theory

Material property degradation method that is used with the mode dependent failure criteria depends on the mode of failure. For the two dimensional lamination theory with the transverse shear deformation effects included, degraded properties for the fiber and matrix failure modes are given separately by Equations (7) and (8).

Fiber failures:

$$(E_1, G_{12}, G_{13}, \nu_{12})_{\text{degraded}} = R \times (E_1, G_{12}, G_{13}, \nu_{12})_{\text{previous}} \quad (7)$$

Matrix failures:

$$(E_2, G_{12}, G_{23}, \nu_{21})_{\text{degraded}} = R \times (E_2, G_{12}, G_{23}, \nu_{21})_{\text{previous}} \quad (8)$$

where factor "R" in Equations (7) and (8) is the degradation factor which can be adjusted to degrade the material properties gradually or suddenly. It should be noted that although in Equations (7) and (8), the plane stress form of the mode dependent failure theory, such as Hashin's failure theory, is assumed to be used, the out-of-plane shear modulus are also degraded in fiber and matrix failure modes, because in the finite element model individual layers are defined as 2D orthotropic material with transverse shear deformation included. Therefore, out-of-plane shear modulus also has to be defined as elastic constants in the material definition of the plies. In the present study, as it is mentioned above, for sudden degradation material property degradation factor of "0.001" is used, and for gradual degradation a factor of "0.5" is used. In case of gradual degradation, plies are allowed to fail repeatedly until the degradation factor reaches "0.001", which is the factor that is used to indicate complete fiber or matrix failure in this study.

For the fiber failure case, Figure 9 shows a schematic drawing which helps in understanding the induced failures better. In case of fiber failure, modulus of the composite in the fiber direction (1) is degraded because in unidirectional composites it is assumed that fibers are the main load carrying members. The transverse load is assumed to be primarily carried by the matrix; therefore modulus of the composite in the transverse direction (2) is not degraded. Since fiber failures cause a loss of stiffness in the fiber direction but the transverse modulus is not degraded, the in-plane Poisson's ratio (ν_{12}) is also degraded by the same degradation factor used in degrading the modulus in the fiber direction. It is generally assumed that fiber failure also induces in-plane shear failure; therefore in-plane shear modulus G_{12} is also degraded. From Figure 9 it can be deduced that for unidirectional composites in-plane shear modulus G_{12} and out-of-plane shear modulus G_{13} are affected similarly from fiber failure. Therefore, out-of-plane shear modulus G_{13} is also degraded by the same degradation factor used in degrading G_{12} . Finally, in case of fiber failures out-of-plane shear modulus G_{23} is not degraded because fiber breakage does not affect the shear modulus in the 2-3 plane as severely as it affects the shear modulus in the 1-3 plane. One further note is that for transversely isotropic materials out-of-plane shear modulus G_{23} is given by $E_2 / 2(1+\nu_{23})$. If one assumes isotropy in the 2-3 plane then shear modulus G_{23} is directly related to transverse modulus E_2 which is not degraded in case of fiber failure. Thus, from a pure mathematical point of view it can be assumed that out-of-plane shear modulus G_{23} is not affected significantly by the fiber failure.

In case of matrix failure, similar arguments can be made in selecting the elastic constants given in Equation (8) which are to be degraded once matrix failure is predicted by the failure theory.

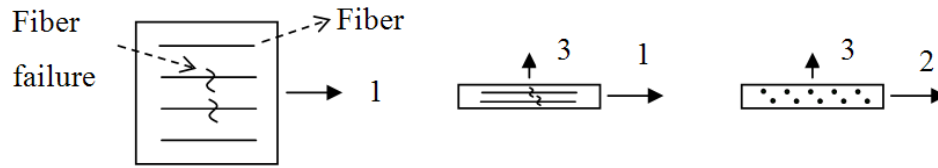


Figure 9: Schematic drawing of fiber failure of a representative element in unidirectional composite

4.2.2 Material Property Degradation Method for Mode Independent Failure Theory

In the current study, in order to demonstrate how the mode independent failure theory is included in the progressive failure analysis, in the case studies Tsai-Wu failure theory[13] is selected as the failure theory which is widely used in progressive failure analysis.

In the literature, material property degradation associated with failure predicted by the Tsai-Wu failure theory is implemented by identifying a mode of failure which is based on the stress component that contributes maximum to the failure index. For instance, if the maximum contribution to the failure index is due to σ_1 then fiber failure is assumed. Similarly, if maximum contribution to failure index is due to combination of σ_2 or τ_{12} , then matrix failure is assumed. However, this method of material property degradation disregards the contribution of all stress components to the failure index, and puts the blame on only one stress component in order to identify a failure mode. In the present study, material property degradation method used with the Tsai-Wu failure theory is modified, and the material property degradation factor, which is selected in the beginning of the analysis, is manipulated to yield two separate degradation factors that

are to be used with fiber and matrix failure modes which are assumed to occur simultaneously. The decision on the separate degradation factors is based on the selection of an appropriate decay function defined in terms of fiber and matrix failure indices. If the pre-selected degradation factor is R , then the requirement from the degradation factor associated with fiber failure (R_f) is that R_f should be equal to 1 when the fiber failure index is 0, and R_f should be equal to R when the fiber failure index is 1. The same logic holds for degradation factor (R_m) associated with the matrix failure. For the intermediate values of the fiber and matrix failure indices, a decay function, which is suitable for the pre-selected degradation factor R , is selected. The choice of the decay function is arbitrary, and it can be tuned so that results of progressive failure analysis match any available experimental failure data. To calculate separate degradation factors associated with fiber and matrix failures, failure indices corresponding to failure modes are separated as:

$$FF = F_1 \sigma_1 + F_{11} \sigma_1^2 + F_{12} \sigma_1 \sigma_2 \times \left(\frac{|\sigma_1|}{|\sigma_1| + |\sigma_2|} \right) \quad (9)$$

$$MF = F_2 \sigma_2 + F_{22} \sigma_2^2 + F_{66} \tau_{12}^2 + F_{12} \sigma_1 \sigma_2 \times \left(\frac{|\sigma_2|}{|\sigma_1| + |\sigma_2|} \right) \quad (10)$$

where FF is the fiber failure index and MF is the matrix failure index, and it is assumed interaction term contributes to both modes of failure, in proportion to the fiber direction and transverse direction axial stresses. In the mode independent Tsai-Wu failure criterion, it is assumed that failure occurs when the summation of the fiber and the matrix failure indices is greater than or equal to one. In the modified application of the Tsai-Wu failure criterion, separate degradation factors associated with the fiber and the matrix failures are calculated only after the condition of the summation of the fiber and

the matrix failure indices being greater than or equal to one is satisfied.

For sudden degradation, it is expected that the degradation factors associated with fiber and matrix failures should decay fast with the failure index, and for gradual degradation, gradual decay of the degradation factors with the fiber and matrix failure indices is more reasonable. Whether sudden or gradual, for all levels of material property degradation an exponential decay function is considered to be appropriate in calculating the separate degradation factors associated with the fiber and matrix failures. If the pre-selected degradation factor is R , then degradation factors, associated with fiber and matrix modes of failure, are proposed to be calculated by the exponential decay functions given in Equation (10).

$$R_f = e^{\ln(R) \times FF} \quad , \quad R_m = e^{\ln(R) \times MF} \quad (11)$$

where R_f and R_m are the separate fiber and matrix degradation factors to be used with the fiber and matrix failure modes, which are assumed to occur simultaneously. The exponential decay functions satisfy the following conditions:

- Separate fiber and matrix degradation factors become "1" when the failure indices are "0", which implies that no material property degradation should be done.
- Separate fiber and matrix degradation factors become equal to the pre-selected degradation factor R , when the failure indices are "1".
- For the intermediate values of the fiber and matrix failure indices (0-1), the multiplication of the separate degradation factors is equal to the pre-selected

degradation factor R . For those material properties which are degraded in both fiber and matrix modes of failure, such as the in-plane shear modulus as shown in Equations (3) and (4), since the material property undergoes successive degradation, it is reasonable to expect that R_f multiplied with R_m to be close to the initially selected degradation factor R .

Following the calculation of separate fiber and matrix degradation factors, Equation (7) and (8) are invoked to degrade the material properties with R being replaced by R_f in Equation (7) and R_m in Equation (8). Such a separation of the preselected degradation factor R is considered to reflect the failure behavior better than selecting a single mode of failure when a mode independent failure theory, such as Tsai-Wu, is used in the progressive failure analysis. As an example of gradual degradation, if the pre-selected gradual degradation factor is 0.9 and fiber and matrix indices are 0.6 and 0.4, respectively, then based on Equation (11) degradation factor associated with fiber failure mode (R_f) is approximately 0.94 and degradation factor associated with matrix failure mode (R_m) is approximately 0.96. Thus, the preselected %10 degradation in the material properties is divided into a %6 degradation in the material property associated with the fiber failure and %4 degradation in material property associated with the matrix failure. It should again be noted that when separate degradation factors are used in conjunction with fiber and matrix failures, which are assumed to occur simultaneously, it can be seen from Equations (7) and (8) that in-plane shear modulus undergoes successive degradation associated with both fiber and matrix failures. Therefore, it is reasonable to expect that R_f multiplied with R_m to be close to the initially selected degradation factor R , and this is indeed the case for the example problem studied.

If sudden degradation of material properties is selected as the method to use in the progressive failure analysis, a function which decays fast with the failure indices should

be used to reflect the sudden degradation of material properties better when the fiber and matrix failure indices take on intermediate values between 0-1. Equation (11) inherently decays fast when the pre-selected degradation factor is a low number implying sudden degradation. In the present study, for sudden degradation of material properties, degradation factor of "0.001" is used. Although the selection of the sudden degradation factor is arbitrary, in the present study the progressive failure analysis results showed that when the material properties of the failed plies are reduced by "1000", in the next load increment the failed ply is not loaded appreciably and subsequent degradation does not change the trend of failure progression. In the present study, exponential decay function shown in Figure 10, is used to calculate the separate degradation factors associated with fiber and matrix failures when the pre-selected sudden degradation factor is $R= 0.001$, and $\ln R=-6.91$. In case of sudden degradation, complete fiber or matrix failures are assumed to occur whenever the degradation factors associated with the fiber or matrix failures become less than or equal to "0.001", or in the general case less than or equal to R . During progressive failure analysis, after the failure is predicted in a ply, separate fiber and matrix degradation factors are calculated and elastic properties are degraded in accordance with Equations (7) and (8). However, failure color coding is invoked whenever the product of the fiber or the product of the matrix degradation factors, of each step of progressive failure analysis, become less than equal to the pre-selected degradation factor. As a final note it should be stated that in the present study, for the mode independent Tsai-Wu failure theory, progressive failure analysis is performed by two different methods. In the first method, the classical approach is used and a failure mode is identified based on the relative magnitudes of the fiber and matrix failure indices, and material property degradations are done based on single mode of failure; i.e. fiber or matrix. In the second method, exponential decay functions given in Equation (11) are used to yield two separate degradation factors that

are to be used with fiber and matrix failure modes which are assumed to occur simultaneously.

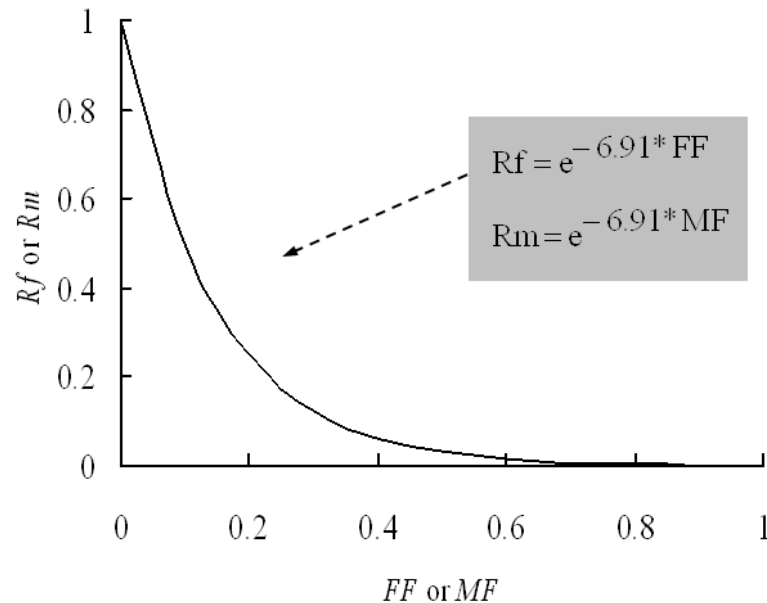


Figure 10: Exponential decay function used to determine separate degradation factors for $R=0.001$

4.3 Linear and Nonlinear Analysis

In the thesis, two dimensional finite element based progressive failure analysis method is used to study the first ply failure and progression of failure of composite laminates with cut-outs under in-plane and out-of-plane loading and geometrically linear and non-linear deformations. The failure analysis of composite laminates subjected to out-of-plane loads is complicated due to the fact that both material and geometric non-linearities become effective, when the loads are increased beyond the first ply failure [6]. Material

non-linearity occurs due to damage accumulation, and geometric non-linearities become effective due to the large displacements which the structure undergoes after first ply failure and before the ultimate failure. In the present study, linear constitutive law is used for material modeling but during the progressive analysis since material properties are degraded, in a way material non-linearity is included in the analysis. However, geometric non-linearity is included by using the non-linear solution types of MSC Nastran during the progressive failure analysis.

Linear analysis assumes a linear relationship between the load applied to a structure and the response of the structure. The stiffness of a structure in a linear analysis does not change depending on its previous state. Linear static problems are solved in one step, and linear analysis can provide a good approximation of a structure's response. A number of important assumptions and limitations are inherent in linear static analysis. Linear analysis is restricted to small displacements, otherwise the stiffness of the structures changes and must be accounted for by regenerating the stiffness matrix. Lastly, loads are assumed to be applied slowly as to keep the structure in equilibrium.

It becomes necessary to consider nonlinear effects in structures where large deformations such as rotations and/or strains occur. In a nonlinear problem, the stiffness of the structure depends on the displacement and the response is no longer a linear function of the load applied. As the structure displaces due to loading, the stiffness changes, and as the stiffness changes the structure's response changes. As a result, nonlinear problems require incremental solution schemes that divide the problem up into steps calculating the displacement, then updating the stiffness. Each step uses the results from the previous step as a starting point. As a result the stiffness matrix must be generated and decomposed many times during the analysis adding time and costs to the analysis [14].

Thus, it can be said that the main difference between linear and non-linear analysis is in whether the stiffness of the structure changes with the deformation or not. If linear constitutive law is used, as in the present study, then it is assumed that stiffness of the structure does not change with the deformation if no failure is induced during the loading process. When the structure deforms under a certain load condition, stiffness of the structure may change if the deformation is large. However, if the deformation is small with respect to the size of the structure, then it can be assumed that the change in the stiffness of the structure is negligible. Small deformation assumption is one of fundamental assumptions of the linear analysis. In linear analysis, since model stiffness never changes, there is no need to update the stiffness while structure deforms.

In non-linear analysis stiffness changes during deformation process and it must be updated by using an iterative solution method in the finite element formulation. It should be noted that if stiffness change is only due to the large deformation, this non-linear behavior is named as geometric nonlinearity [21].

Geometric nonlinear effects play an important role in large deformation applications. According to Kirchhoff and Love plate theory, small deformation theory is valid for deflections under 20 % of the plate thickness or 2 % of the small span length. But since geometric non-linear effects are also related with boundary conditions as well as dimensions, the behavior of the structure should be also examined while deciding on using geometric nonlinearity in the finite element analysis. The word “large” in large deformation in geometrically nonlinear analysis means that the displacements invalidate the small displacement assumptions inherent in the equations of linear analysis.

Another aspect of geometric nonlinear analysis involves follower forces. If the load is sufficient to cause large deformation in the structure, then in the deformed configuration, the load follows the structure to its deformed state. Capturing this behavior requires the iterative update techniques of nonlinear analysis. Figure 11 shows a slender cantilever beam subject to an initially vertical end load. If it is assumed that the load is sufficient to cause large displacements, in the deformed configuration, the load is no longer vertical, and it follows the structure to its deformed state.

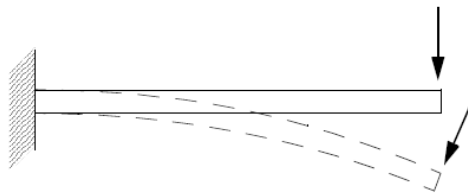


Figure 11: Follower force effect

It should be noted that in structural problems the loading may be such as to follow the structure as it deforms, or the load might remain fixed in direction. These situations are often referred to as “non-conservative” and “conservative” loading respectively. In the former, the proportions of the load acting in-plane and transverse to the structure changes. Thus, follower forces not only affect the load vector, but also affects the structural stiffness through stress stiffening effects. In geometric non-linear analysis, pressure follows the structure since it is applied to an element face. However, concentrated forces may or may not remain fixed in direction. Depending on the application concentrated forces can also be made to follow the structure.

In case of geometric nonlinearity, there are two distinct deformation types to consider:

- i) Large displacement, small strain: In large displacement small strain deformation type, the structure undergoes under large rotations as shown in

Figure 12(a), but the strains remain small. In this deformation type, stiffness matrix is simply transformed to account for rotation. Therefore, large displacement small strain solutions are cheaper than the full large strain solutions [21].

- ii) Large displacement, large strain: Large displacement, large strain deformation occurs when the strains also become large as shown in Figure 12(b). In such cases the whole element shape, hence the stiffness matrix, changes. Thus, stiffness matrix cannot be transformed by a rotation matrix.

In either case, the stiffness matrix is a function of the deformation, and the problem is non-linear.

Geometric nonlinear analysis are also used in large strain applications like metal forming that strains exceed 100% [21].

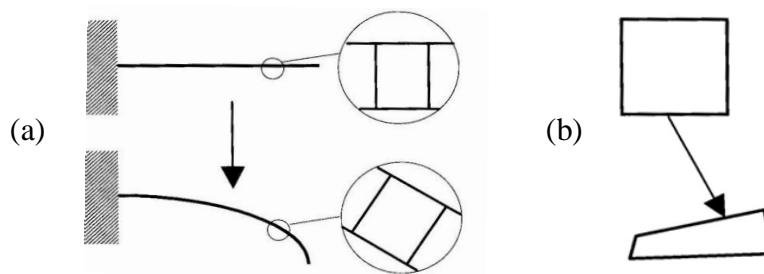


Figure 12: Examples of (a) large displacement, small strain (b) large displacement, large strain [21]

In this study, all types of geometric non-linear analysis have been used and comparisons between different load conditions and solution types have been performed. MSC Nastran

solution types like SOL101 (Linear static analysis), SOL106 (Nonlinear static, Large deformation-small strain) and SOL600 (Implicit Nonlinear, Large deformation-large strain) are implemented into progressive failure analysis to evaluate effects of in-plane and out-of-plane loads on the first ply failure and progression of failure in composite laminates. Throughout the study, pressure forces are allowed to follow deformation and axial loads are assumed to have fixed direction as shown in Figure 13.

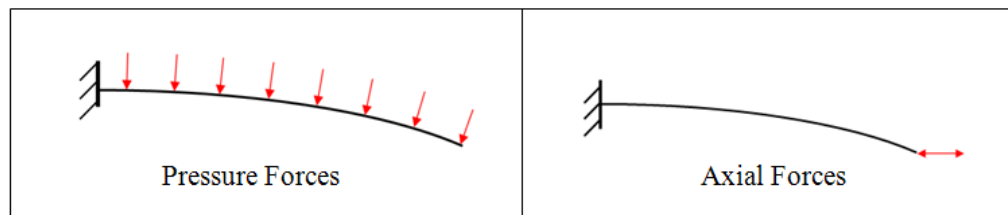


Figure 13 : Follower Forces

On the other hand, since the material nonlinearity effects due to the failure in the composite have been taken into account by degrading material properties in an average sense, it can be assumed that there is no need to use material nonlinearity option in analysis [6].

The detailed information about nonlinear analysis types and solution parameters are presented in Appendix B.

CHAPTER 5

RESULTS AND DISCUSSIONS

5.1 Verification of PCL Code by Hand Calculation

In this section, the first ply failure and ultimate loads obtained from the PCL code are verified by using the Classical Lamination Theory (CLT) [15]. Firstly, hand calculation of CLT is performed for a defined case study and then the same case problem is solved by the PCL code and hand calculation and PCL code results are compared with each other.

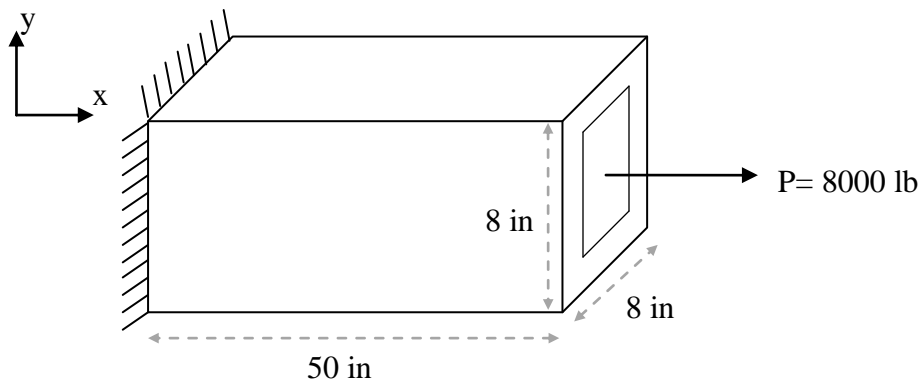


Figure 14: Geometry and boundary conditions of box beam

For the case study, a square cross-section box beam has been defined as shown in Figure 14. Box is made of 3 layer E-glass/epoxy laminate with a stacking sequence [0/90/0]. The total thickness of the laminate is 0.015 inch and mechanical properties of the plies

are shown in Table 1. Box beam is subjected to an axial force of 8000 lb, as shown in Figure 14.

Table 1: Material properties for E-glass/epoxy material

| Material Properties | | Value |
|-----------------------------------|------------|----------|
| Longitudinal Young's Modulus | E_{11} | 7800 ksi |
| Transverse Young's Modulus | E_{22} | 2602 ksi |
| Poisson's Ratio | ν_{12} | 0.24 |
| In-Plane Shear Modulus | G_{12} | 1300 ksi |
| Longitudinal Tensile Strength | X_T | 150 ksi |
| Longitudinal Compression Strength | X_C | 150 ksi |
| Transverse Tensile Strength | Y_T | 4 ksi |
| Transverse Compression Strength | Y_C | 20 ksi |
| In-Plane Shear Strength | T | 6 ksi |

If the box is assumed as a flat plate by unwrapping the edges, the loaded edge length will be four times the edge length of the box. So the applied load per unit length can be expressed as:

$$N_x = \frac{P}{\text{Circumference}} = \frac{8000 \text{ lb}}{4 \times 8 \text{ inch}} = 250 \text{ lb}$$

Since N_y and N_{xy} do not exist, the stress resultant vector will be $N = \begin{bmatrix} N_x \\ N_y \\ N_z \end{bmatrix} = \begin{bmatrix} 250 \\ 0 \\ 0 \end{bmatrix}$.

Under the assumptions of CLT which is based on Kirchhoff-Love classical plate theory, the resultant forces and moments can be written in terms of mid-plane extensional strains and curvatures as:

$$\begin{bmatrix} N \\ M \end{bmatrix} = \begin{bmatrix} A & B \\ B & D \end{bmatrix} \begin{bmatrix} \varepsilon^0 \\ \kappa \end{bmatrix} \quad (12)$$

where “A” is the extensional stiffness, “B” is bending-extension coupling stiffness and “D” is bending stiffness matrix and they can be calculated as follows;

$$\begin{aligned} A_{ij} &= \sum_{k=1}^N (\bar{Q}_{ij})_k (z_k - z_{k-1}) \\ B_{ij} &= \frac{1}{2} \sum_{k=1}^N (\bar{Q}_{ij})_k (z_k^2 - z_{k-1}^2) \\ D_{ij} &= \frac{1}{3} \sum_{k=1}^N (\bar{Q}_{ij})_k (z_k^3 - z_{k-1}^3) \end{aligned} \quad (13)$$

where \bar{Q}_{ij} is the transformed reduced stiffness matrix which is in the material coordinate system and “ z_k ” is the directed distance to the top of the k^{th} ply and “ z_{k-1} ” is the directed distance to the bottom of the k^{th} ply from the mid-surface of laminate. Also for the orthotropic material under plane stress case, reduced stiffness matrix is by Equation (14).

$$Q_{ij} = \begin{bmatrix} Q_{11} & Q_{12} & 0 \\ Q_{12} & Q_{22} & 0 \\ 0 & 0 & Q_{66} \end{bmatrix} \quad (14)$$

where

$$Q_{11} = \frac{E_1}{1-\nu_{12}\nu_{21}}, \quad Q_{12} = \frac{\nu_{12}E_1}{1-\nu_{12}\nu_{21}}, \quad Q_{22} = \frac{E_2}{1-\nu_{12}\nu_{21}}, \quad Q_{66} = G_{12} \quad (15)$$

The elements of the reduced stiffness matrix in the material coordinate system are given in Table 2.

Table 2: Reduced stiffness's for plies

| Ply Orientation | Q ₁₁ (ksi) | Q ₁₂ (ksi) | Q ₂₂ (ksi) | Q ₆₆ (ksi) |
|-----------------|-----------------------|-----------------------|-----------------------|-----------------------|
| 0° | 7960 | 650 | 2655 | 1300 |
| 90° | 2655 | 650 | 7960 | 1300 |

In the described case study, since the laminate is mid-plane symmetric bending-extension coupling stiffness matrix vanishes. Also due to the absence of moment in the case study, there is only extensional strain, and it can be calculated by multiplying the inverse of “A” matrix by force vector [15].

For the reduced stiffness values shown in Table 2, “A” and “A⁻¹” matrices are obtained as;

$$[A] = \begin{bmatrix} 92.87 & 9.75 & 0 \\ 9.75 & 66.35 & 0 \\ 0 & 0 & 19.5 \end{bmatrix} \times 10^3 \text{ (lb/in)} \quad (16)$$

$$[A]^{-1} = \begin{bmatrix} 10.93 & 1.605 & 0 \\ 1.605 & 15.3 & 0 \\ 0 & 0 & 51.28 \end{bmatrix} \times 10^{-6} \text{ (in/lb)} \quad (17)$$

By using $[\epsilon^0] = [A]^{-1}[N]$ and $[\sigma] = [\bar{Q}][\epsilon^0]$ equations, the stress values at the mid-plane of plies are determined and they are tabulated in Table 3.

Table 3: Ply stresses in material coordinate system

| Ply Orientation | σ_1 (ksi) | σ_2 (ksi) | τ_{12} (ksi) |
|-----------------|------------------|------------------|-------------------|
| 0° | 21.566 | 0.714 | 0 |
| 90° | -1.418 | 6.994 | 0 |

For the obtained stress values, if the failure indices are checked by using Tsai-Hill failure theory shown in Equation (18).

$$FI = \frac{\sigma_1^2}{X^2} + \frac{\sigma_2^2}{Y^2} - \frac{\sigma_1 \sigma_2}{X^2} + \frac{\tau_{12}^2}{S^2} \quad (18)$$

The failure index for 0° plies is determined as "0.0518" and since it is lower than "1", no failure is expected in these plies. But failure index value for the 90° ply is calculated as "3.07", so it can be said that failure is predicted in the inner ply. At this point, load needs to be scaled down to the first ply failure load level to calculate the first ply failure load and to start the progressive failure analysis correctly. Since failure index calculation in Tsai-Hill typically corresponds to square of applied load over allowable load, the new load on the laminate can be calculated by dividing current load to the square root of failure index as follows;

$$P_{\text{new}} = \frac{8000 \text{ lb}}{\sqrt{3.07}} = 4563 \text{ lb} \quad , \quad N_{x,\text{new}} = 142.6 \text{ lb/in} \quad (19)$$

Thus, 4563 lb corresponds to the first ply failure load, and at this load level 90° ply fails. If it is assumed that ply has completely failed and it doesn't have any contribution to stiffness matrix, the updated "A" matrix is calculated as;

$$[A] = \begin{bmatrix} 79.6 & 6.5 & 0 \\ 6.5 & 2.65 & 0 \\ 0 & 0 & 1.3 \end{bmatrix} \times 10^3 \text{ (lb/in)} \quad (20)$$

By applying same calculation procedure for remaining 0° plies, stress values in the 0° plies can be obtained as;

$$\sigma_1 = 14.267 \text{ ksi}, \sigma_2 = -0.59 \times 10^{-3} \text{ ksi} \quad (21)$$

The Tsai-Hill theory failure index for the just calculated stress state is 9.04×10^{-3} . Since the failure index is lower than one, after first ply failure of the 90° ply, 0° plies can sustain the first ply load, implying the box beam has residual strength. To calculate the ultimate failure load of the box beam, the first ply failure load must be scaled as shown in Equation (22). The scaled load for the failure of the remaining 0° plies would be the ultimate failure load of the laminate.

$$P_{\text{ultimate}} = \frac{4563 \text{ lb}}{\sqrt{9.04 \times 10^{-3}}} = 48000 \text{ lb} \quad (22)$$

To verify the calculations performed by the PCL code, the same case study has also been analyzed by using the developed PCL code. But while performing progressive failure, instead of scaling the applied load for the purpose of evaluating the first ply or the ultimate failure load directly, the load is increased from an initial value up to the ultimate failure step by step. The prepared finite element model for this iterative analysis is shown in Figure 15. To make one to one correspondence with the hand calculation, box beam is unwrapped and it is treated as a laminate with a width which is four times the edge length of the square box beam.

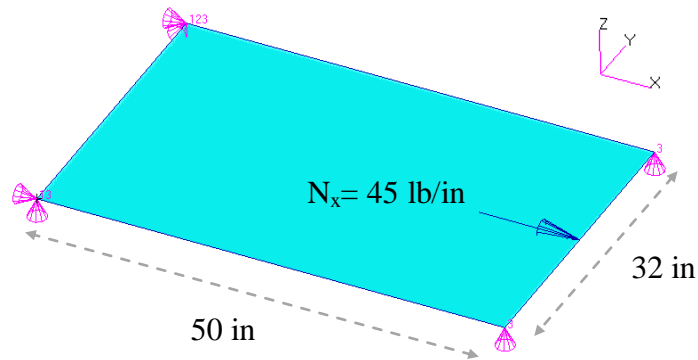


Figure 15: Geometry and boundary conditions of the unwrapped box beam with an initial load of 45 lb/in

In the model, the box geometry is directly simulated by a plate as assumed in previous analysis and only one shell element used. One end of the laminate is simply-supported and the loaded end is supported in the "z" direction only. The use of single shell element is justified, because in the hand calculation boundary effects are also not considered. As an initial load value 45 lb/in is selected and it is increased by 100 lb/in in each increment to obtain first ply and ultimate failure load values which are close to the CLT results. Since complete ply failure concept has been used in CLT for this study, in finite element based iterative progressive failure analysis, all elastic constants of failed ply are degraded to small values.

According to the results of the PCL run, the first ply failure load is obtained as 4640 lb and ultimate failure load is obtained as 49440 lb. Although there are some differences between results of the classical lamination theory based hand calculation and the PCL code, these differences are due to the selected load increment which is 100 lb/in. If it is desired to get sensitive failure loads, the load increment has to be decreased. However, for the purpose of verifying the accuracy of the results determined by the PCL code, the

calculated first ply failure load and ultimate load results are considered to be satisfactory.

5.2 Verification of PCL Code by Test Results

As a second case study, in this section, verification of the developed PCL code and progressive failure analysis methodology is performed by comparing the results of the PCL code with the results of experiments performed by Chang et.al [3] and analysis results of Sleight [7]. For a 20-ply laminate which has a centrally located circular cut-out, progressive failure analysis has been performed and first ply failure and ultimate failure loads are determined and compared with the corresponding failure loads given by Chang et.al. [3] and Sleight [7].

Specimen material consists of T300/1034-C carbon fiber reinforced epoxy layers with nominal ply thickness 0.1308 mm. The stacking sequence is $[0 / (\pm 45)_3 / 90_3]_s$. As shown in Figure 16; laminate length is 203.2 mm, width is 25.4 mm and diameter of the central cut-out is 6.35 mm. As in a typical tensile test, the sides of the specimen are free and loaded ends are clamped. Material properties of the test specimen are tabulated in Table 4.

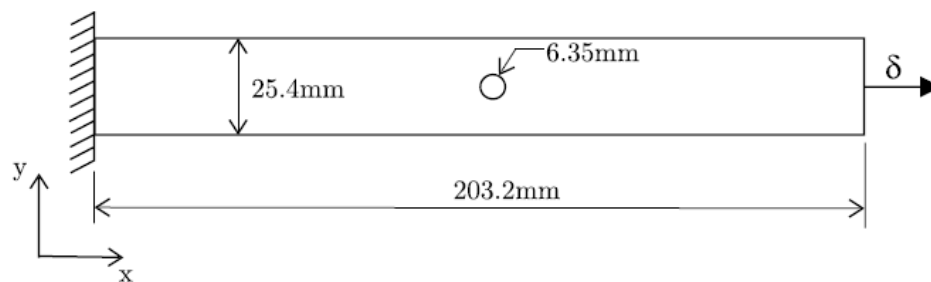


Figure 16: Tensile test specimen [7]

Table 4: Material properties for T300/1034-C carbon/epoxy [3]

| Material Properties | | Value |
|-----------------------------------|------------|--------------|
| Longitudinal Young's Modulus | E_{11} | 146858.3 MPa |
| Transverse Young's Modulus | E_{22} | 11376.3 MPa |
| Poisson's Ratio | ν_{12} | 0.30 |
| In-Plane Shear Modulus | G_{12} | 6184.6 MPa |
| Longitudinal Tensile Strength | X_T | 1730.5 MPa |
| Longitudinal Compression Strength | X_C | 1378.9 MPa |
| Transverse Tensile Strength | Y_T | 66.5 MPa |
| Transverse Compression Strength | Y_C | 268.2 MPa |
| In-Plane Shear Strength | T | 133.7 MPa |

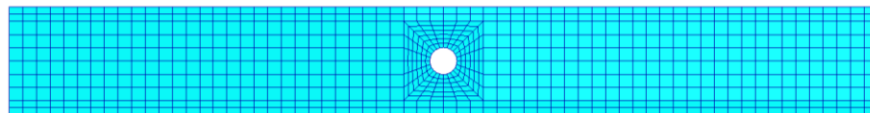


Figure 17: 2D Finite element model of test specimen

Since the finite element results of the Sleight[7] is also compared as well as the experimental results of Chang et.al. [3], the same two dimensional finite element model has been prepared in MSC Patran as shown in Figure 17. Moreover, same displacement increment has been used for the purpose of comparing the load / displacement curves directly. In this particular example, load is applied by enforced displacement at the free end of the laminate. An initial displacement of 0.0127 mm is applied to the laminate and

in each load step the displacement is incremented by 0.0254 mm. Sleight [7] used a degradation factor of 10^{-20} in sudden degradation. It was mentioned before that since small degradation factors causes crashes in MSC Nastran matrix operations, in this study 10^{-3} has been used as the degradation factor. One source of the deviations between the results of Sleight [7] and the results of the present study is considered to be due to the differences in the degradation factor.

The comparison of load/displacement curves are shown in Figure 18. The load/displacement curve of the Sleight [7] is obtained by digitalizing graphic stated in referenced article and also it does not contain the load drop-off region. As shown in figure, developed method predicts higher first ply failure and ultimate failure loads than other studies.

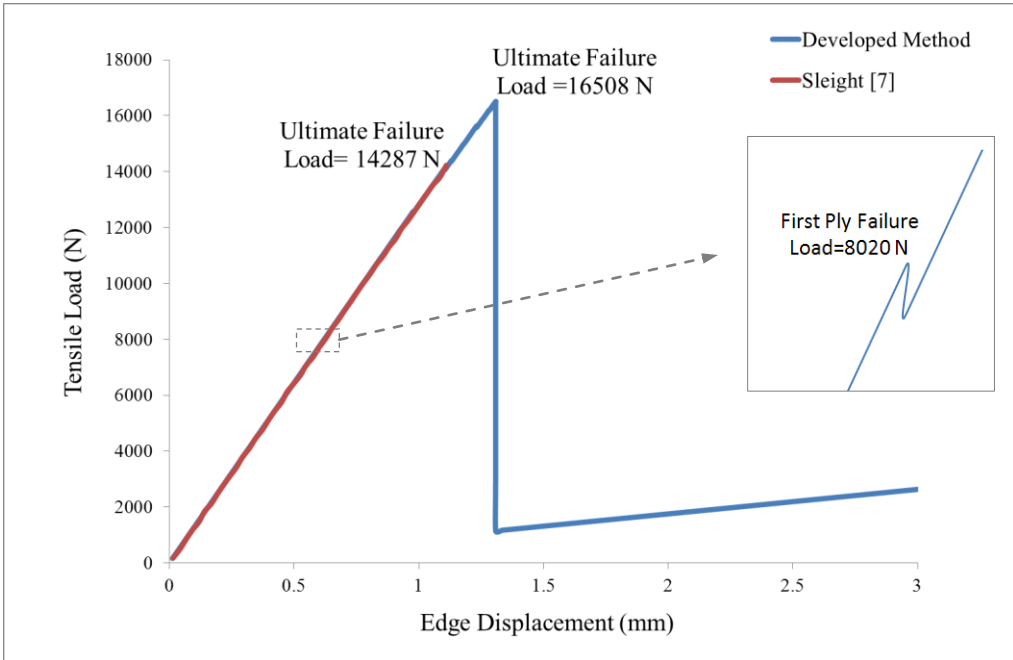


Figure 18: Comparison of load / displacement curves

Table 5 compares the first ply failure and ultimate failure loads determined by the PCL code and the results presented in the report by Sleight [7]. It is noticed that although the load displacement curves of the present analysis and Sleight are on top of each other, there is % 18 differences between the first ply loads. However, ultimate failure load determined by the PCL code is within %5 of the experimental result, and more close to the experimental result of Chang [3] than the ultimate load predicted by Sleight [7]. In the presented analysis, ultimate load predicted is higher than the experimentally determined ultimate load. Therefore, the ultimate load predicted by in the present analysis is not conservative, and this is a disadvantage in strength prediction. However, it should be noted that decision criteria on the ultimate load may change from analyst to analyst. In the verification study the ultimate load is taken as the load at which a very sharp drop in the constraints forces, at the free edge where the input displacement is applied, is observed as shown in Figure 18.

Table 5: Comparison of failure loads based on the failure criterion of Hashin

| Study | First Ply Failure Load (N) | Ultimate Failure Load (N) |
|---------------------------------|----------------------------|---------------------------|
| Developed Method, PCL | 8020 | 16508 |
| Sleight, COMET [7] | 6761 | 14287 |
| Chang, Experimental results [3] | Unavailable | 15671 |

During the progressive failure analysis, up to the first ply failure load, the degradation method does not have any effect on the results. Therefore, while comparing results of developed method with the results of Sleight [7], failure prediction methods and stress evaluation are the issues that should be concentrated on. When the progressive methodology of Sleight[7] is examined, it is noticed that failure predictions have been made by using stresses calculated at Gauss points. If failure is detected in any Gauss

point, the degradation has been performed for the material properties of the associated Gauss point.

It is known that in finite element method, first stresses are obtained in Gauss points and then they are extrapolated to the element nodes and to the centroid of the element. For this reason, it can be assumed that centroid stress is an average value and the stress value at the one of Gauss points may be higher than centroid stress. So, the reason of obtaining higher first ply failure load than Sleight [7] can be explained by justifying this issue in MSC Nastran. However, stress results at Gauss points are only available for 3D elements in MSC Nastran. For this reason, a different 3D finite element model has been developed as shown in Figure 19, and failure predictions based on both centroid and Gauss point stresses have been made for the first ply failure load of 6761 N of Sleight [7].

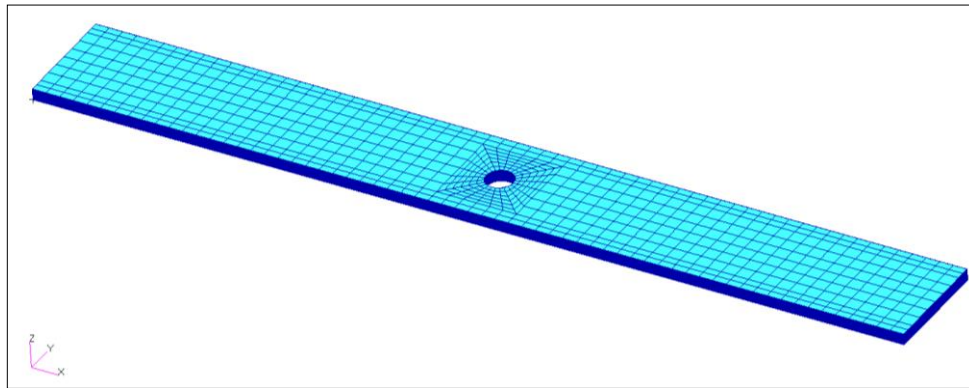


Figure 19: 3D Finite element model prepared for Gauss stress check

In Table 6, for the most critical hex8 element which has "8" Gauss points, the stress values and failure indices are listed at element center and each Gauss point. Failure indices are calculated based on the in-plane stresses utilizing the failure criterion of Hashin. Failure indices are given in the fourth column in Table 6.

Table 6: Stress results of Gauss points and centroid for the most critical element

| LOCATION | σ | MPa | Hashin Failure Index | Failure Mode |
|----------|----------|--------|----------------------|----------------|
| Center | X | -22.93 | 0.895 | Matrix Tensile |
| | Y | 62.46 | | |
| | XY | 6.73 | | |
| Gauss-1 | X | -21.05 | 0.700 | Matrix Tensile |
| | Y | 55.31 | | |
| | XY | 5.29 | | |
| Gauss-2 | X | -30.64 | 0.709 | Matrix Tensile |
| | Y | 55.65 | | |
| | XY | 5.49 | | |
| Gauss-3 | X | -30.16 | <u>1.110</u> | Matrix Tensile |
| | Y | 69.42 | | |
| | XY | 8.32 | | |
| Gauss-4 | X | -20.71 | <u>1.104</u> | Matrix Tensile |
| | Y | 69.25 | | |
| | XY | 8.16 | | |
| Gauss-5 | X | -15.79 | 0.694 | Matrix Tensile |
| | Y | 55.10 | | |
| | XY | 5.05 | | |
| Gauss-6 | X | -25.12 | 0.703 | Matrix Tensile |
| | Y | 55.44 | | |
| | XY | 5.24 | | |
| Gauss-7 | X | -24.50 | <u>1.123</u> | Matrix Tensile |
| | Y | 69.85 | | |
| | XY | 8.21 | | |
| Gauss-8 | X | -15.43 | <u>1.117</u> | Matrix Tensile |
| | Y | 69.69 | | |
| | XY | 8.05 | | |

For the first ply failure load of Sleight [7] no failure is observed at the element center as in the two dimensional model which is used in the progressive failure analysis in the PCL code. However, since the stress values at some of Gauss points are higher than the stresses at the centroid of the element, the failure indices obtained from Hashin's failure theory are greater than "1". Although there is no failure at the element center, if Gauss

points are taken into consideration for failure, it can be assumed that failure is initiated in the laminate.

According to the results for the three dimensional model, it can be concluded that since stress values of Gauss points are more critical than the stress values at the centroid of the element, failure initiation can be earlier and lower first ply failure loads can be obtained. This example explains the difference between failure load determined by the PCL code developed in the present study and the first ply load determined by Sleight [7]. This explanation is also valid for the difference between ultimate failure loads because early failure initiation causes lower ultimate failure loads.

Another factor contributing to the difference in the ultimate loads determined in the present study and by Sleight [7] could be due to the use of different material property degradation factors. As it is discussed before in the present study material property degradation factor is taken as "0.001" which is higher than the degradation factor used by Sleight. It should be noted that the effect of degradation factor on the ultimate failure becomes less and less when the degradation factor is further reduced, because degraded plies take up negligible load. However, one cannot claim that the difference between the degradation factors used in the present study and by Sleight has no effect on the ultimate failure load. From Table 5 it can be seen that the difference in the first ply failure loads is 1259 N whereas the difference in ultimate failure load is 2221 N. After the first ply failure, in the load range between first ply failure and ultimate failure, the difference in the residual load that the laminate can sustain is 962 N which is smaller than the difference in the first ply failure load. It is considered that the main reason for the difference in the first ply failure load is due to the different stress recovery points used by Sleight [7] and in the present study. After the first ply failure, considering that the difference in the residual loads becomes less than the difference in the first ply failure, it

can be inferred that the effect of using different stress recovery points on the failure indices becomes less significant compared to the effect of using different stress recovery points on the evaluation of failure indices for the determination of the first ply failure load. It is noted that after the first ply failure, although there is also a difference in the degradation factors, the difference in the residual loads is less compared to the difference in first ply failure loads. This is an indication that the effect of using different stress recovery points has less influence on the ultimate loads than it has on the first ply failure load. It is considered that once the material property degradation starts, the degraded elements do not take up appreciable load and therefore stress in these elements are less. The additional load goes to the intact elements and stresses in these elements become higher such that probability of predicting failure based on the stresses at the element centers increases. It should also be noted that the use of different degradation factors also has an effect on the difference in the ultimate loads. As it is seen in Table 5, a very low degradation factor, as used by Sleight [7], would underestimate the residual strength capacity of the material.

As a final comment it can be stated that, in progressive failure analysis, it is very hard to find an excellent match of the ultimate failure load with experimental results. Because, in progressive failure analysis, degradation method, degradation factor and failure theory used, all have a significant effect on the failure progression.

Nevertheless, it can be said that results presented in this verification section gave satisfactory feedback on the reliability of the PCL code developed in the thesis study. Thus, PCL code can be used with enough confidence to study the effect of linear and non-linear analysis on the failure progression of composite laminated under combined loading.

5.3 Description of the Model and Laminate Definition

In the present study, a rectangular laminate with a central cut-out is used as the model which employed in the case studies associated with the progressive failure analyses. Figure 20 shows the geometry, boundary definition and shell finite element mesh of the 400 mm x 200 mm composite laminate with a circular cut-out of 100 mm in diameter at the center. Boundaries are of the laminate denoted as W,E,N,S and H indicating the West, East, North, South and cut-out boundaries, where the boundary conditions (1: x displacement ; 2: y displacement ; 3: z displacement ; 4: x-rotation; 5: y rotation) are specified, respectively.

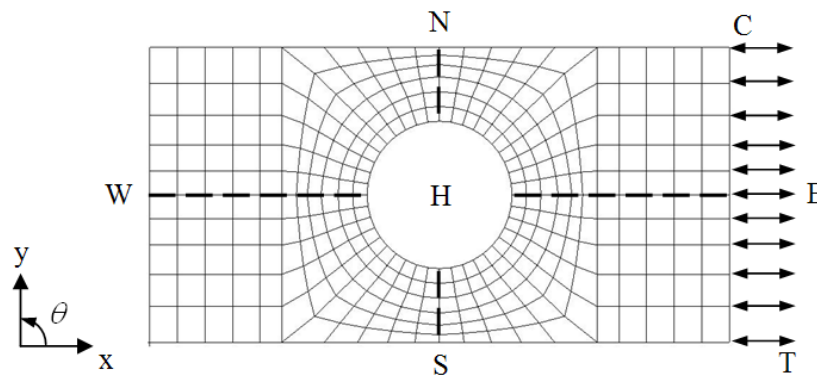


Figure 20: Laminate geometry and boundary definitions

Composite laminate is composed of eight, 0.1308 mm thick T300/N5208 pre-preg plies and it is a balanced symmetric laminate with a stacking sequence $[0/90/45/-45]_S$.

Material properties of the layer material are shown in Table 7.

Table 7: Material properties for T300/N5208 [22]

| Material Properties | | Value |
|-----------------------------------|------------|------------|
| Longitudinal Young's Modulus | E_{11} | 132380 MPa |
| Transverse Young's Modulus | E_{22} | 10760 MPa |
| Poisson's Ratio | ν_{12} | 0.24 |
| In-Plane Shear Modulus | G_{12} | 5660 MPa |
| Interlaminar Shear Modulus | G_{13} | 5660 MPa |
| Out-Plane Shear Modulus | G_{23} | 3380 MPa |
| Longitudinal Tensile Strength | X_T | 1513.4 MPa |
| Longitudinal Compression Strength | X_C | 1696 MPa |
| Transverse Tensile Strength | Y_T | 44 MPa |
| Transverse Compression Strength | Y_C | 44 MPa |
| In-Plane Shear Strength | T | 86.87 MPa |

Progressive failure analysis of the cut-out laminate is performed for four different load cases summarized in Table 8. Boundary conditions are applied along the W, E, N, S and H edges, and the numbers specified next to the edges in Table 8 indicate the degrees of freedom which are fixed. In the load cases studied, in-plane load is applied through nodal forces which act at each node from the east edge E as shown in Figure 20, and uniform pressure is applied on the top surface. For the tensile loading, symmetry

boundary conditions are applied along the mid-lines between the outer boundaries and the inner boundary, as shown in Figure 20 and indicated in Table 8. In the analyses performed, as it is mentioned before, for the combined pressure and axial loading, pressure is allowed to follow deformation but axial load is assumed to have a fix direction.

Table 8: Load cases and boundary conditions

| Load Cases ¹ | | Boundary conditions |
|-------------------------|------|-----------------------------------|
| 1 | T | W,E:3; W-H, E-H:2,4; N-H, S-H:1,5 |
| 2 | P | W,E,N,S: 1,2,3 |
| 3 | P +T | W: 1,2,3; N,S,E:2,3 |
| 4 | P+C | W: 1,2,3; N,S,E:2,3 |

¹ T: Tension, C: Compression, P: Pressure

5.4 Mesh Sensitivity Study

While performing a finite element based progressive failure analysis, it is a good practice to check mesh density of the model. This way, optimum mesh size can be determined in terms of achieving accuracy with reasonable computational effort. In this study, after verifying the developed method by using the CLT and results of previous works and experiments in the literature, various case studies involving different loading conditions, solution types, failure theories and degradation types have been performed. During these practices, the laminate defined in Section 5.3 is used. Therefore, in this section the particular laminate is analyzed by using different mesh sizes. However, since a load controlled progressive failure analysis is used in the most of case studies performed, instead of displacement controlled analysis as in the test verification given

above, load controlled progressive failure analysis has been used in the mesh sensitivity study.

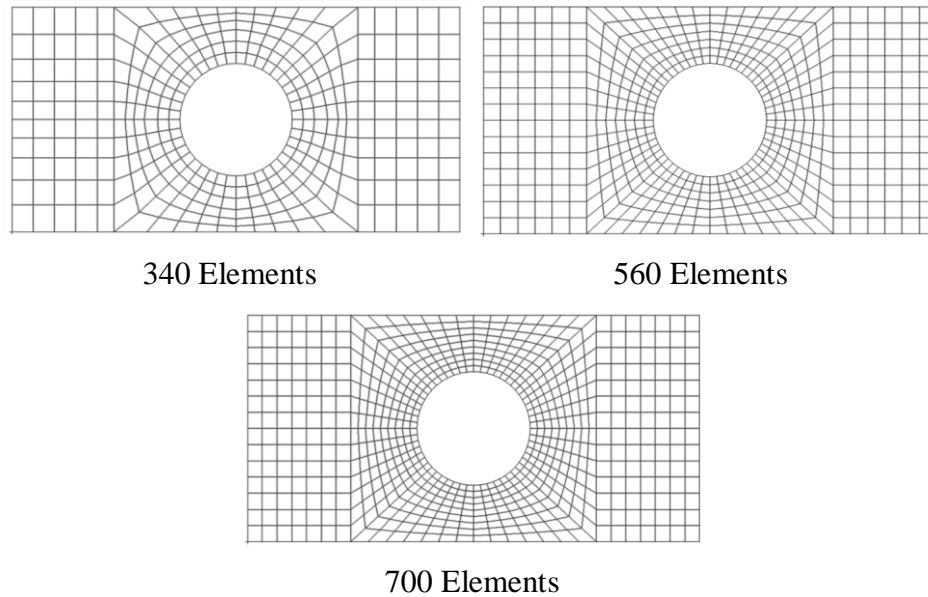


Figure 21: Finite element models for mesh sensitivity check

In Figure 21, three alternatives used for the mesh sensitivity check have been shown. In the coarsest model there are 340 elements and in the finest model there are 700 elements. While performing progressive failure analysis for different mesh sizes, combined pressure and tension case has been used and the resultant displacement values have been collected from the middle point of loaded edge. The comparison of the load/displacement curves of the three alternatives are shown in Figure 22. The sequence of load applications is such that first pressure is applied until first ply failure, and then pressure is kept constant and tensile load is increased with increments until ultimate failure.

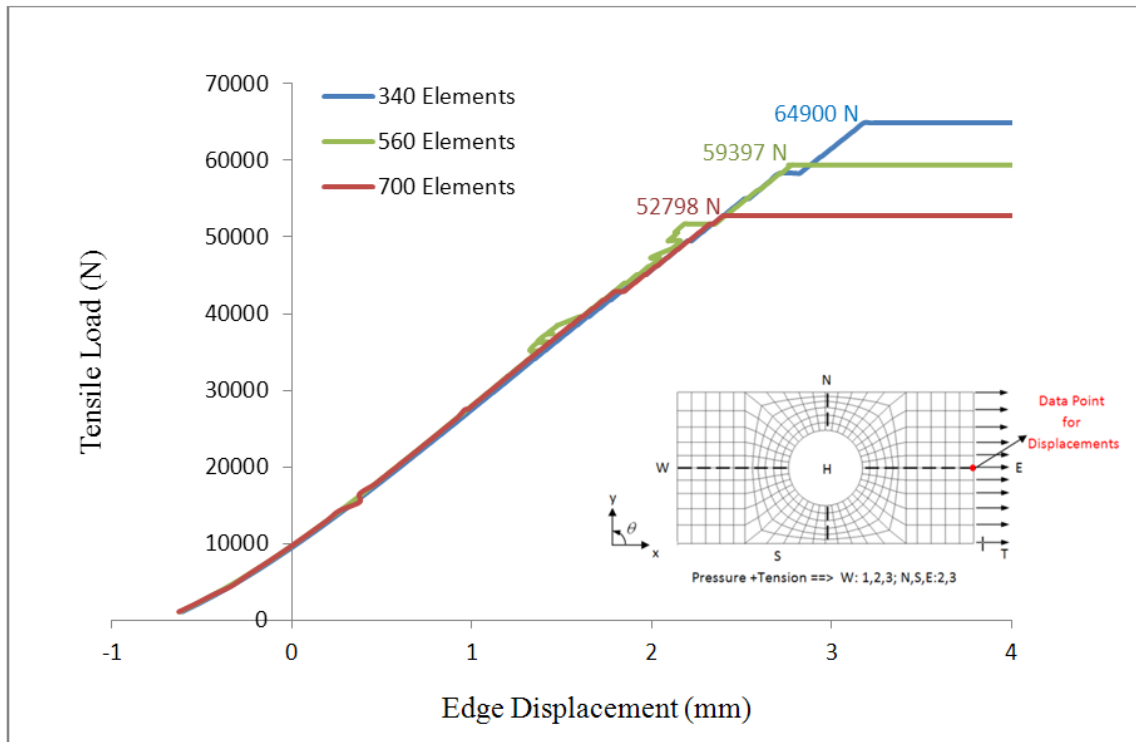


Figure 22: Load/displacement curves of different mesh sizes for the combined pressure and tension loads by using SOL600 nonlinear analysis

In the load controlled progressive failure analysis, ultimate failure load corresponds to the load level at which the edge displacement increases indefinitely without increasing the load due to continuous failure caused by the degraded elements.

It can be noticed that from Figure 22 that fine mesh predicts the lowest ultimate failure load, and for coarser mesh ultimate failure load is higher. To understand the reason of this difference in the ultimate failure loads with the mesh size, Figure 23 which shows the state of failure progressions for the finest and the coarsest mesh configurations is examined. In Figure 23, failure progressions are compared at the same pressure and in-

plane tensile loading. According to the failure progression plots, in fine mesh, failure initiated and reached ultimate failure load earlier than the coarse mesh case. Because, in coarse mesh stress concentration near the hole is distributed to a larger area due to the size of the elements but in fine mesh stress remains localized. In addition, in the fine mesh case since element centers are closer to the hole edge and failure calculations are performed for the stresses at element centers, failure initiation occurs earlier than failure progression is higher compared to the coarse mesh case.

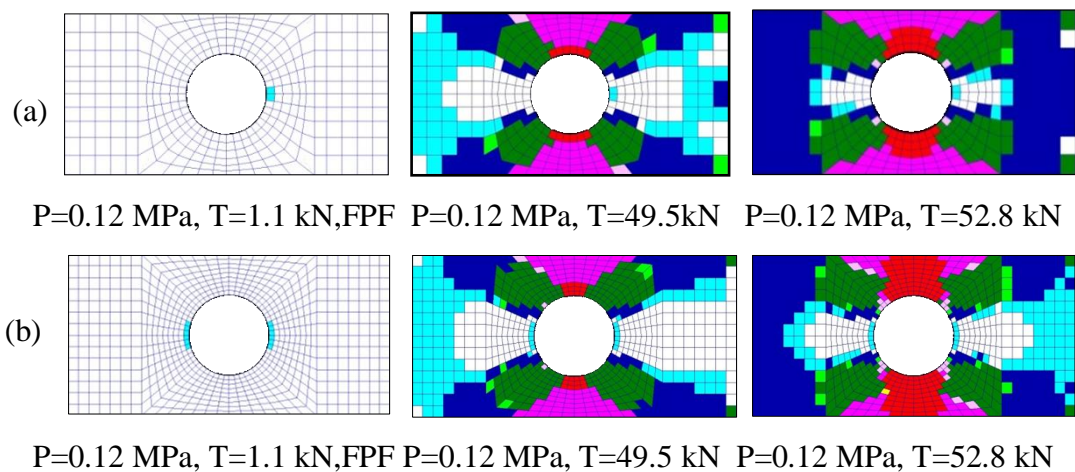


Figure 23: Comparison of failure progression plots (a) 340 elements (b) 700 elements

Consequently, it can be concluded that mesh sensitivity has an important effect on evaluating first ply and ultimate failures of laminates. By increasing mesh alternatives, an optimum mesh size can be obtained by checking the convergence of the ultimate failure load. However, it should also be noted that fine mesh models cause excessive solution time and computational effort especially in nonlinear analysis. For this reason, while deciding on an appropriate mesh size, one has to be careful not to use very fine mesh and obtain unnecessarily very accurate ultimate failure load. Ultimate failure load

gives an indication about the residual strength of the laminate. One can always use a factor of safety on ultimate failure load which is determined based on a relatively coarser mesh analysis and eliminate the need of using very fine meshes which effectively results in high computational time.

The aim of this study is to develop a PCL code that enables user to perform progressive failure analysis and compare the results of various cases containing different loading conditions, solution types, failure theories and degradation types by changing the related parameters of interest. Considering the computational difficulties associated with the solution time and convergence issues, it has been decided to employ the coarse mesh model in the subsequent progressive failure analyses that are presented in the thesis.

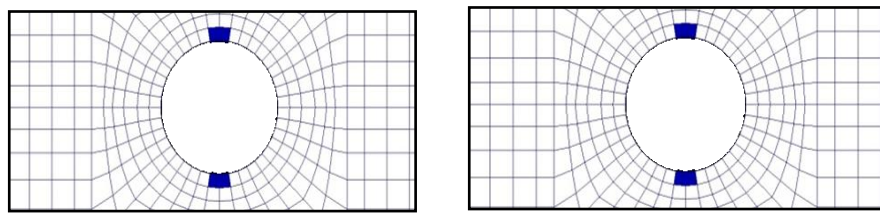
But while comparing the results of analysis with an experiment such as the example given in Section 5.2, it is possible to be forced to use finer mesh to have more accurate results. However, the finite element model used for comparison in mentioned section has been checked for mesh sensitivity in Sleight [7] and according to the results of that study, coarse model is satisfactory enough for first ply and ultimate failure predictions.

Mesh sensitivity study is also performed by using simple nonlinear static runs instead of progressive failure analysis for different element numbers and presented in Appendix C.

5.5 Pure Tensile Loading (Load Case 1)

Progressive failure analysis of the composite laminate, under pure gradual tensile loading, is performed by the linear static (SOL 101) and implicit non-linear (SOL 600) solution types of MSC Nastran [14] using Hashin's failure theory and sudden material property degradation scheme. Figure 24 shows the common first ply failure (FPF)

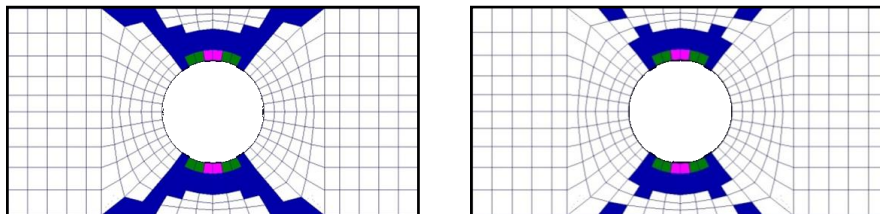
locations determined by the two solvers. First ply failure loads are determined as 14.52 kN by both linear and geometrically non-linear analysis, and first ply failure mode is identified as the matrix tension in the 90 plies (plies 2 and 7). Figure 25 gives failure progression plots obtained by the linear and non-linear analysis at an intermediate load level. In case of pure in-plane tensile loading, geometrically non-linear analysis and linear analysis predict similar failure progression plots, as expected. Therefore, the use of linear analysis for pure in-plane tensile loading is justified.



(a) Linear Analysis

(b) Non-Linear Analysis

Figure 24: First ply failure; Load case: 1; T=14.52 kN; Failure Theory: Hashin; R=0.001



(a) Linear analysis

(b) Non-Linear analysis

Figure 25: Failure progression; Load case: 1; T=29.04 kN; Failure Theory: Hashin; R=0.001

5.6 Pure Pressure Loading (Load Case 2)

Progressive failure analysis results for pure pressure loading are obtained by using the implicit non-linear solution type of MSC Nastran. Figure 26 shows four failure plots corresponding to load levels between the first ply pressure and ultimate failure. In case of pure pressure loading, initial failure occurs near the edge of the cut-out along the W-E

line. It is seen that although the laminate has same boundary conditions along the four edges for load case 2, for the particular laminate failure progression is not symmetric with respect to the cut-out, but failure shows somewhat anti-symmetric spread with respect to the cut-out. Figure 26(c) and Figure 26(d) show the somewhat anti-symmetric failure progression more clearly. Anti-symmetric appearance of failure progression is attributed to the position of the $\pm 45^\circ$ layers within the laminate. For the particular laminate, -45° layers are closer to the mid-plane of the laminate, therefore there are slight differences among the in-plane stresses in the 45° and -45° layers.

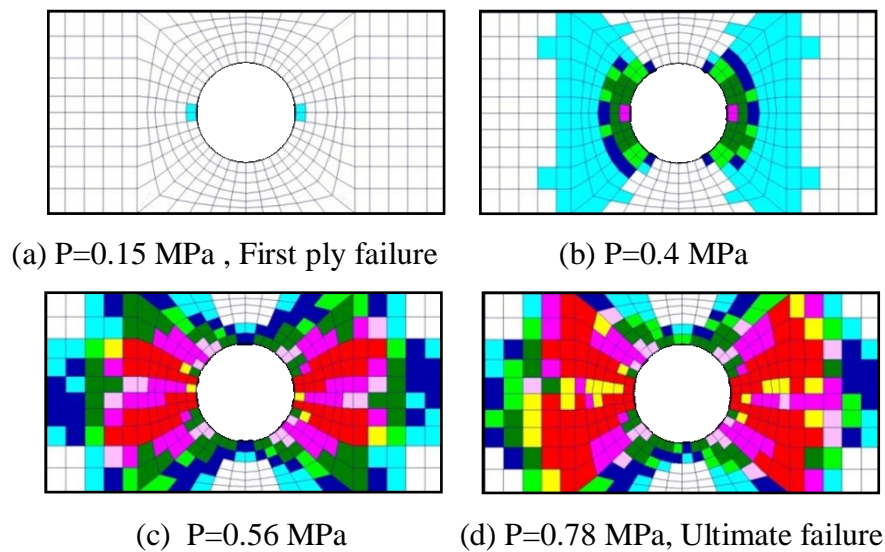


Figure 26: Failure progression; Load case: 2; Non-linear analysis; Failure Theory: Hashin; R=0.001

For the pre-preg material, since the transverse strength (Y_t) is very low, matrix tension is seen to be the dominant failure mode in most load cases. As shown in Figure 27, under the pressure loading transverse stress, which contributes to the matrix tensile failure in the 45° ply (3^{rd} ply) of the elements along the 45° line, is slightly higher than the transverse stress in the -45° ply (4^{th} ply) of the elements along the -45° line. Slight

differences in the stresses are the main cause for the anti-symmetric appearance of failure progression. However, if there is only tension load on the laminate, failure would not show an anti-symmetric progression since laminate is mid-plane symmetric.

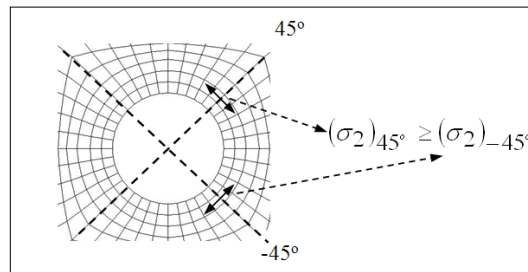


Figure 27: Comparison of transverse stresses in the 45° and -45° plies along the diagonal lines

As it is shown in Figure 28, under pure pressure loading, failure progression plots are also obtained at the same pressure loads using the Tsai-Wu failure theory in the classical sense. In the classical application of the failure theory proposed by Tsai-Wu, a single mode of failure is assumed to occur based on the relative magnitudes of the fiber and matrix failure indices. Therefore, there is no provision for the simultaneous failure of the fiber and the matrix. Figure 26 and Figure 28 show that failure progressions predicted by the failure criteria proposed by Hashin and Tsai-Wu are similar. Although failure is slightly more spread when Tsai-Wu failure theory is used, ultimate failure pressures predicted by the progressive failure analysis using the failure criteria proposed by Hashin and Tsai-Wu are approximately equal to each other. Interestingly, when failure theory proposed by Hashin is used, ultimate failure is predicted to occur along the shorter side of the laminate, somewhere between the cut-out and the left and right edges of the laminate. On the other hand, Tsai-Wu failure theory predicts the ultimate failure along the longer edge of the laminate, as indicated by the red elements which imply failure of all the plies. It should be noted that in the present analysis ultimate failure load

is taken as the load when all plies of elements along a line fail according to the failure theory used.

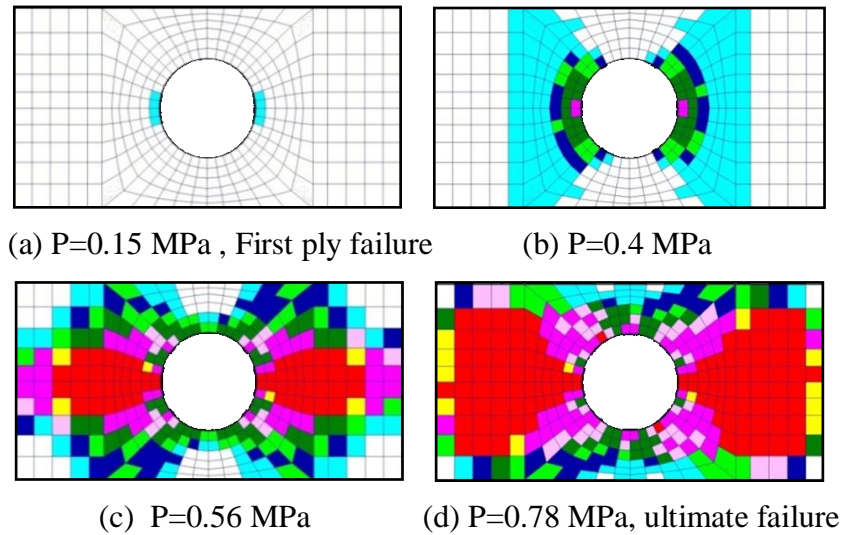


Figure 28: Failure progression; Load case: 2; Nonlinear analysis; Failure Theory: Tsai-Wu-Classical; R=0.001

5.7 Gradual Tensile Loading under Constant Pressure (Load Case 3)

Progressive failure analysis of the composite laminate with cut-out is performed under combined tensile and pressure loading by employing the Hashin and Tsai-Wu failure criteria using the sudden material property degradation scheme with a degradation factor of "0.001". In load case 3, Tsai-Wu failure theory is first applied in the classical sense and then in the modified sense as described in Section 4.2.2. In the present study, during the progressive failure analysis, application of the Tsai-Wu failure theory in the modified sense is referred to as the modified Tsai-Wu failure theory. In the gradual tensile loading under constant pressure, initially first ply failure is determined at pure pressure loading, which is determined as 0.12 MPa, and following the first ply failure,

pressure is kept constant and tensile load is gradually increased until ultimate failure. Figure 29- Figure 31 show the failure progression plots between the first ply failure (FPF) and ultimate failure for the Hashin, Tsai-Wu failure theory applied in classical sense and Tsai-Wu failure theory applied in the modified sense, respectively. In Figure 29- Figure 31, the total tensile load of 1.1 kN corresponds to a nodal force of 100 N which is the incremental nodal force used in the progressive failure analysis. For the incremental tensile nodal force of 100 N, there has been no change in the first ply failure mode, therefore in Figure 29- Figure 31 the first total incremental tensile load is also shown together with the first ply failure pressure. Modified Tsai-Wu failure theory is applied by determining separate degradation factors, given by Equation (11), associated with fiber and matrix failures which are assumed to occur simultaneously every time the failure index of the failure theory proposed by Tsai-Wu exceeds one. However, failure color coding is implemented only in case of complete fiber or matrix failures, which are assumed to occur whenever the elastic constants associated with fiber failure ($E_1, G_{12}, G_{13}, \nu_{12}$) or with matrix failure ($E_2, G_{12}, G_{23}, \nu_{21}$), are degraded below the pre-selected sudden degradation factor R times the initial values of the elastic constants.

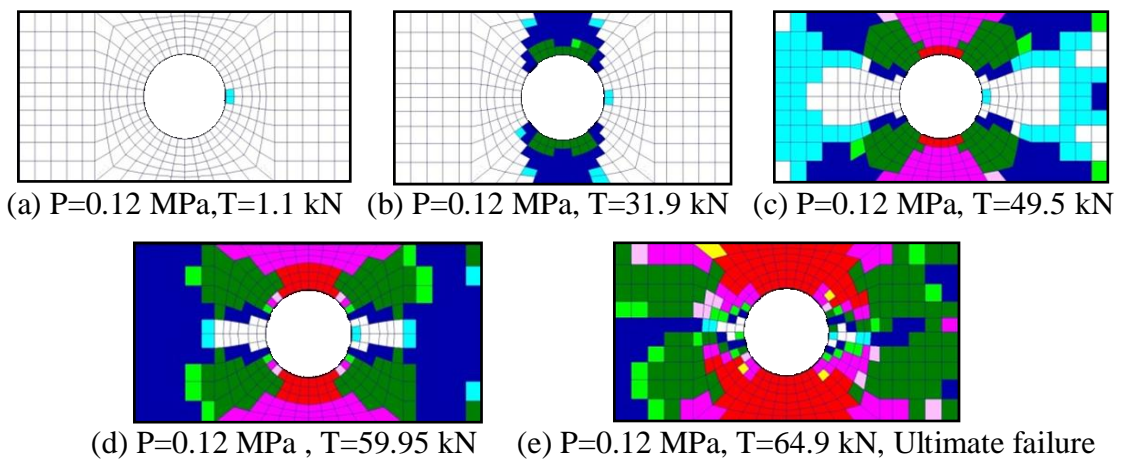


Figure 29: Failure progression; Load case: 3; Nonlinear analysis; Failure Theory: Hashin; $R=0.001$

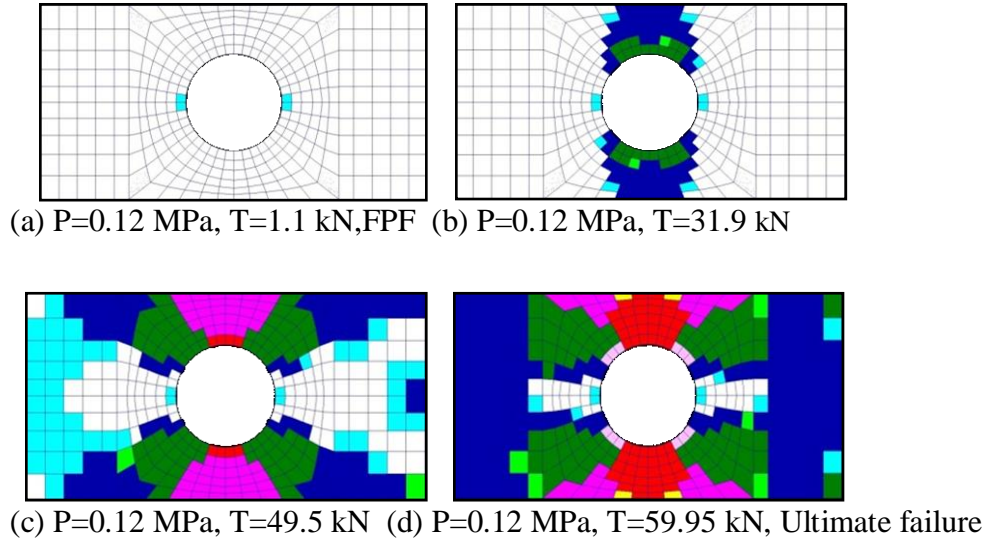


Figure 30: Failure progression; Load case:3; Nonlinear anal.; Failure Crit.: Tsai-Wu-
Classical; $R=0.001$

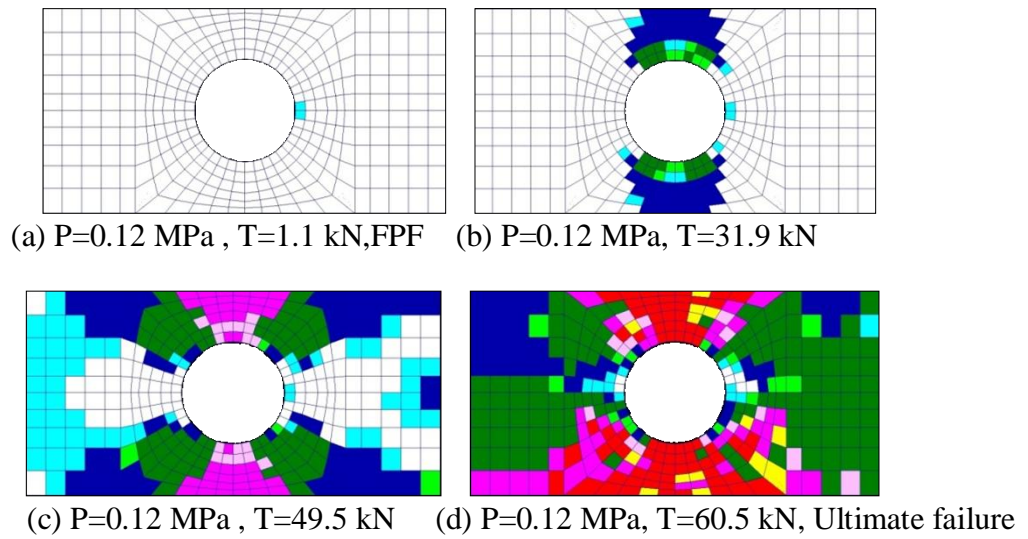


Figure 31: Failure progression; Load case:3; Nonlinear anal.; Failure Crit.: Tsai-Wu-
Modified; $R=0.001$

For the combined tension and pressure loading, Hashin, classical and modified Tsai-Wu failure criteria all predict first ply failure, under pure pressure loading, at the intersection of the W-E axis and the edge of the cut-out in the 0° bottom ply (ply 1) in matrix tension mode. It is noted that in load case 3, pressure loading also causes axial loading in the y-direction in the laminate. Although the axial stresses in the x-direction at the intersection of the edge of the cut-out and the N-S direction are higher than the y-direction axial stresses at the intersection of the edge of the cut-out and the W-E direction, matrix tension failure is found to be more critical due to low transverse strength of T300/N5208 pre-preg layer. Therefore, first ply failure occurs at the intersection of W-E axis and the edge of the cut-out in the 0° bottom ply in matrix tension mode. However, after the first ply failure, as the tensile force is increased gradually, failure progresses along the N-S direction of the laminate from the edge of the hole, as expected. In Figure 29-Figure 31, ultimate failure is evident due to the failure of all plies of all elements along the N-S direction from the edge of the cut-out.

Comparison of Figure 29-Figure 31 reveal that failure progression plots drawn at the intermediate load levels, below the ultimate failure load, are very similar to each other for the three failure criteria used in the progressive failure analysis. It is observed that the use of the failure theory proposed by Hashin in the progressive failure analysis, results in the highest ultimate failure load. Modified Tsai-Wu failure theory proposed in this study gives slightly higher ultimate failure load compared to the classical Tsai-Wu failure theory. It should be noted that in the modified application of the Tsai-Wu failure theory, when failure is predicted in a ply, both fiber and matrix properties are degraded simultaneously but with degradation factors greater than the initially selected degradation factor R . Therefore, in a way modified application of the Tsai-Wu failure theory leads to somewhat gradual degradation in the progressive failure analysis. However, since simultaneous degradation of the elastic properties associated with fiber

and matrix failures is allowed, failure is more dispersed in a ply. Therefore, it is deemed that modified application of the Tsai-Wu failure theory represents the state of failure in the laminate better, compared to the classical application of the Tsai-Wu failure theory in the progressive failure analysis.

In case of combined gradual tensile loading under constant pressure, first ply failure loads and the spread of failure at an intermediate load level due to linear and geometrically non-linear analysis are compared in Figure 32 and Figure 33. Hashin's failure theory is used in both linear and non-linear analysis. Figure 32 shows that linear analysis predicts a first ply failure pressure of 0.006 MPa, which is much lower compared to the first ply failure pressure of 0.12 MPa predicted by the non-linear analysis. First ply failure is predicted in ply 1 in matrix tension mode, both by linear and non-linear analysis.

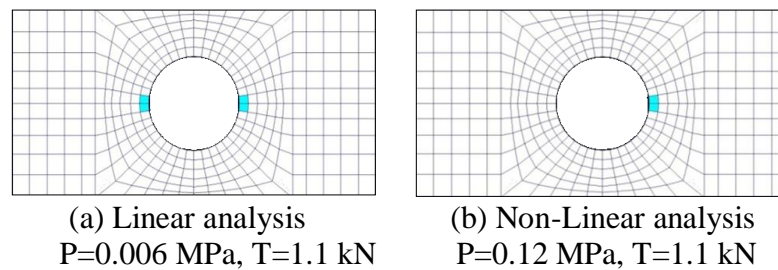


Figure 32: First ply failures; Load case: 3; Failure Theory: Hashin; $R=0.001$

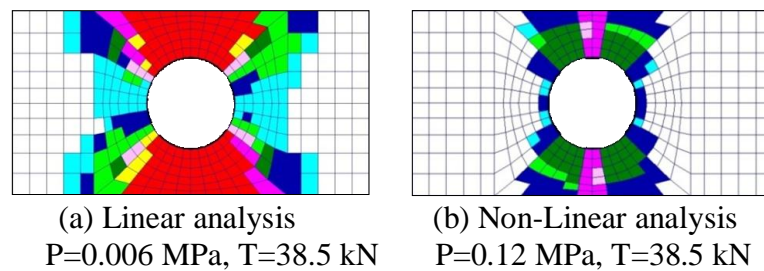


Figure 33: Failure progression; Load case: 3; Failure Theory: Hashin; $R=0.001$

Figure 33 compares the failure progression at a tensile load of 38.5 kN which is applied on the laminate after the occurrence of the first ply failure due to pure pressure. Figure 33 shows that in case of out-of-plane loading, linear analysis highly overestimate the state of failure in the laminate. As Figure 33(a) shows, in case of linear analysis ultimate failure of the laminate has already occurred at the tensile load of 38.5 kN, whereas in case of non-linear analysis laminate has not reached its ultimate failure load. It is known that in case of geometric non-linearity, diaphragm stresses cannot be ignored, and the elongation of the fibers in the central plane of the laminate is not negligible, and the laminate stiffens as it deflects laterally due to the pressure load. Thus, for the combined pressure and tensile loading, non-linear analysis predicts much lower stresses compared to linear analysis. It should be noted that even though pressure is not increased after the first ply failure and for the pure tension case geometric non-linearity is not effective, for the combined tensile loading under constant pressure, significant differences are observed between the failure progression plots predicted by the linear and non-linear analysis.

For the combined pressure and tensile loading, Figure 34 and Figure 35 compares the first ply failure and failure progression plots which are determined by the linear and non-linear analysis using the Tsai-Wu failure theory applied in the classical sense. In case of linear analysis, first ply failure is predicted in plies "1" and "8" in matrix tension mode, whereas non-linear analysis predicts first ply failure only in ply "1" in matrix tension mode. Failure progression plots given in Figure 35 show that linear analysis again highly overestimates the state of failure in the laminate even though pressure is not increased after the first ply failure. Also while solution time for nonlinear analysis of combined pressure and tensile loading is around "7" hours, for linear analysis solution time decreases to "2" hours, approximately.

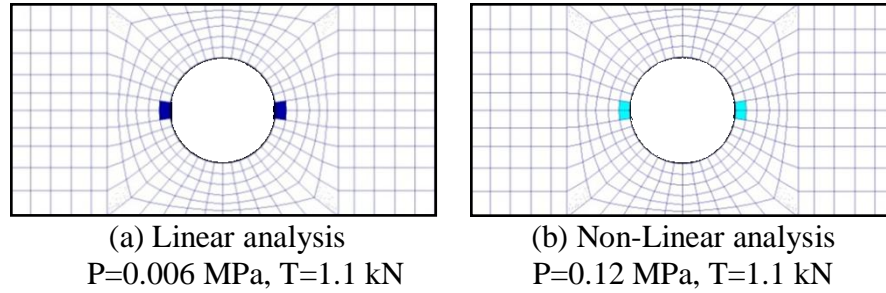


Figure 34: First ply failures; Load case: 3; Failure Theory: Tsai-Wu-Classical; $R=0.001$

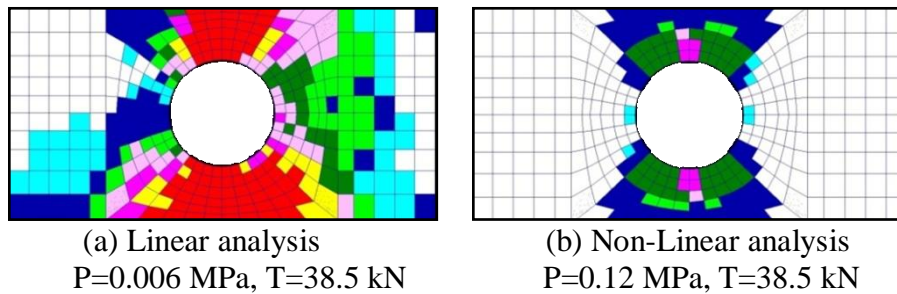


Figure 35: Failure progression; Load case: 3; Failure Theory: Tsai-Wu-Classical;
 $R=0.001$

5.8 Gradual Compressive Loading under Constant Pressure (Load Case 4)

Under combined compressive and pressure loading, initial comparison of the linear and non-linear progressive failure analysis of the composite laminate is performed by employing the Tsai-Wu failure theory in the classical sense, and by using the sudden material property degradation scheme with a degradation factor of "0.001". Figure 36 compares the first ply failures predicted by the linear and non-linear analysis. During the progressive failure analysis, first ply failure is determined for the pure pressure loading, and following the first ply failure, pressure is kept constant and compressive load is gradually increased and failure is progressed. In Figure 36, the total compressive load of 1.1 kN corresponds to a nodal force of 100 N which is the incremental nodal force used

in the progressive failure analysis as in the combined pressure and tensile load case. In case of linear analysis, first ply failure is predicted in plies "1" and "8" in matrix tension mode, whereas non-linear analysis predicts first ply failure only in ply "1" in matrix tension mode. Figure 37 shows the comparison of the failure progression plots obtained by the linear and non-linear analysis at an intermediate compressive load of 14.3 kN, which is applied after the first ply failure due to the pure pressure loading. In case of compression loading under constant pressure, as Figure 37 clearly shows, non-linear analysis predicts more widespread failure compared to the linear analysis unlike the tensile loading under constant pressure.

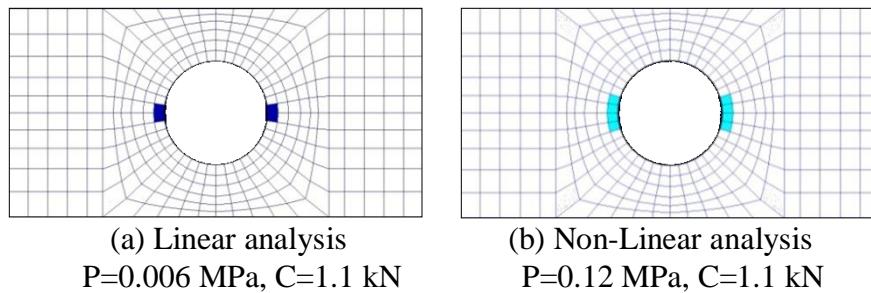


Figure 36: First ply failures; Load case: 4; Failure Theory: Tsai-Wu-Classical; $R=0.001$

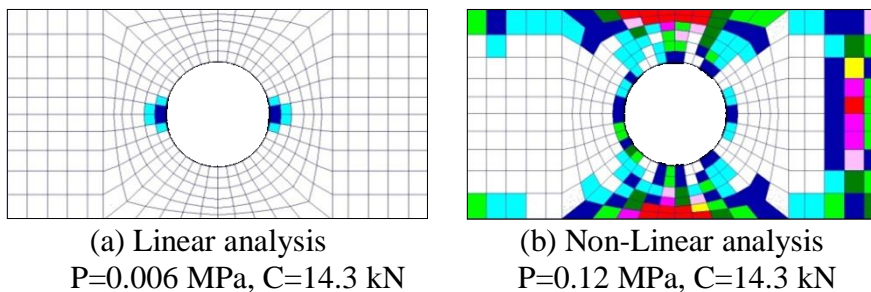


Figure 37: Failure progression; Load case: 4; Failure Theory: Tsai-Wu-Classical; $R=0.001$

Figure 38 shows the failure plots determined by the modified application of the Tsai-Wu failure theory at a compressive load of 11 kN at which the non-linear analysis nearly predicts ultimate failure.

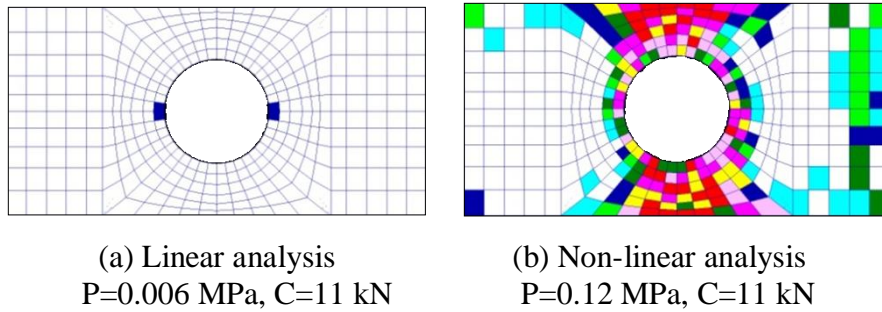


Figure 38: Failure progression; Load case: 4; Failure Theory: Tsai-Wu-Modified;
 $R=0.001$

Comparison of Figure 37(b) and Figure 38(b) shows that for the combined pressure and compression load case, modified application of Tsai-Wu failure theory predicts more failure around the edge of the cut-out compared to the classical application of the Tsai-Wu failure theory in the progressive failure analysis.

To understand the reason for higher failure progression in case of non-linear analysis in load case 4, deformation and stress contour plots of linear and non-linear analysis are compared in Figure 39-Figure 41. For the particular load level, Figure 40 and Figure 41 show the maximum stresses among the 8 layers in the laminate.

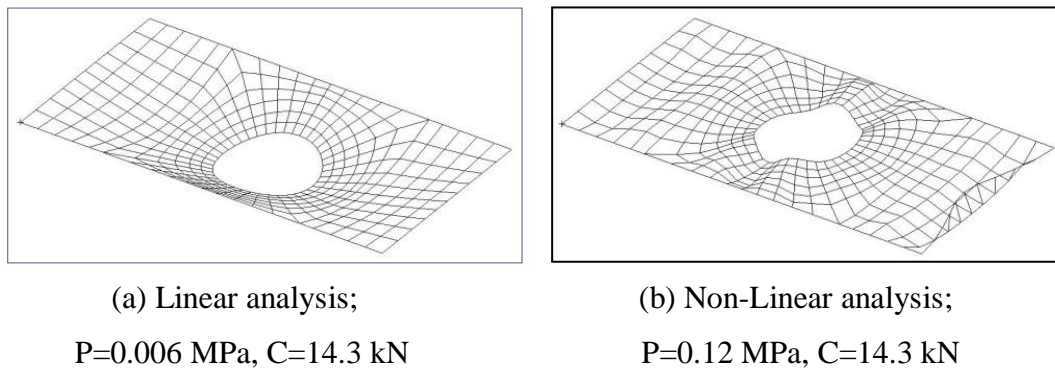
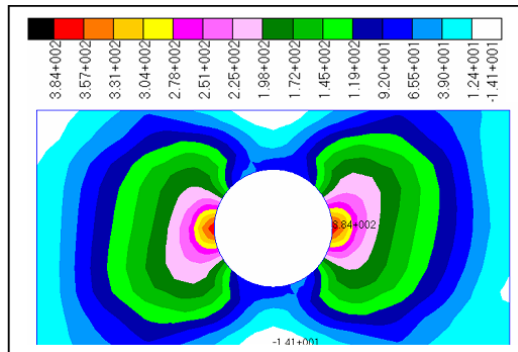
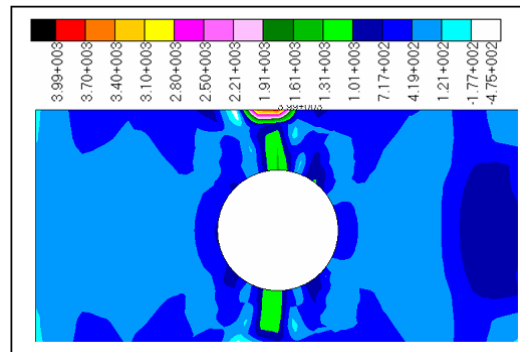


Figure 39: Deformation Plots; Load case: 4; Failure Theory: Tsai-Wu-Classical;
 $R=0.001$

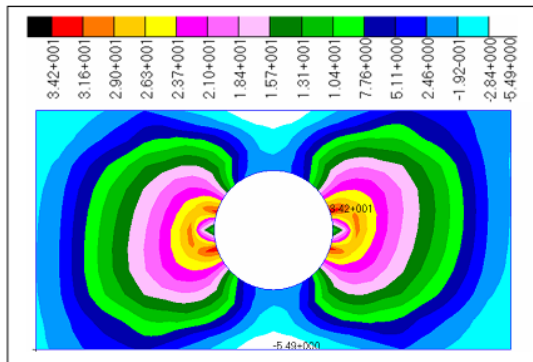


(a) Linear analysis;
 P=0.006 MPa, C=14.3 kN

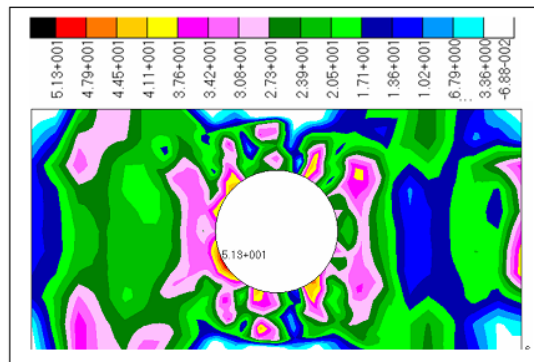


(b) Non-Linear analysis;
 P=0.12 MPa, C=14.3 kN

Figure 40: Maximum σ_1 Stress (MPa); Load case : 4; Failure Theory: Tsai-Wu-Classical; $R=0.001$



(a) Linear analysis;
 P=0.006 MPa, C=14.3 kN



(b) Non-linear analysis;
 P=0.12 MPa, C=14.3 kN

Figure 41: Maximum σ_2 Stress (MPa); Load case: 4; Failure Theory: Tsai-Wu-Classical; $R=0.001$

Figure 39 shows that in case of combined pressure and compression loading, when the compressive load is increased, due to the secondary bending, large deformation effects become more influential and non-linear analysis predicts more realistic deformation, which is evident from the wrinkles that occur in the laminate. Figure 39 shows that

wrinkles, which form in the laminate in the non-linear analysis, are absent in the deformation plot obtained by the linear analysis. As shown in Figure 40 and Figure 41, local bending causes higher stress state in the laminate, and the maximum fiber direction stress (σ_1) and maximum transverse direction stress (σ_2), as well as maximum in-plane shear stress, predicted by the non-linear analysis are significantly higher than the corresponding stresses predicted by the linear analysis. Due to the higher stress state predicted by the non-linear analysis, failure is more spread as shown in Figure 37(b) compared to the failure progression predicted by the linear analysis shown in Figure 37(a). It should be noted that in case of non-linear analysis, when the compressive load is increased after the first ply failure pressure is reached, the laminate also gets compressed in the width (y) direction, because in load case 4 the longer side edges of the laminate are not allowed to move in the width (y) direction. Therefore, as it is seen in Figure 37(b) all plies of the elements, near the intersection of the N-S direction and the longer side edges of the laminate, fail at the particular total compressive load of 14.3 kN which is applied after the first ply failure pressure. Fiber direction stress plot also confirms that the intersection of the N-S direction and the longer side edges of the laminate is the critical region because of the higher fiber direction stress, as evident in Figure 37(b). It is also noted that in case of non-linear analysis, local bending near the right edge of the laminate where the compressive load is applied, causes higher stresses near the right edge compared to the stresses determined by the linear analysis. Therefore failure plot given in Figure 37(b) shows many elements with different number of failed plies near the right edge of the laminate where the in-plane load is applied. Local bending of the laminate, near the edge where the load is applied, is clearly seen in Figure 39(b) which shows that near the right edge, laminate undergoes large rotation which is absent in the linear analysis. It can be concluded that in case of combined pressure and compression loading, linear analysis underestimates the failure state unlike the combined pressure and tensile loading.

In case of combined pressure and compression loading, due to the local bending predicted by the non-linear analysis, simultaneous degradation of the elastic properties, associated with fiber and matrix failures allowed in the modified application of the Tsai-Wu failure theory, is considered to be the main reason for higher dispersion of failure compared to the classical application of the Tsai-Wu failure theory. As shown in Figure 37(b) and Figure 38(b), even at a lower compressive load, modified application of the Tsai-Wu failure theory causes more failure compared to the classical application of the Tsai-Wu failure theory.

Failure progression plots for the combined pressure/compression and combined pressure/tension load cases are compared in Figure 42 and Figure 43, respectively. For the combined pressure and tension case, Figure 42 gives the failure plots at the same load level as the combined pressure and compression load case. Figure 42 and Figure 43 clearly show that due to the secondary bending effect of the compressive load, as well as the non-linear deformation effects which are more pronounced in the combined pressure and compression load case, laminate is more stressed and failure is more spread compared to the state of failure for the combined pressure and tension case. In case of combined pressure and compression, since pressure is allowed to follow deformation, follower load effect due to pressure is also more pronounced compared to the follower load effect due to pressure for the combined pressure and tension case. Figure 42 also shows that under combined pressure and compression, Tsai-Wu failure theory, applied in the classical sense, predicts larger failure progression compared to the Hashin's failure theory. This example shows that the effect of using a particular failure theory on the failure progression is also highly dependent on the load case. Depending on the load case, failure criteria proposed by Hashin and Tsai-Wu may predict similar failure progression, as in combined pressure and tension case, or may predict very different

failure progression, as in combined pressure and compression case.

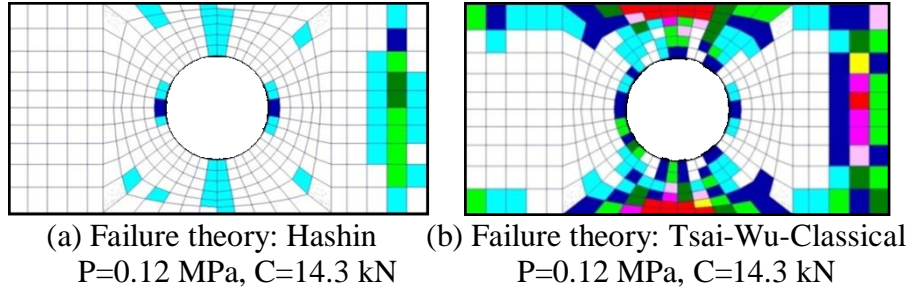


Figure 42: Failure progression; Combined pressure and compression; Non-linear anal.;
 $R=0.001$

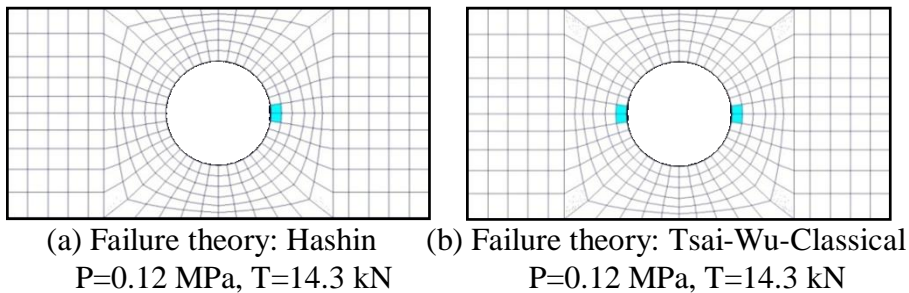


Figure 43: Failure progression; Combined pressure and tension; Non-linear anal.;
 $R=0.001$

5.9 Effect of Degradation Factor on the Failure Progression

As a final case study, the effect of degradation factor on the ultimate failure load is investigated for the pure tensile loading by using gradual degradation. In case of gradual degradation, a degradation factor of "0.5" is used, and plies are allowed to fail repeatedly until the degradation factor becomes "0.001", which is the factor that is used to indicate complete fiber or matrix failure in this study.

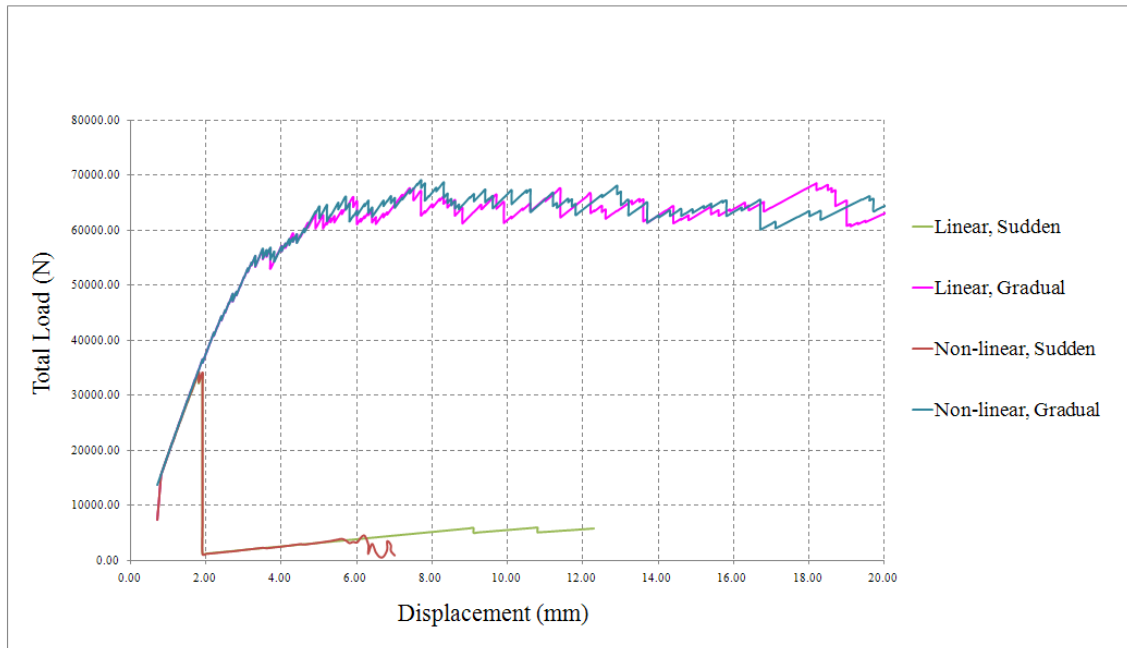


Figure 44: Load/displacement curves of sudden and gradual degradation used linear/non-linear progressive failure analysis

In Figure 44, the comparison of sudden and gradual degradation for linear and non-linear (SOL106) progressive failure analysis is shown. It should be noted that the load displacement curve in Figure 44 is obtained for displacement controlled loading. That is, input displacements are specified at the East edge of the laminate, as shown in Figure 20, and total constraint force, which corresponds to the total load applied, is calculated by the finite element analysis. Since geometric nonlinear effects are negligible for pure tension load case, as mentioned in previous sections, ultimate load values are also close for linear and nonlinear analysis. But, when gradual degradation is used in the progressive failure analysis, a higher ultimate failure load is predicted. For the particular gradual degradation factor of "0.5", ultimate failure load that is predicted is almost twice the ultimate failure load predicted by the progressive failure analysis performed using sudden degradation with a factor of "0.001". This result is in accordance with the

previous studies in the literature, such as the work of Reddy et.al [6]. Higher ultimate load in case of higher degradation factor is reasonable because in case of sudden degradation, elastic constants are reduced to small values irrespective of the damage accumulated. As stated by Reddy et.al [6], the actual size of damage in a ply is usually very small compared to the size of the finite element used. Therefore, sudden material property degradation scheme would be more meaningful to be used with the finite element models which have very fine meshes. Whereas for coarser meshes, the use of sudden degradation would cause higher failure progression, and therefore lower ultimate failure load compared to the use of gradual degradation during the progressive failure analysis.

Also, it can be noticed that for sudden degradation load drop-off occurs after ultimate failure load. However, in gradual degradation, load remains in an interval without dropping off suddenly and laminate continues to elongate substantially in the direction of the loading. It is considered that in gradual degradation the effect of the failure is shared by the elements more homogenously, and instead of a sudden load drop-off, laminate fails at a constant load level by exhibiting excessive deformation as seen in the load displacement curve given in Figure 44. For this reason, in gradual degradation, the ultimate failure load is assumed to have occurred at the load level at which all elements along a line, which divides a structure into two pieces, fail.

Figure 45(a) and (b) show the estimated ultimate failure loads and state of failure at the ultimate failure loads for the sudden and gradual degradation of material properties, respectively.

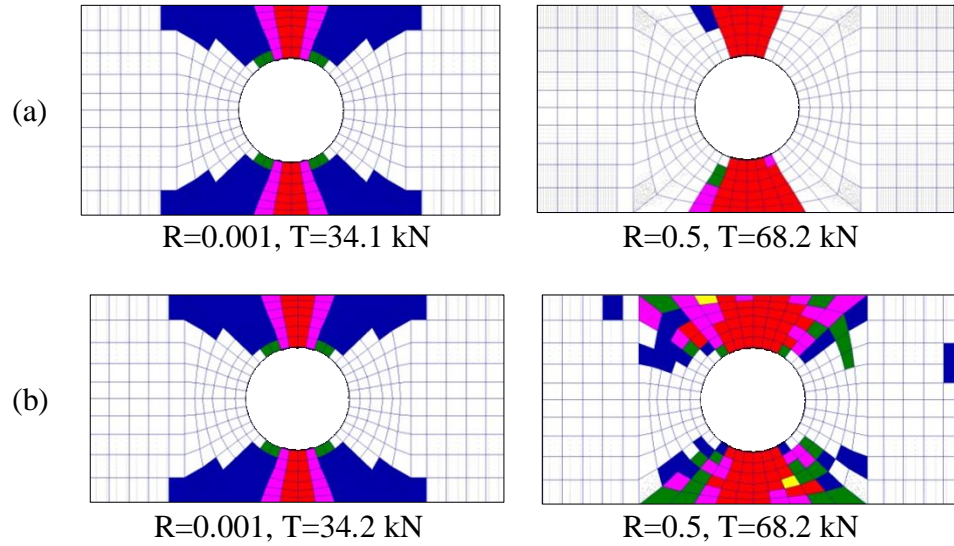


Figure 45: Ultimate failure loads; Load case: 1; (a) Linear analysis (b) Non-linear analysis; Failure theory: Hashin

In the non-linear progressive failure analysis of sudden and gradual degradation, SOL106 (Non-linear Static Analysis) is used. But, when SOL600 (Implicit Non-linear Analysis) is used for same cases; it is observed that higher ultimate loads are predicted as shown in Figure 46. In this case, tension test is assumed to be performed under load control.

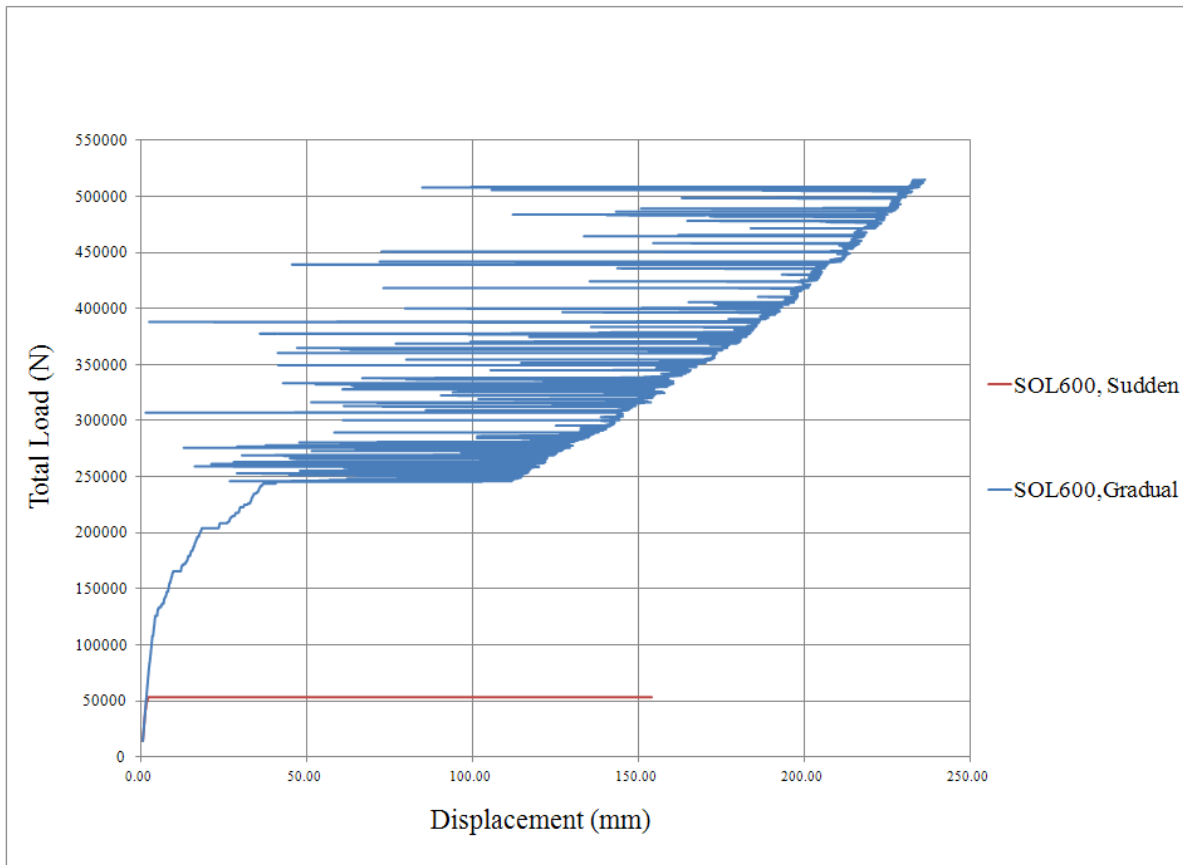


Figure 46: Load/displacement curves of sudden and gradual degradation : SOL600 non-linear progressive failure analysis

When sudden degradation is used in the progressive failure analysis of pure tension case, ultimate failure load is obtained as 53.9 kN by using SOL600 as the non-linear solver. From Figure 46, it can be seen that for load controlled pure tension test, ultimate failure load corresponds to the load at which the East edge of the laminate shows drastic displacement. On the other hand, for gradual degradation, prediction of the ultimate failure load by using the load/displacement curve and failure progression plots is not straightforward. As it is seen in Figure 46, for the gradual degradation case, abrupt change in the displacement of the East edge of the laminate occurs at a load level of

about 250 kN. However at this load level, overall degradation factor for any ply is not lower than "0.001" which is the degradation factor which is assumed to signify complete failure of the ply. Therefore, if complete failure of a ply is assumed to occur when the degradation factor becomes less than "0.001", then one can comment that for the gradual degradation case ultimate load is very high. However, at such high load levels displacement of the laminate is very high, and it is not possible for the laminate to keep its integrity at such high load/displacement levels. Figure 46 shows that even at a load level of 250 kN, the end displacement is about 4 cm which is unrealistically large. It is noted that implicit nonlinear solver of MSC Nastran SOL 600 takes large strain into account unlike SOL 106. Therefore, it is considered that higher ultimate loads predicted by SOL 600 could be due to the large strain formulation that is included in the analysis. Considering the variation of ultimate loads predicted by different non-linear solution types of MSC Nastran, it can be concluded that large strain effect may be important on the ultimate load levels, especially when there are highly distorted elements due to the large deformation of the laminate during the progressive failure analysis. As a final note, it is recommended that different non-linear finite element solvers be employed to check the progressive failure analysis results of the present study using gradual degradation of material properties. In addition, it is highly recommended that tests be performed to verify ultimate failure loads, and decide on the best degradation methodology to be used in progressive failure analysis.

CHAPTER 6

CONCLUSIONS AND FUTURE WORKS

In this thesis, a PCL code is developed which has the capability of performing progressive failure analysis of composite structures under combined in-plane and out-of-plane loadings, using linear and non-linear solution types of MSC Nastran. With the developed code, comparative study of linear and geometrically non-linear progressive failure analysis of composite structures is performed. As the sample structure, a composite laminate with a central cut-out is taken, and progressive failure analysis of the laminate is conducted by employing different solution types, failure criteria, material property degradation schemes, and different combination of in-plane and out-of-plane loads. It is noted that in most of the previous studies on progressive failure analysis of composites, single load case is used. Progressive failure analysis of composites under combined loads is particularly important for thin walled aerospace structures which are usually subjected to combined in-plane and out-of-plane loads. A major objective of the present study was to investigate the significance of geometrically non-linear analysis on the progressive failure response of composite laminates under combined in-plane and out-of-plane loading. For this purpose, different ply and constituent based failure criteria and material property degradation schemes have been coded into a PCL code in MSC Nastran. During the progressive failure analysis, failure is progressed by employing material property degradation factor, which can be adjusted to allow any level of degradation of material properties, such as sudden or gradual, upon the prediction of failure in a ply. The developed code is verified by comparing the results of the code it against the hand calculation based results obtained by the Classical Lamination Theory and previous experimental results in the literature. Mesh sensitivity is checked by

comparing the first ply failure and ultimate failure predicted by the use of different mesh densities, and the most appropriate finite element model is used for the comparison of different case studies. For mode independent failure criteria, a method is proposed for the determination of separate degradation factors associated with fiber and matrix failures which are assumed to occur simultaneously. The proposed method is demonstrated on the failure theory proposed by Tsai-Wu.

Based on the results of these progressive failure analyses, the following main conclusions are drawn:

- Under combined pressure and tensile loading, for constant pressure levels just sufficient for the first ply failure of the laminate and gradual tensile loading after the first ply failure, linear analysis highly overestimates the state of failure in the laminate.
- Combined pressure and compression loading causes higher failure progression compared to combined pressure and tension loading, due to the secondary bending effect of the compressive load, as well as the non-linear deformation effects which are more pronounced in the combined pressure and compression load case.
- The effect of using a particular failure theory on the failure progression is highly dependent on the load case. Depending on the load case, failure criteria proposed by Hashin and Tsai-Wu may predict similar failure progression, as in combined pressure and tension case, or may predict very different failure progression, as in combined pressure and compression case.

- In the modified application of the Tsai-Wu failure criterion, when failure is predicted in a ply, both fiber and matrix properties are degraded simultaneously but with degradation factors greater than the initially selected degradation factor R . Therefore, in a way modified application of the Tsai-Wu failure criterion leads to somewhat gradual degradation in the progressive failure analysis. However, since simultaneous degradation of the elastic properties associated with fiber and matrix failures is allowed, failure is more dispersed in a ply. Therefore, it is deemed that modified application of the Tsai-Wu failure criterion represents the state of failure in the laminate better, compared to the classical application of the Tsai-Wu failure criterion in the progressive failure analysis.
- For the combined pressure and compression loading, due to the local bending effect predicted by the non-linear analysis, simultaneous degradation of the elastic properties, associated with fiber and matrix failures allowed in the modified application of the Tsai-Wu failure theory, causes higher dispersion of failure compared to the classical application of the Tsai-Wu failure theory in the progressive failure analysis.
- Progressive failure analysis with gradual degradation of material properties results in higher ultimate loads compared to the using sudden degradation. Depending on the finite element mesh size, the degradation factor must be selected accordingly in order to reflect the true failure progression behavior more closely. It is recommended that different non-linear finite element solvers be employed to check the progressive failure analysis results of the present study using gradual degradation of material properties. In addition, it is highly recommended that tests be performed to verify ultimate failure loads and decide on the best degradation methodology to be used in progressive failure analysis.

- Under combined out-of-plane and in-plane loading, linear analysis can significantly overestimate the failure progression, as in combined pressure and tension case, or underestimate the failure progression, as in combined pressure and compression case, compared to geometrically non-linear analysis.

In the current methodology, only intra-laminar failures are considered. The present work can be extended to the inter-laminar failures by employing an appropriate polynomial failure equation. This way, delamination can also be predicted by including the interlaminar stresses in the failure equation. Upon the prediction of delamination, out-of-plane elastic constants would be degraded such that the out-of-plane stresses are reduced to very low values. Such an extension of the present work would be very valuable since interlaminar failures are very critical in laminated composite structures.

In the present study, for mode independent failure criteria, a method is proposed for the determination of separate degradation factors for fiber and matrix failures which are assumed to occur simultaneously. More case studies should be performed using the proposed method of material property degradation to substantiate its use in the progressive failure analysis. In this respect, more experimental studies have to be performed to predict ultimate failure loads of composite laminates. A rigorous method has to be devised to determine the separate degradation factors associated with fiber and matrix failures which are assumed to occur simultaneously. If more experimental results are available, fiber and matrix degradation factors can be tuned such that the results of the progressive failure analyses match with the experimental results more closely.

More study has to be conducted on the use of degradation method such as sudden or gradual degradation. The effect of using different degradation strategy has to be evaluated by comparing the failure predictions of progressive failure analysis with the

experimental results. It is considered that if more experimental results are available, then degradation scheme can be tuned so that failure predictions of progressive failure analyses are more reliable. Therefore, it is imperative that more experimental work on the failure of composite laminates under combined in-plane and out-of-plane loading has to be conducted in the future.

REFERENCES

- [1] M. J. Hinton, A.S. Kaddour and P.D. Soden. A further assessment of the predictive capabilities of current failure theories for composite laminates: comparison with experimental evidence, *Composite Science and Technology*, 64(3-4), 549-588 (2004).
- [2] U. Icardi, S. Locatto and A. Longo. Assessment of recent theories for predicting failures of composite laminates, *Appl. Mech. Rev.*, 60(2), 76-86 (2007).
- [3] F.K. Chang and K.Y. Chang. A Progressive damage model for laminated composites containing stress concentrations, *Journal of Composite Materials*, 21, 834-855 (1987).
- [4] S. Tolson and N. Zabaras. Finite element analysis of progressive failure in laminated composite plates, *Computers and Structures*, 38(3), 361-376 (1991).
- [5] Y.S. Reddy and J.N. Reddy. Linear and non-linear failure analysis of composite laminates with transverse shear, *Composites Science and Technology*, 44, 227-255 (1992).
- [6] Y.S.N. Reddy, C.M.D. Moorthy and J.N. Reddy. Non-linear progressive failure analysis of laminated composite plates, *Int. J. Non-Linear Mechanics*, 30(5), 629-649 (1995).
- [7] D.W. Sleight. Progressive failure analysis methodology for laminated composite structures, NASA/TP-1999-209107 (1999).
- [8] S. Basu, A.M. Waas and D.R. Ambur. Prediction of progressive failure in multidirectional composite laminated panels, *International Journal of Solids and Structures*, 44(9), 2648-2676 (2007).
- [9] T.E. Tay, G.Liu, V.B.C. Tan, X.S. Sun and D.C. Pham. Progressive failure analysis of composites, *Journal of Composite Materials*, 42(18), 1921-1966 (2008).

- [10] M.R. Garnish and V.M.K. Akula. Review of degradation models for progressive failure analysis of fiber reinforced composites, *Applied Mechanics Reviews*, 62, 1-33 (2009).
- [11] MSC. Software, PCL and Customization Guide (2005).
- [12] Z. Hashin. Failure criteria for unidirectional fiber composites, *Journal of Applied Mechanics*, 47, 329-334 (1980).
- [13] S.W. Tsai. A General theory of strength for anisotropic materials, *Journal of Composite Materials*, 5(1), 58-80 (1971).
- [14] MSC. Software, Document Library (2005).
- [15] R. M. Jones, *Mechanics of Composite Materials*, 2nd Ed., Taylor and Francis Inc., Philadelphia (1999).
- [16] M. N. Nahas, Survey of Failure and Post-Failure Theories of Laminated Fiber-Reinforced Plastics and Composites, *Journal of Composite Technology and Research*, 8(4), 138-153 (1986).
- [17] C. S. Lopes, Z. Gurdal, P. P. Camanho and B.F. Tatting. Progressive Failure Analysis of Tow-Placed Variable-Stiffness Composite Panels, *International Journal of Solid and Structures*, 44, 8493-8516 (2007).
- [18] J. D. Lee. Three Dimensional Finite Element Analysis of Damage Accumulation in Composite Laminate, *Computers and Structures*, 15(3), 335-350 (1982).
- [19] S.C. Tan. A Progressive Failure Model for Composite Laminates Containing Openings, *Journal of Composite Materials*, 25(5), 556-577 (1991).
- [20] Z.G. Apalak, M.K. Apalak and M.S. Genc. Progressive Damage Modeling of an Adhesively Bonded Composite Single Lap Joint Under Flexural Loads at the Mesoscale Level, *Journal of Reinforced Plastics and Composites*, 26(9), 903-953 (2007).
- [21] A. D. Crocombe. How to tackle non-linear finite element analysis, NAFEMS Ltd. (2001).

- [22] O.O. Ochoa and J.N. Reddy. Finite Element Analysis of Composite Laminates, 1st Ed., Kluwer Academic Publishers, Netherlands (1992).
- [23] MSC Software, PCL Reference Manual Code Examples (2005).
- [24] MSC Software, Nastran Preference Guide (2010).
- [25] MSC Software, Nastran Implicit Nonlinear (SOL600) User's Guide (2010).
- [26] MSC Software, Nastran Quick Reference Guide (2010).
- [27] Z. Hashin and A. Rotem. A Fatigue Failure Criterion for Fiber Reinforced Materials, Journal of Composite Materials, 7, 448-464 (1973).
- [28] R.M. Christensen. Tensor Transformations and Failure Criteria for the Analysis of Fiber Composite Materials, Journal of Composite Materials, 22, 874-897 (1988).
- [29] J.D. Lee. Three Dimensional Finite Element Analysis of Damage Accumulation in Composite Laminate, Computers and Structures, 15, 335-350 (1982).
- [30] S.W. Tsai. Strength Characteristics of Composite Materials, NASA CR-224 (1965).
- [31] R. Hill. A Theory of Yielding and Plastic Flow of Anisotropic Metals, Proceedings of the Royal society of London, A (193), 281-297 (1948).
- [32] O. Hoffman. The Brittle Strength of Orthotropic Materials, Journal of Composite Materials, 1, 200-206 (1967).

APPENDIX A

PCL CODE

PCL is a command language which is used for creating functions, applications, graphics and user interfaces in MSC Patran. It has a similar code structure as in Fortran or C but also there are specific function commands enables to use MSC Patran abilities. By embedding specific function commands in developed code structure with the help of control statements, variables, operators, any operation can be performed within possibilities of MSC Patran.

The most commonly used expressions used in the developed progressive failure analysis PCL code are explained below. For basic PCL examples, these expressions can be employed. However, for further information PCL customization and code example documents of MSC Software should be referenced [11][23] .

A1.Data Types

The type, scope and dimension of the variables used in code must be declared before. Real, integer and string type variables are frequently employed in PCL codes.

A1.1 Real

A real variable is defined by adding “REAL” keyword in front of the variable name as:

REAL x, y, diameter

Real constants must have at least one digit before and after the decimal point and also plus or minus sign may be used optionally.

x = 1200.5

A1.2 Integer

An integer variable is defined by adding “INTEGER” keyword in front of the variable name as:

INTEGER a, b, element_id

Integer constants don't have fractional part. In other words there is no digit after the decimal point. Similar to the real variables, plus or minus sign may be used for integers optionally.

element_id = 10

A1.3 String

A string variable is defined by adding “STRING” keyword in front of the variable name and maximum string length as a positive integer within square brackets after variable name as:

STRING name [20], data_type [10]

A character string consists of double quotes and a string of characters. While defining a string, the maximum string length should be defined by taking into consideration the probable length of the string. An example for a string constant is shown below.

name = "murat"

A2.Arrays

Any data type can be represented in an array due to the needs while constructing a code structure. Array size can be declared at the beginning or by use of virtual arrays an infinite sized array can be employed. Array definition is made by declaring any number of subscripts in parentheses separated by commas, after the variable type identifier. Figure A1 explains the array definition for an integer array "I" which has 3 rows and 5 columns.

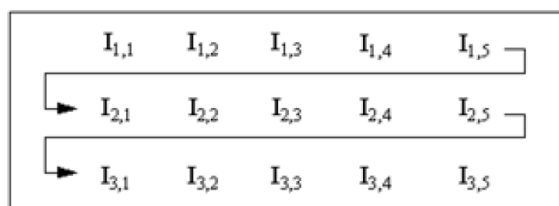


Figure A1: Integer array, INTEGER I (3, 5)

Instead of directly allocated array, if it is not possible to estimate the array size, virtual arrays can be used by using keyword "VIRTUAL" in place of subscripts as follow;

REAL mydata (VIRTUAL)

Also post-allocation may be performed to specify upper and lower bounds by using `SYS_ALLOCATE_ARRAY` command.

A3.Operators

In Table A1: Basic operators used in PCL, operators used for basic operations in PCL are shown. By employing these operators with variables, constants, specific functions and expressions can be built for the purpose of performing PCL runs. Detailed information about the operator usage can also be obtained from PCL customization document [11].

Table A1: Basic operators used in PCL

| Operators | | | | | | Definitions |
|-----------|----|----|----|----|----|----------------------------------|
| + | - | | | | | Unary Plus or Minus, Logical Not |
| ** | | | | | | Exponentiation |
| * | / | | | | | Multiplication and Division |
| + | - | | | | | Addition and Subtraction |
| // | | | | | | String Concatenation |
| < | > | <= | >= | == | != | Relational Operators |
| | && | | | | | Logical Or, Logical And |
| += | -= | = | | | | Increment, Decrement, Assignment |

A4.Control Statements

A4.1 Simple If Then

The simple “IF” statement is shown below. The logical expression in the parenthesis is checked by “IF” and if the answer is true than statement begin with “THEN” is performed. If the answer is false then no operation is done.

IF (logical expression) THEN statement

A4.2 If Then Else

Similar to “*Simple If Then*”, logical expression is checked by “IF” and then if answer is true than statements are executed and then skipped to look at “END IF” clause. But answer is false then other logical expressions given in “ELSE IF” clause are controlled. If again all answers are false then code skips to “ELSE” and executes defined statements under “ELSE”.

IF (logical expression) THEN

statements...

ELSE IF (logical expression) THEN

statements...

ELSE

statements...

END IF

A4.3 For

The “FOR” statement is used to create loops.. It starts by assigning the first numeric value to the variable. Then it performs the defined statements between “FOR” and “END FOR”. For the interval declared in the parenthesis following “FOR”, it repeats the same procedure.

```
FOR (variable=numeric expression TO numeric expression)  
statements...  
END FOR
```

A4.4 Repeat

The “REPEAT” statement repeats the defined statements up to the “UNTIL” clause. If the answer of logical expression stated after “UNTIL” is false, then performed statements are repeated again. If the answer is true, then “REPEAT” loop is finished.

```
REPEAT  
statements...  
UNTIL (logical expression)
```

A4.5 Break and Continue

“BREAK” and “CONTINUE” statements are only used within “FOR” or “REPEAT” statements. If “BREAK” statement is used, then code skips to the “END” statement, and

terminates the loop. On the other hand, if “CONTINUE” statement is used then loop continues to repeat until the current code block is finished.

```
FOR  
IF (logical expression) THEN  
BREAK           -----  
END IF  
END FOR   ←-----
```

```
FOR  
IF (logical expression) THEN  
CONTINUE       -----  
END IF       ←-----  
END FOR
```

A5. PCL Structure

PCL code starts with the “FUNCTION” and end with “END FUNCTION” keywords. Between these keywords, there needs to be declarations, statements and specific commands. Also after the “FUNCTION” keyword, the name of the current function should be specified. A simple PCL code structure is shown as follows;

```
FUNCTION fname  
declarations...  
statements...  
(and/or)  
END FUNCTION
```

A6. Running PCL

For running a prepared PCL code in the MSC Patran interface, user should embed and run the PCL code by using command line. If any error is detected during embedding or running process, MSC Patran gives the causes of these errors in same command line. Besides, the operations done by PCL code are written and saved in session files, so execution of the code can also be followed from updated session files.

For embedding and running the PCL code, firstly the related PCL files should be placed in working directory of MSC Patran. And then following keywords is entered in command line, respectively.

```
!! INPUT filename.pcl  
fname()
```

A7. PCL Example

In this section, developed PCL code for the purpose of performing progressive failure analysis is presented. For the gradual tensile load under constant pressure, by using SOL600 as nonlinear solution, 0.001 as degradation factor for sudden degradation and Hashin as failure theory, the defined laminate is analyzed with the help of presented code.

FUNCTION code()

\$ Input laminate and finite element model properties are recognized and assigned to variables-----

INTEGER v,mat,e,chan

REAL

a,l,t,o,s,ply,e1(VIRTUAL),e2(VIRTUAL),poisson12(VIRTUAL),s12(VIRTUAL),s23(VIRTUAL),s13(VIRTUAL)

db_count_materials(mat)

db_count_elems(e)

db_get_matl_prop_value2(mat,40,a,l,t,o,s,v,ply)

dump ply

dump mat

\$Distinct material properties are created for the each ply of the each element-----

INTEGER counto,plyids(VIRTUAL),symmetry,ar,el

REAL thick(VIRTUAL),orient(VIRTUAL),off

STRING

mat_name[40],thick2[90](VIRTUAL),orient2[90](VIRTUAL),e_1[90](VIRTUAL),e_2[90](VIRTUAL) @
,poisson_12[90](VIRTUAL),s_12[90](VIRTUAL),s_23[90](VIRTUAL),s_13[90](VIRTUAL)

LOGICAL flag

sys_allocate_array(thick,1,ply)

sys_allocate_array(orient,1,ply)

sys_allocate_array(plyids,1,ply)

db_get_comp_lam_ids_by_id(mat,40,mat_name,counto,plyids,thick,orient,symmetry,off,flag)

sys_allocate_array(thick2,1,ply)

sys_allocate_array(orient2,1,ply)

FOR (ar=1 TO ply)

thick2(ar)="//str_from_real(thick(ar))

orient2(ar)="//str_from_real(orient(ar))

END FOR

```
sys_allocate_array(e1,1,ply)
sys_allocate_array(e2,1,ply)
sys_allocate_array(poisson12,1,ply)
sys_allocate_array(s12,1,ply)
sys_allocate_array(s23,1,ply)
sys_allocate_array(s13,1,ply)
sys_allocate_array(e_1,1,ply)
sys_allocate_array(e_2,1,ply)
sys_allocate_array(poisson_12,1,ply)
sys_allocate_array(s_12,1,ply)
sys_allocate_array(s_23,1,ply)
sys_allocate_array(s_13,1,ply)
```

FOR (e1=1 TO ply)

```
db_get_matl_prop_value2(plyids(e1),2,a,l,t,o,s,v,e1(e1))
db_get_matl_prop_value2(plyids(e1),3,a,l,t,o,s,v,e2(e1))
db_get_matl_prop_value2(plyids(e1),5,a,l,t,o,s,v,poisson12(e1))
db_get_matl_prop_value2(plyids(e1),8,a,l,t,o,s,v,s12(e1))
db_get_matl_prop_value2(plyids(e1),9,a,l,t,o,s,v,s23(e1))
db_get_matl_prop_value2(plyids(e1),10,a,l,t,o,s,v,s13(e1))
```

```
e_1(e1)=""//str_from_real( e1(e1) )
e_2(e1)=""//str_from_real( e2(e1) )
poisson_12(e1)=""//str_from_real( poisson12(e1) )
s_12(e1)=""//str_from_real( s12(e1) )
S_23(e1)=""//str_from_real( s23(e1) )
s_13(e1)=""//str_from_real( s13(e1) )
```

END FOR

INTEGER z,w

```
STRING name[40],name2[40],name3[40],name4[40],name5[90],stack[90](VIRTUAL)
@
,sequence[90](VIRTUAL),proparray[90](5),name6[90],stiff[90](7)
```

```
sys_allocate_array(stack,1,ply)
sys_allocate_array(sequence,1,ply)
```

```

FOR ( w=1 TO ply )

FOR ( z=1 TO e )

name="mat_"//str_from_integer( w )//"_ " //str_from_integer( z )

stiff(1)=e_1(w)
stiff(2)=e_2(w)
stiff(3)=poisson_12(w)
stiff(4)=s_12(w)
stiff(5)=s_23(w)
stiff(6)=s_13(w)
stiff(7)=" "

ui_answer_message (28003218, "YES")
material.create( "Analysis code ID", 1, "Analysis type ID", 1, name, @
0,"Date: 01-May-11 Time: 14:36:41", "2d Orthotropic", 5, "Directionality", @
4, "Linearity", 1, "Homogeneous", 0, "Linear Elastic", 1, @
"Model Options & IDs", ["" , "" , "" , "" , ""],[0, 0, 0, 0, 0], "Active Flag", @
1, "Create", 10, "External Flag", FALSE, "Property IDs", ["Elastic Modulus 11",
"Elastic Modulus 22", "Poisson Ratio 12", "Shear Modulus 12", "Shear Modulus 23",
"Shear Modulus 13"], [2, 3, 5, 8, 9, 10, 0], "Property Values", stiff )
ui_answer_message (28003218, "YES")

END FOR
ui_answer_message (28003218, "YES")
END FOR
ui_answer_message (28003218, "YES")

FOR ( z=1 TO e )
FOR (w=1 TO ply)
name5="mat_"//str_from_integer( w )//"_ " //str_from_integer( z )
stack(w) = name5
sequence(w)= ""//str_from_integer( w )
END FOR

name2="laminate_"//str_from_integer( z )

mat_create_lam3( name2, "" , 1, stack , thick2, orient2, sequence, counto, "" , "Create" )
name6="m:laminate_"//str_from_integer( z )

```

```

proparray(1)=name6
proparray(2)="Coord 0"
proparray(3)=""
proparray(4)=""
proparray(5)=""
name3="composite_ "//str_from_integer( z )
name4="Elm"//" "//str_from_integer( z )
ui_answer_message (29002020, "YESFORALL")
elementprops_create( name3, 51, 25, 35, 1, 3, 20, [13, 20, 4037, 4111, 4213] @
, [5, 9, 1, 1, 4], proparray, name4 )
END FOR

```

\$Loading and solution parameters are defined -----

```

STRING loop[10], force[20](4)
REAL i
INTEGER n,c
n=0
c=0
i=100.0
REPEAT
virtual_open_scratch(chan)
IF ( c ==1 ) THEN
i+=100.0
force(1)="<"//str_from_real( i)//", 0., 0.>"
force(2)=""
force(3)=""
force(4)=""
loadsbc_modify2( "tension", "tension", "Force", "Nodal", "", "Static", ["Node 1:6
37:41"], "FEM", "Coord 0", "1.", force, [ "", "", "", "" ] )
END IF
c=1
n+=1
loop="analiz"//str_from_integer( n )
ui_answer_message (6022070 , "YES")
mscnastran_subcase.create( "600", "LC_2T", "This is a default subcase." )
mscnastran_subcase.create_char_param( "LOAD CASE", "LC_2T" )
mscnastran_subcase.create_char_param( "SUBCASE TITLE", @
"This is a default subcase." )
mscnastran_subcase.create_char_param( "SUBCASE SUBTITLE", "LC_2T" )
mscnastran_subcase.create_char_param( "SUBCASE LABEL", "" )

```

```

mscnastran_subcase.create_char_param( "SUBCASE TITLE FLAG", "ON" )
mscnastran_subcase.create_char_param( "SUBCASE SUBTITLE FLAG", "OFF" )
mscnastran_subcase.create_char_param( "SUBCASE LABEL FLAG", "OFF" )
mscnastran_subcase.create_int_param( "RESULTS INTERVALS", 2 )
mscnastran_subcase.create_char_param( "ECHO MARC INPUT FILE", "ON" )
mscnastran_subcase.create_char_param( "RESULTS IN MARC PRINT FILE", "OFF" )
mscnastran_subcase.create_char_param( "DISPLACEMENTS", "1" )
mscnastran_subcase.create_char_param( "DISPLACEMENTS 1", @
"DISPLACEMENT(SORT1,REAL)=0" )
mscnastran_subcase.create_char_param( "ELEMENT STRESSES", "1" )
mscnastran_subcase.create_char_param( "ELEMENT STRESSES 1", @
"STRESS(SORT1,REAL,VONMISES,BILIN)=0;PARAM,NOCOMPS,1" )
mscnastran_subcase.create_char_param( "CONSTRAINT FORCES", "1" )
mscnastran_subcase.create_char_param( "CONSTRAINT FORCES 1", @
"SPCFORCES(SORT1,REAL)=0" )
mscnastran_subcase.create_char_param( "INTERMEDIATE OUTPUT OPTION", "No"
)
mscnastran_subcase.create_int_param( "INTEGRATION PTS", 5 )
mscnastran_subcase.create_char_param( "STRAIN, PLASTIC COMPONENTS (321)",
"ON" )
mscnastran_subcase.create_char_param( "STRESS, CAUCHY COMPONENTS (341)",
"ON" )
mscnastran_subcase.create_char_param( "SHELL LAYER OUTPUT REQUESTS", "" )
mscnastran_subcase.create_char_param( "MARC Nodal POST CODE Defaults", "ON"
)
mscnastran_subcase.create_char_param( "SUBCASE WRITE", "ON" )
mscnastran_subcase.create_char_param( "SUBCASE DIRECT TEXT POS", "OFF" )
mscnastran_subcase.create_int_param( "SUBCASE INPUT 0", 0 )
mscnastran_subcase.create_char_param( "ADVANCED ANALYSIS TYPE", "NL
STATIC" )
mscnastran_subcase.create_char_param( "SOLUTION TYPE", "NONLINEAR
STATIC" )
mscnastran_subcase.create_char_param( "GEOMETRIC", @
"Large Displacement/Large Strains" )
mscnastran_subcase.create_char_param( "LOADS FOLLOW", "STIFFNESS" )
mscnastran_subcase.create_char_param( "INCREMENT TYPE CODE", "FXDSTAT" )
mscnastran_subcase.create_char_param( "INCREMENT TYPE", "Fixed" )
mscnastran_subcase.create_int_param( "INCREMENTS", 10 )
mscnastran_subcase.create_char_param( "DEACTIVATE OPTION", "Manual" )

ui_answer_message (6022037 , "YES")

```

```

jobfile.open( loop, "ANALYZE NO JOBFILE" )
msc_delete_old_files( loop, ".bdf", ".op2" )
jobfile.write_spl( "/* Jobfile for PATNAS created %A% at %A% */", ["16-Apr-11" @
, "17:10:24"] )
jobfile.writec( "", "TRANSLATOR = pat3nas" )
jobfile.writec( "DATABASE", "E:\calisma\3103_3d.db" )
jobfile.writec( "JOBNAME", loop )
jobfile.writec( "ANALYSIS TITLE", "MSC.Nastran job created on 12-Apr-11 at" // @
" 20:40:26" )
jobfile.writec( "ANALYSIS SUBTITLE", "" )
jobfile.writec( "ANALYSIS LABEL", "" )
jobfile.writec( "", "" )
jobfile.writec( "OBJECT", "Entire Model" )
jobfile.writec( "METHOD", "Full Run" )
jobfile.writec( "", "" )
jobfile.writec( "MODEL SUFFIX", ".bdf" )
jobfile.writec( "RESULTS SUFFIX", ".op2" )
jobfile.writec( "", "" )
jobfile.writec( "", "/*" )
jobfile.writec( "", " * File Search Path Declaration" )
jobfile.writec( "", " */" )
jobfile.writec( "", "" )
jobfile.writec( "File Search Path",
"E:\MSC.Software\Patran\2008_r2\shareware\msc\unsupported\utilities\extra_files" )
jobfile.writec( "File Search Path",
"E:\MSC.Software\Patran\2008_r2\shareware\msc\unsupported\utilities\plb" )
jobfile.writec( "File Search Path",
"E:\MSC.Software\Patran\2008_r2\shareware\msc\unsupported\utilities\icons" )
jobfile.writec( "File Search Path", "E:\Documents and Settings\murat gunel" )
jobfile.writec( "File Search Path", "E:\MSC.Software\Patran\2008_r2" )
jobfile.writec( "File Search Path", "E:\MSC.Software\Patran\2008_r2\helpfiles" )
jobfile.writec( "File Search Path", "E:\MSC.Software\Patran\2008_r2\alters" )
jobfile.writec( "File Search Path", "E:\MSC.Software\Patran\2008_r2\icons" )
jobfile.writec( "File Search Path", "E:\MSC.Software\Patran\2008_r2\bin" )
jobfile.writec( "File Search Path", "E:\MSC.Software\Patran\2008_r2\bin\exe" )
jobfile.writec( "File Search Path", "E:\Documents and Settings\murat gunel" )
jobfile.writec( "File Search Path",
"E:\MSC.Software\Patran\2008_r2\mscprocor_files\dmap" )
jobfile.writec( "File Search Path",
"E:\MSC.Software\Patran\2008_r2\mscprocor_files\plb" )

```

```

jobfile.writec( "File Search Path",
"E:\MSC.Software\Patran\2008_r2\mscprocor_files\lib" )
jobfile.writec( "File Search Path",
"E:\MSC.Software\Patran\2008_r2\mscprocor_files\icons" )
jobfile.writec( "File Search Path", "E:\MSC.Software\Patran\2008_r2\mscexplore_files\"
)
jobfile.writec( "File Search Path",
"E:\MSC.Software\Patran\2008_r2\shareware\msc\unsupported\utilities\icons" )
jobfile.writec( "File Search Path",
"E:\MSC.Software\Patran\2008_r2\shareware\msc\unsupported\utilities\plb" )
jobfile.writec( "File Search Path",
"E:\MSC.Software\Patran\2008_r2\shareware\msc\unsupported\utilities\extra_files" )
jobfile.writec( "", "" )
jobfile.writec( "", "/*" )
jobfile.writec( "", " * Translation Parameters" )
jobfile.writec( "", " */" )
jobfile.writec( "", "" )
$# STRING [3] = "600"
jobfile.writec( "DATA OUTPUT", "OP2" )
jobfile.writec( "OUTPUT2 REQUESTS", "P3 Built In" )
jobfile.writec( "OUTPUT2 FORMAT", "Binary" )
jobfile.writec( "DIVISION TOLERANCE", "1.0e-08" )
jobfile.writec( "NUMERICAL TOLERANCE", "1.0e-04" )
jobfile.writec( "WRITING TOLERANCE", "1.0e-21" )
jobfile.writec( "GEOM CHECK", "INFORM" )
jobfile.writec( "SORTED BULK", "NO" )
jobfile.writec( "CARD FORMAT", "either" )
jobfile.writec( "NODE COORDINATES", "reference frame" )
jobfile.writec( "COORD COORDINATES", "global" )
jobfile.writec( "MSC.Nastran VERSION", "2008." )
jobfile.writec( "WRITE STORED PRECISION", "FALSE" )
jobfile.writec( "PROPS ON ELEM ENTRY", "FALSE" )
jobfile.writec( "CONTINUATION ENTRY", "FALSE" )
jobfile.writec( "PCOMPG ENTRY", "FALSE" )
jobfile.writec( "CONVERT CBAR CBEAM", "FALSE" )
jobfile.writec( "ITERATIVE SOLVER", "FALSE" )
jobfile.writec( "MODEL TOLERANCE", "0.0049999999" )
jobfile.writec( "ELEMENT PROPERTY OFFSET", "0" )
jobfile.writec( "MATERIAL PROPERTY OFFSET", "0" )
jobfile.writec( "TABLE OFFSET", "0" )
jobfile.writec( "LOAD SET OFFSET", "0" )

```

```

jobfile.writec( "LOAD CASE OFFSET", "0" )
jobfile.writec( "CONTROL SET OFFSET", "0" )
jobfile.writec( "RIGID ELEMENT OFFSET", "0" )
jobfile.writec( "SCALAR POINT OFFSET", "0" )
jobfile.writec( "BEGINNING CONTINUATION MARKER", "+ A" )
jobfile.writec( "NUMBER ONLY", "ON" )
jobfile.writec( "BEGINNING NUMBER", "OFF" )
jobfile.writec( "TRAILING NUMBER", "OFF" )
jobfile.writec( "SYNTAX NUMBER", "ON" )
jobfile.writec( "SYNTAX MARKER", "." )
jobfile.writec( "EXTERNAL SUPERELEMENT METHOD", "NONE" )
jobfile.writec( "", "" )
jobfile.writec( "", "/*" )
jobfile.writec( "", " * Solution Parameters" )
jobfile.writec( "", " */" )
jobfile.writec( "", "" )
jobfile.writec( "SOLUTION TYPE", "IMPLICIT NONLINEAR" )
jobfile.writei( "SOLUTION SEQUENCE", 600 )
jobfile.writec( "MASS CALCULATION", "" )
jobfile.writec( "DATA DECK ECHO", "" )
jobfile.writec( "PLATE RZ STIFFNESS FACTOR", "" )
jobfile.writec( "MAXIMUM PRINTED LINES", "" )
jobfile.writec( "MAXIMUM RUN TIME", "" )
jobfile.writec( "WT-MASS CONVERSION", "" )
jobfile.writec( "NODE ID FOR WT-GENER", "" )
jobfile.writec( "RIGID ELEMENT TYPE", "" )
jobfile.writec( "USE XDB OP2", "ON" )
jobfile.writei( "CONTACT-DEFORMABLE-DEFORMABLE METHOD", 0 )
jobfile.writei( "CONTACT-CRITERION", 0 )
jobfile.writei( "CONTACT-DERIVATION", 0 )
jobfile.writei( "CONTACT-REL_ABS", 0 )
jobfile.writec( "RESTART TYPE", "None" )
jobfile.writec( "DOMAIN DECOMPOSE", "Automatic" )
jobfile.writei( "DOMAIN 0", 1 )
jobfile.writec( "SINGLE POST FILE", "" )
jobfile.writec( "DOMAIN OBJECT", "Entire Model" )
jobfile.writec( "METIS METHOD", "Best" )
jobfile.writec( "DOMAIN ISLAND REMOVAL", "" )
jobfile.writec( "COARSE GRAPH", "" )
jobfile.writei( "MDOF DATA", 0 )
jobfile.writec( "CELL WRITE", "ON" )

```

```

jobfile.writei( "CELL INPUT 0", 0 )
jobfile.writec( "FMS WRITE", "ON" )
jobfile.writei( "FMS INPUT 0", 0 )
jobfile.writec( "EXEC WRITE", "ON" )
jobfile.writei( "EXEC INPUT 0", 0 )
jobfile.writec( "CASE WRITE", "ON" )
jobfile.writei( "CASE INPUT 0", 0 )
jobfile.writec( "BULK WRITE", "ON" )
jobfile.writei( "BULK INPUT 0", 0 )
jobfile.writec( "CELL DTI POSITION", "START" )
jobfile.writec( "FMS DTI POSITION", "START" )
jobfile.writec( "EXEC DTI POSITION", "START" )
jobfile.writec( "CASE DTI POSITION", "START" )
jobfile.writec( "BULK DTI POSITION", "START" )
jobfile.writec( "", "END" )
jobfile.close( )
mscnastran_job.associate_subcases( "600", loop, 1, ["LC_2T"] )
analysis_submit( "MSC.Nastran", loop, TRUE )
STRING result[20], result2[20]
result=loop/"./"op2"
result2="./"result
jobfile.open( loop, "RESULTS" )
jobfile.write_spl( "/* Jobfile for NASPAT created %A% at %A% */", ["16-Apr-11" @
, "17:18:24"] )
jobfile.writec( "", "TRANSLATOR = naspat3" )
jobfile.writec( "DATABASE", "E:\calisma\3103_3d.db" )
jobfile.writec( "JOBNAME", loop )
jobfile.writec( "RESULTS FILE", result2 )
jobfile.writec( "", "" )
jobfile.writec( "OBJECT", "Result Entities" )
jobfile.writec( "ANALYSIS TYPE", "Structural" )
jobfile.writec( "", "" )
jobfile.writec( "", "/*" )
jobfile.writec( "", " * File Search Path Declaration" )
jobfile.writec( "", " */" )
jobfile.writec( "", "" )
jobfile.writec( "File Search Path", "E:\MSC.Software\Patran\2008_r2\bin" )
jobfile.writec( "File Search Path", "E:\MSC.Software\Patran\2008_r2\icons" )
jobfile.writec( "File Search Path", "E:\MSC.Software\Patran\2008_r2\alters" )
jobfile.writec( "File Search Path", "E:\MSC.Software\Patran\2008_r2\helpfiles" )
jobfile.writec( "File Search Path", "E:\MSC.Software\Patran\2008_r2" )

```

```

jobfile.writec( "File Search Path", "E:\Documents and Settings\murat gunel" )
jobfile.writec( "File Search Path",
"E:\MSC.Software\Patran\2008_r2\shareware\msc\unsupported\uti@" )
jobfile.writec( "", "ities\icons" )
jobfile.writec( "File Search Path",
"E:\MSC.Software\Patran\2008_r2\shareware\msc\unsupported\uti@" )
jobfile.writec( "", "ities\plb" )
jobfile.writec( "File Search Path",
"E:\MSC.Software\Patran\2008_r2\shareware\msc\unsupported\uti@" )
jobfile.writec( "", "ities\extra_files" )
jobfile.writec( "File Search Path", "E:\MSC.Software\Patran\2008_r2\mscexplore_files\
)
jobfile.writec( "File Search Path",
"E:\MSC.Software\Patran\2008_r2\mscprocor_files\icons" )
jobfile.writec( "File Search Path",
"E:\MSC.Software\Patran\2008_r2\mscprocor_files\lib" )
jobfile.writec( "File Search Path",
"E:\MSC.Software\Patran\2008_r2\mscprocor_files\plb" )
jobfile.writec( "File Search Path",
"E:\MSC.Software\Patran\2008_r2\mscprocor_files\dmap" )
jobfile.writec( "File Search Path", "E:\Documents and Settings\murat gunel" )
jobfile.writec( "File Search Path", "E:\MSC.Software\Patran\2008_r2\bin\exe" )
jobfile.writec( "", "" )
jobfile.writec( "", "/*" )
jobfile.writec( "", " * Translation Parameters" )
jobfile.writec( "", " */" )
jobfile.writec( "", "" )
jobfile.writec( "DIVISION TOLERANCE", "1.0E-8" )
jobfile.writec( "NUMERICAL TOLERANCE", "1.0E-4" )
jobfile.writec( "MODEL TOLERANCE", "0.0049999999" )
jobfile.writec( "ROTATIONAL NODAL RESULTS", "OFF" )
jobfile.writec( "STRESS/STRAIN INVARIANTS", "OFF" )
jobfile.writec( "PRINCIPAL DIRECTIONS", "OFF" )
jobfile.writec( "CREATE P-ORDER FIELD", "OFF" )
jobfile.writec( "ELEMENT RESULTS POSITIONS", "Nodal    " )
jobfile.writec( "NASTRAN VERSION", "2008." )
jobfile.writec( "TITLE DESCRIPTION", "ON" )
jobfile.writec( "", "END" )
jobfile.close( )
ui_answer_message (6020053, "YESFORALL")
analysis_import( "MSC.Nastran", loop, "Results File", result2, @

```

TRUE)

```
STRING analysis_string[VIRTUAL]
STRING nastran_exec[80]
sys_get_env("NASTRAN_EXECUTABLE", nastran_exec)
$ dump nastran_exec
analysis_string = nastran_exec //" " // "D:\calisma" // "\" // loop //" .bdf"
write("Running Analysis... Please Wait~~~^_^")
db_commit_raw()
utl_process_spawn(analysis_string, TRUE)
$ dump analysis_string
db_start_transaction_raw()
sys_free_string(analysis_string)
INTEGER m,array(5)
STRING entity [20]
INTEGER reslocx,reslocy,reslocxy
INTEGER nresx,nresy,nresxy
INTEGER idsx(VIRTUAL),idsy(VIRTUAL),idsxy(VIRTUAL)
INTEGER nresultsx(VIRTUAL),nresultsy(VIRTUAL),nresultszy(VIRTUAL)
INTEGER minlocx(12),data_typex,minlocy(12),data_typey,minlocxy(12),data_typedxy
INTEGER maxlocx(12),maxlocy(12),maxlocxy(12)
INTEGER lam
REAL resultsx(VIRTUAL),resultsy(VIRTUAL),resultszy(VIRTUAL)
sys_allocate_array(resultsx,1,e)
sys_allocate_array(resultsy,1,e)
sys_allocate_array(resultszy,1,e)
sys_allocate_array(nresultsx,1,e)
sys_allocate_array(nresultsy,1,e)
sys_allocate_array(nresultszy,1,e)
sys_allocate_array(idsx,1,e)
sys_allocate_array(idsy,1,e)
sys_allocate_array(idsxy,1,e)
res_utl_clear_result ()
FOR( lam=1 TO ply)
STRING layername[90]
INTEGER layerid
layername="Layer"//" " //str_from_integer( lam )
res_data_get_layerpos_id(layername,layerid)
entity="Elm 1"//": " //str_from_integer( e )

INTEGER pid,lid
```

```

db_get_primary_res_id("Stress Tensor",pid)
db_get_load_case_id("LC_2T",lid)
array(1)=lid
array(2)=2*n
array(3)=pid
array(4)=1
array(5)=layerid
res_utl_extract_elem_results(array, entity, "XX", "c" , "AsIs", data_typex, reslocx,
nresx, idsx, nresultsx, resultsx, minlocx, maxlocx)
res_utl_extract_elem_results(array, entity, "YY", "c" , "AsIs", data_typey, reslocy,
nresy, idsy, nresultsy, resultsy, minlocy, maxlocy)
res_utl_extract_elem_results(array, entity, "XY", "c" , "AsIs", data_typexy, reslocxy,
nresxy, idxy, nresultxy, resultsxy, minlocxy, maxlocxy)
STRING modified_mat[90],fails[90]
INTEGER mat_id

```

\$Elastic properties used in failure detection-----

```

REAL xt,xc,yc,yt,ts
xt=1513.40
xc=-1696.00
yt=44.00
yc=-44.00
ts=86.87

```

\$Degradation parameters-----

```

REAL src
src=0.001
REAL deg_e1,deg_e2,deg_v12,deg_s12,deg_s13,deg_s23
STRING strdeg_e1[50],strdeg_e2[50],strdeg_v12[50], @
strdeg_s12[50],strdeg_s13[50],strdeg_s23[50]
INTEGER found
REAL e1_base,e2_base,v12_base,s12_base,s23_base,s13_base

```

\$Failure detection process-----

```

REAL fbt, fbc, mtt, mtc
FOR ( m=1 TO e )
IF ((resultsx(m)+resultsy(m)+resultscy(m))==0.0) THEN
write("NO SOLUTION!!!!!!!!!! CHECK MARC RESULT FILES")
BREAK
END IF
IF (resultsx(m) > 0 ) THEN
  IF( (((resultsx(m)/xt)**2.0)+((resultscy(m)/ts)**2.0)) >=1.00 ) THEN
fbt=(((resultsx(m)/xt)**2.0)+((resultscy(m)/ts)**2.0))
dump fbt
write("Fiber Tensile at...")
dump m
fails="Elm"//" " //str_from_integer( m )
uil_toolbar.wireframe( )
ga_group_create( "ply"//"_" //str_from_integer( lam ) )
ga_group_entity_add( "ply"//"_" //str_from_integer( lam ), fails )
ga_group_entity_remove( "default_group", fails )
ga_group_current_set( "default_group" )
gm_plot_erase_fem( 0 )
modified_mat="mat_"//str_from_integer( lam )// "_" //str_from_integer( m )
material.rename( modified_mat, modified_mat )
db_get_material_id_from_name(modified_mat, mat_id)
db_get_matl_prop_value2(mat_id, 2, 0, 0, 0, 0, 0, found, e1_base)
db_get_matl_prop_value2(mat_id, 3, 0, 0, 0, 0, 0, found, e2_base)
db_get_matl_prop_value2(mat_id, 8, 0, 0, 0, 0, 0, found, s12_base)
db_get_matl_prop_value2(mat_id, 5, 0, 0, 0, 0, 0, found, v12_base)
db_get_matl_prop_value2(mat_id, 10, 0, 0, 0, 0, 0, found, s13_base)
db_get_matl_prop_value2(mat_id, 9, 0, 0, 0, 0, 0, found, s23_base)
deg_e1=src*(e1_base)
deg_s12=src*(s12_base)
deg_v12=src*(v12_base)
deg_s13=src*(s13_base)

```

\$Redegradation is not allowed in sudden degradation-----

```

IF ( e1_base < 132379.0 ) THEN
deg_e1=e1_base
deg_s12=s12_base
deg_v12=v12_base
deg_s13=s13_base
END IF

```

```

strdeg_e1="//str_from_real( deg_e1 )
strdeg_s12="//str_from_real( deg_s12 )
strdeg_v12="//str_from_real( deg_v12 )
strdeg_s13="//str_from_real( deg_s13 )
IF ( (mth_abs(deg_v12))>=(deg_e1/e2_base)**0.5 ) THEN
write("VIOLATION FOUND DUE TO DEGRADATION")
BREAK
ELSE IF ( (mth_abs((deg_v12*e2_base)/deg_e1))>=(e2_base/deg_e1)**0.5 ) THEN
write("VIOLATION FOUND DUE TO DEGRADATION")
BREAK
ELSE IF ( (1-(deg_v12*((deg_v12*e2_base)/deg_e1 )))<=0 ) THEN
write("VIOLATION FOUND DUE TO DEGRADATION")
BREAK
END IF
STRING degfbt[50](5)
degfbt(1)=strdeg_e1
degfbt(2)=strdeg_v12
degfbt(3)=strdeg_s12
degfbt(4)=strdeg_s13
degfbt(5)="
dump degfbt
material.create( "Analysis code ID", 1, "Analysis type ID", 1, modified_mat, mat_id,
"DatC: 01-Nov-0 TimC: 18:27:00", "2d Orthotropic", 5, "Directionality", @
4, "Linearity", 1, "Homogeneous", 0, "Linear Elastic", 1, "Model Options & IDs", [""
"", "", "", ""], [0, 0, 0, 0, 0], "Active Flag", 1, "Modify", 31, @
"External Flag", FALSE, "Property IDs", ["Elastic Modulus 11", "Poisson Ratio 12",
"Shear Modulus 12", "Shear Modulus 13"], [2, 5, 8, 10, 0], @
"Property Values", degfbt )
c=0
END IF
END IF
IF (resultsx(m) < 0 ) THEN
IF( (resultsx(m)/xc)**2.0 >=1.00 ) THEN
fbc=(resultsx(m)/xc)**2.0
dump fbc
write("Fiber Compression at...")
dump m
fails="Elm"//" "//str_from_integer( m )
uil_toolbar.wireframe( )
ga_group_create( "ply"//"_ "//str_from_integer( lam ) )

```

```

ga_group_entity_add( "ply"//"_"//str_from_integer( lam ), fails )
ga_group_entity_remove( "default_group", fails )
ga_group_current_set( "default_group" )
gm_plot_erase_fem( 0 )
modified_mat="mat_"//str_from_integer( lam )//"_"//str_from_integer( m )
material.rename( modified_mat, modified_mat )
db_get_material_id_from_name(modified_mat,mat_id)
db_get_matl_prop_value2(mat_id,2,0,0,0,0,found,e1_base)
db_get_matl_prop_value2(mat_id,3,0,0,0,0,found,e2_base)
db_get_matl_prop_value2(mat_id,8,0,0,0,0,found,s12_base)
db_get_matl_prop_value2(mat_id,5,0,0,0,0,found,v12_base)
db_get_matl_prop_value2(mat_id,10,0,0,0,0,found,s13_base)
db_get_matl_prop_value2(mat_id,9,0,0,0,0,found,s23_base)
deg_e1=src*(e1_base)
deg_s12=src*(s12_base)
deg_v12=src*(v12_base)
deg_s13=src*(s13_base)

```

\$Redegradation is not allowed in sudden degradation-----

```

F ( e1_base < 132379.0 ) THEN
deg_e1=e1_base
deg_s12=s12_base
deg_v12=v12_base
deg_s13=s13_base
END IF

```

```

strdeg_e1=""//str_from_real( deg_e1 )
strdeg_s12=""//str_from_real( deg_s12 )
strdeg_v12=""//str_from_real( deg_v12 )
strdeg_s13=""//str_from_real( deg_s13 )
IF ( (mth_abs(deg_v12))>=(deg_e1/e2_base)**0.5 ) THEN
write("VIOLATION FOUND DUE TO DEGRADATION")
BREAK
ELSE IF ( (mth_abs((deg_v12*e2_base)/deg_e1))>=(e2_base/deg_e1)**0.5 ) THEN
write("VIOLATION FOUND DUE TO DEGRADATION")
BREAK
ELSE IF ( (1-(deg_v12*((deg_v12*e2_base)/deg_e1 )))<=0 ) THEN
write("VIOLATION FOUND DUE TO DEGRADATION")
BREAK

```

```

END IF
STRING degfbc[50](5)
degfbc(1)=strdeg_e1
degfbc(2)=strdeg_v12
degfbc(3)=strdeg_s12
degfbc(4)=strdeg_s13
degfbc(5)=""
dump degfbc
material.create( "Analysis code ID", 1, "Analysis type ID", 1, modified_mat, mat_id,
"DatC: 01-Nov-0 Time: 18:27:00", "2d Orthotropic", 5, "Directionality", @
4, "Linearity", 1, "Homogeneous", 0, "Linear Elastic", 1, "Model Options & IDs", [""
"", "", "", ""], [0, 0, 0, 0, 0], "Active Flag", 1, "Modify", 31, @
"External Flag", FALSE, "Property IDs", ["Elastic Modulus 11", "Poisson Ratio 12",
"Shear Modulus 12", "Shear Modulus 13"], [2, 5, 8, 10, 0], @
"Property Values", degfbc )
c=0
END IF
END IF
IF (resultsy(m) > 0 ) THEN
  IF( (((resultsy(m)/yt)**2.0)+((resultsxy(m)/ts)**2.0)) >=1.00 ) THEN
    mtt=(((resultsy(m)/yt)**2.0)+((resultsxy(m)/ts)**2.0))
    dump mtt
    write("Matrix Tensile at...")
    dump m
    fails="Elm"//" _//str_from_integer( m )
    uil_toolbar.wireframe( )
    ga_group_create( "ply"//" _//str_from_integer( lam ) )
    ga_group_entity_add( "ply"//" _//str_from_integer( lam ), fails )
    ga_group_entity_remove( "default_group", fails )
    ga_group_current_set( "default_group" )
    gm_plot_erase_fem( 0 )
    modified_mat="mat_"//str_from_integer( lam )//" _//str_from_integer( m )
    material.rename( modified_mat, modified_mat )
    db_get_material_id_from_name(modified_mat,mat_id)
    db_get_matl_prop_value2(mat_id,2,0,0,0,0,found,e1_base)
    db_get_matl_prop_value2(mat_id,5,0,0,0,0,found,v12_base)
    db_get_matl_prop_value2(mat_id,3,0,0,0,0,found,e2_base)
    db_get_matl_prop_value2(mat_id,8,0,0,0,0,found,s12_base)
    db_get_matl_prop_value2(mat_id,9,0,0,0,0,found,s23_base)
    deg_e2=src*(e2_base)
    deg_s12=src*(s12_base)

```

```
deg_s23=src*(s23_base)
```

\$Redegradation is not allowed in sudden degradation-----

```
IF ( e2_base < 10755.0 ) THEN
```

```
deg_e2=e2_base
```

```
deg_s12=s12_base
```

```
deg_s23=s23_base
```

```
END IF
```

```
strdeg_e2="//str_from_real( deg_e2 )
```

```
strdeg_s12="//str_from_real( deg_s12 )
```

```
strdeg_s23="//str_from_real( deg_s23 )
```

```
IF ( (mth_abs(v12_base))>=(e1_base/deg_e2)**0.5 ) THEN
```

```
write("VIOLATION FOUND DUE TO DEGRADATION")
```

```
BREAK
```

```
ELSE IF ( (mth_abs((v12_base*deg_e2)/e1_base))>=(deg_e2/e1_base)**0.5 ) THEN
```

```
write("VIOLATION FOUND DUE TO DEGRADATION")
```

```
BREAK
```

```
ELSE IF ( (1-(v12_base*((v12_base*deg_e2)/e1_base )))<=0 ) THEN
```

```
write("VIOLATION FOUND DUE TO DEGRADATION")
```

```
BREAK
```

```
END IF
```

```
STRING degmtt[50](4)
```

```
degmtt(1)=strdeg_e2
```

```
degmtt(2)=strdeg_s12
```

```
degmtt(3)=strdeg_s23
```

```
degmtt(4)=""
```

```
dump degmtt
```

```
material.create( "Analysis code ID", 1, "Analysis type ID", 1, modified_mat, mat_id,
```

```
"Date: 01-May-11 Time: 14:36:41", "2d Orthotropic", 5, "Directionality", @
```

```
4, "Linearity", 1, "Homogeneous", 0, "Linear Elastic", 1, "Model Options & IDs", [""
```

```
""", "", "", ""], [0, 0, 0, 0, 0], "Active Flag", 1, "Modify", 31, @
```

```
"External Flag", FALSE, "Property IDs", ["Elastic Modulus 22", "Shear Modulus 12",
```

```
"Shear Modulus 23"], [3, 8, 9, 0], @
```

```
"Property Values", degmtt )
```

```
c=0
```

```
END IF
```

```
END IF
```

```
IF (resultsy(m) < 0 ) THEN
```

```

IF(((resultsy(m)/yc)*((yc/(2.0*ts))**2.0)-
1.0))+((resultsy(m)/(2.0*ts))**2.0)+((resultscopy(m)/(ts))**2.0)>=1.00 ) THEN
mtc=(((resultsy(m)/yc)*((yc/(2.0*ts))**2.0)-
1.0))+((resultsy(m)/(2.0*ts))**2.0)+((resultscopy(m)/ts)**2.0))
dump mtc
write("Matrix Compression at...")
dump m
fails="Elm"//" " //str_from_integer( m )
uil_toolbar.wireframe( )
ga_group_create( "ply"//"_" //str_from_integer( lam ) )
ga_group_entity_add( "ply"//"_" //str_from_integer( lam ), fails )
ga_group_entity_remove( "default_group", fails )
ga_group_current_set( "default_group" )
gm_plot_erase_fem( 0 )
modified_mat="mat_"//str_from_integer( lam )/"_" //str_from_integer( m )
material.rename( modified_mat, modified_mat )
db_get_material_id_from_name(modified_mat,mat_id)
db_get_matl_prop_value2(mat_id,2,0,0,0,0,found,e1_base)
db_get_matl_prop_value2(mat_id,3,0,0,0,0,found,e2_base)
db_get_matl_prop_value2(mat_id,8,0,0,0,0,found,s12_base)
db_get_matl_prop_value2(mat_id,5,0,0,0,0,found,v12_base)
db_get_matl_prop_value2(mat_id,9,0,0,0,0,found,s23_base)
deg_e2=src*(e2_base)
deg_s12=src*(s12_base)
deg_s23=src*(s23_base)

$Redegradation is not allowed in sudden degradation-----

IF ( e2_base < 10755.0 ) THEN
deg_e2=e2_base
deg_s12=s12_base
deg_s23=s23_base
END IF

strdeg_e2=""//str_from_real( deg_e2 )
strdeg_s12=""//str_from_real( deg_s12 )
strdeg_s23=""//str_from_real( deg_s23 )
IF ( (mth_abs(v12_base))>=(e1_base/deg_e2)**0.5 ) THEN
write("VIOLATION FOUND DUE TO DEGRADATION")
BREAK
ELSE IF ( (mth_abs((v12_base*deg_e2)/e1_base))>=(deg_e2/e1_base)**0.5 ) THEN

```

```

write("VIOLATION FOUND DUE TO DEGRADATION")
BREAK
ELSE IF ( (1-(v12_base*((v12_base*deg_e2)/e1_base )))<=0 ) THEN
write("VIOLATION FOUND DUE TO DEGRADATION")
BREAK
END IF
STRING degmtc[50](4)
degmtc(1)=strdeg_e2
degmtc(2)=strdeg_s12
degmtc(3)=strdeg_s23
degmtc(4)=""
dump degmtc
material.create( "Analysis code ID", 1, "Analysis type ID", 1, modified_mat, mat_id,
>Date: 01-May-11 Time: 14:36:41", "2d Orthotropic", 5, "Directionality", @
4, "Linearity", 1, "Homogeneous", 0, "Linear Elastic", 1, "Model Options & IDs", [""
"", "", "", ""], [0, 0, 0, 0, 0], "Active Flag", 1, "Modify", 31, @
"External Flag", FALSE, "Property IDs", ["Elastic Modulus 22", "Shear Modulus 12",
"Shear Modulus 23"], [3, 8, 9, 0], @
"Property Values", degmtc )
c=0
END IF
END IF
END FOR
END FOR

```

\$Graphical representation of failure-----

```

sys_poll_option( 2 )
ga_display_lines_set( "general", 50 )
sys_poll_option( 0 )
gm_hilight_string("Curve 1:730",12)
FOR( m=1 TO e)
INTEGER cnt0
INTEGER segment0
gm_segment_create(segment0)
db_count_groups_for_entity(m, 124, cnt0)
IF (cnt0==1) THEN
gm_draw_entity(segment0,6,3,m)
ELSE IF (cnt0==2) THEN
gm_draw_entity(segment0,12,3,m)
ELSE IF (cnt0==3) THEN

```

```

gm_draw_entity(segment0,2,3,m)
ELSE IF (cnt0==4) THEN
gm_draw_entity(segment0,10,3,m)
ELSE IF (cnt0==5) THEN
gm_draw_entity(segment0,15,3,m)
ELSE IF (cnt0==6) THEN
gm_draw_entity(segment0,5,3,m)
ELSE IF (cnt0==7) THEN
gm_draw_entity(segment0,3,3,m)
ELSE IF (cnt0==8) THEN
gm_draw_entity(segment0,1,3,m)
END IF
END FOR
STRING jpg[50],jpg2[50]
jpg="Increment"//str_from_integer( n )//"_Load_"//str_from_real( i )
jpg2=jpg//".jpg"
gm_write_image( "JPEG", jpg2, "Overwrite", 0., 0., 1., 1., 100, "Viewport" )
UNTIL ( n == 300)
END FUNCTION

```

APPENDIX B

NONLINEAR SOLUTION PARAMETERS

In this section, nonlinear solution parameters used in the progressive failure analysis are presented. Based on the nonlinear solution user guides of MSC Nastran [24][25], solution parameters are defined through the MSC Patran interface and bulk data cards which are explained in more detail in the following sections.

B1. Nonlinear Static Analysis (MSC Nastran, SOL106)

For the purpose of performing nonlinear analysis by using SOL106 solution sequence, “Nonlinear Static” option is selected from “Solution Type” interface of MSC Patran. Then, as shown in Figure B1, in “Solution Parameters” interface, automatic constraint, large displacements or follower forces selections can be made.

As it was mentioned before, SOL106 has only large displacement and small strain solving capability. If problem needs to be provided large strain capability, implicit nonlinear SOL600 should be used. However, SOL106 is mostly preferred since it is a fast and simple way of solving basic nonlinear problems. It should be noted that in aerospace applications geometric non-linearity due to large strain is less encountered compared to the non-linearity due to large displacement and rotations.

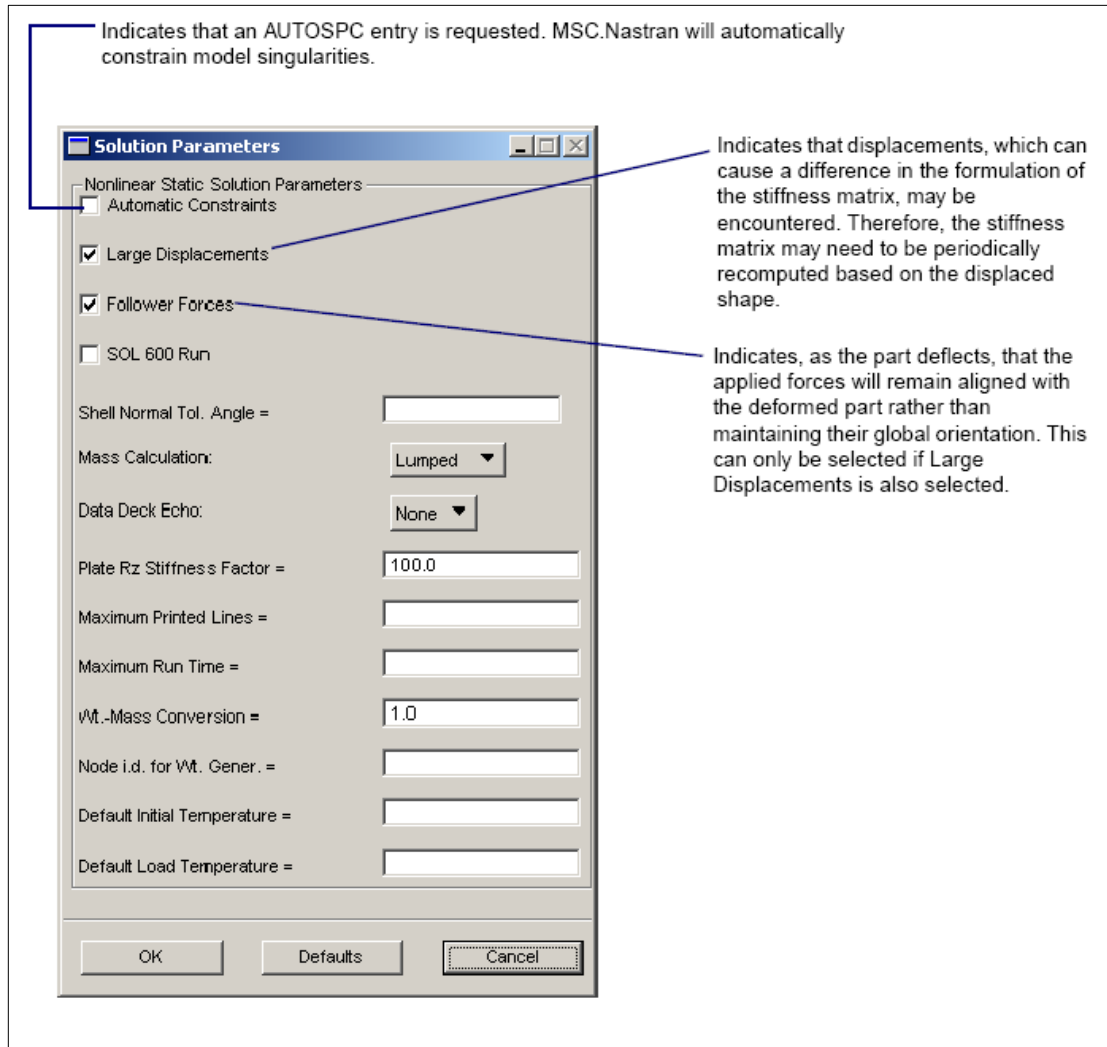


Figure B1: SOL106 solution parameters [24]

The important parameters used in nonlinear static analysis SOL106 are defined by the “NLPARM” entry in bulk data file. It controls the iterative and incremental solution procedure during the nonlinear analysis. Parameters stated in “NLPARM” entry can be adjusted to obtain optimum solution path. However, since it is too hard to estimate optimum values for each specific problem, default settings which are obtained with the help of considerable number of numerical experiments are assigned for general purpose.

| 1 | 2 | 3 | 4 | 5 | 6 | 7 | 8 | 9 | 10 |
|--------|--------|------|------|---------|-------|---------|---------|--------|----|
| NLPARM | ID | NINC | DT | KMETHOD | KSTEP | MAXITER | CONV | INTOUT | |
| | EPSU | EPSP | EPSW | MAXDIV | MAXQN | MAXLS | FSTRESS | LSTOL | |
| | MAXBIS | | | | MAXR | | RTOLB | | |

Figure B2: NLPARM card for SOL106 solutions [26]

In Figure B2 the typical card format for “NLPARM” entry is shown. And also declarations of important parameters defined in this card like NINC, KMETHOD, KSTEP, MAXITER, CONV, INTOUT are shown in Figure B3.

The image shows a 'Subcase Parameters' dialog box with several sections and fields. Annotations with arrows point to specific fields and sections, providing their functions:

- Number of Load Increments = 10:** Defines the number of increments to be used to apply the full load. This is the NINC field.
- Matrix Update Method: Automatic:** Defines what method to use to control the stiffness. Matrix updates as the load is incrementally applied. This parameter can have one of three settings: Automatic, Semi-Automatic, or Controlled Iter. This defines the setting of the KMETHOD field.
- Number of Iterations per Update = 5:** Defines the number of iterations to be used after each matrix update. This is the KSTEP field.
- Allowable Iterations per Increment = 25:** Defines the limit for the number of iterations that can be done in any given increment. This is the MAXITER field.
- Displacement Tolerance = 1.0e-03:** (Under Convergence Criteria)
- Load Tolerance = 0.01:** (Under Convergence Criteria)
- Work Tolerance = 0.01:** (Under Convergence Criteria)
- Arc-Length Method ...:** Opens a subordinate form to activate the Arc-Length Method which is turned OFF by default. The Arc-Length Method is used to explore post-buckling paths.
- Normal Modes:** Activates a normal mode analysis of the prestressed system at the end of the subcase.
- Buckling:** Activates a buckling analysis at the end of the subcase.
- OK / Cancel:** Opens subordinate form to define eigenvalue extraction parameters.

Figure B3: SOL106 subcase parameters [24]

Here, “NINC” field defines the number of increments to be used in subcase process. Load in the current subcase, that is total load minus the load in preceding subcase, is divided by defined increment number by “NINC” to obtain incremental loading. “KMETHOD” and “KSTEP” fields determine the stiffness matrix update strategy for the specified problem. There are three options as “AUTO”, ”SEMI” and “ITER” for the “KMETHOD” field and “AUTO” is default method which works well. It uses quasi-Newton, line search and/or bisection method to evaluate solution as soon as possible without updating stiffness matrix. Since there is no stiffness matrix update in “AUTO” methods, sometimes it is hard to find solutions for highly nonlinear problems. In “SEMI” method, the stiffness matrix is updated after first iteration and for this reason it is more efficient than “AUTO” method for problems have convergence difficulty. Moreover, In “ITER” method stiffness matrix is updated at every “KSTEP”th iterations. Here “KSTEP” defined the number of iterations to be used after each matrix update. Although frequent updates increases solution time, it is highly recommended for highly nonlinear problems. The allowed number of iterations per load increment is given in “MAXITER” field. If number of iterations exceeds the “MAXITER” without convergence, the load increment is bisected and analysis is repeated again. Besides, the convergence is checked according to the specified criteria in “CONV” field. Displacement, load or work criteria combinations can be selected as shown in Figure B3. Finally, output requests for displacement or stress results are defined by the “INTOUT” field. If “YES” entry is used, then all output for every increment is obtained. If “NO” entry is used, then only the output at last increment or the load step is obtained.

Also a bulk data example for SOL106 run is presented in Figure B4.

```

$ NASTRAN input file created by the Patran 2008r2 input file translated
$ on April 19, 2011 at 20:47:16.
$ Direct Text Input for Nastran System Cell section
$ Direct Text Input for File Management Section
$ Direct Text Input for Executive Control
$ Nonlinear Static Analysis, Database
SOL 106
CEND
$ Direct Text Input for Global Case Control Data
TITLE = MSC.Nastran job created on 19-Apr-11 at 20:43:47
ECHO = NONE
SUBCASE 1
  TITLE=This is a default subcase.
  NLPARM = 1
  SPC = 2
  LOAD = 2
  DISPLACEMENT(PLOT, SORT1, REAL)=ALL
  SPCFORCES(PLOT, SORT1, REAL)=ALL
  STRESS(PLOT, SORT1, REAL, VONMISES, BILIN)=ALL
$ Direct Text Input for this Subcase
BEGIN BULK
$ Direct Text Input for Bulk Data
PARAM POST -1
PARAM AUTOSPC NO
PARAM LGDISP 1
PARAM, NOCOMPS, 0
PARAM PRTMAXIM YES
NLPARM 1 15 ITER 1 25 NO
$ Elements and Element Properties for region : prop
$ Composite Property Record created from P3/PATRAN composite material
$ record : pcomp.2
$ Composite Material Description :
PCOMP 1 | 0. 0.
      1 .1308 0. YES 1 .1308 90. YES
      1 .1308 45. YES 1 .1308 -45. YES
      1 .1308 -45. YES 1 .1308 45. YES
      1 .1308 90. YES 1 .1308 0. YES

```

Figure B4: SOL106 bulk data example

B2.Implicit Nonlinear Analysis (MSC Nastran, SOL600)

Implicit nonlinear solution module (SOL600) is developed for the use of MSC Marc capabilities under the control of MSC Nastran system. Since Marc is a solver which is specialized in solving of complicated nonlinear problems which contain geometric, material or contact nonlinearities, SOL600 may be preferred for problems which is not possible to be handled by SOL106.

However, appropriate selection of the parameters used in the solution of complicated problems is very important to obtain accurate results. In this section, solution parameters used in SOL600 runs is presented with their explanations.

For the purpose of performing nonlinear analysis by using SOL600 solution sequence, "Implicit Nonlinear Static" option is selected from "Solution Type" interface of MSC Patran. Then, as shown in Figure B5, from the "Solution Parameters" interface the result output format can be selected.

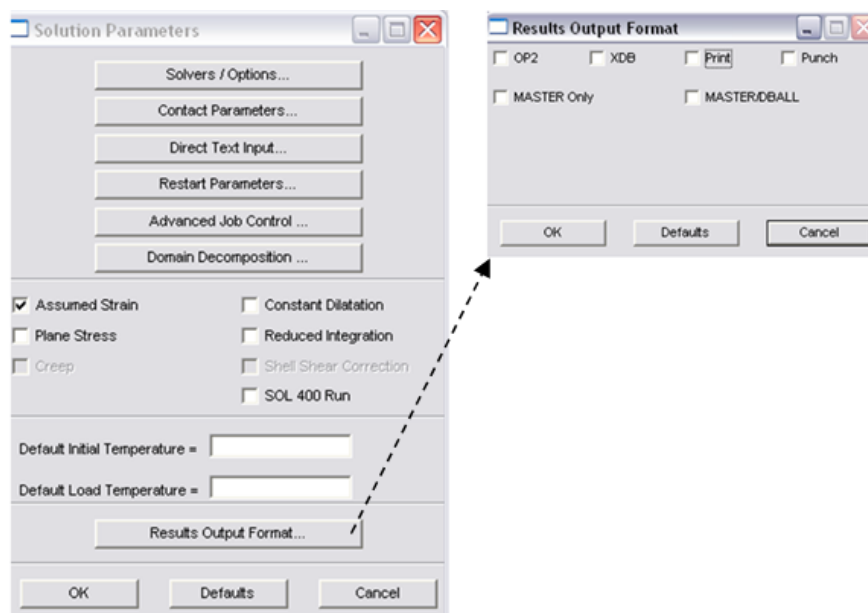


Figure B5: SOL600 solution parameters [24]

If none of the shown result output formats like "op2" or "xdb" is selected, the default result output format of Marc "t16" is generated. But it should be noted that Marc calculates the true stresses for finite elements which means that it takes into consideration the deformed body while calculating stresses. In addition, stresses are calculated by taking into account not only the deformed area but also the coordinate

transformation due to deformation. After calculating stress results of all elements in model, Marc translates the stress results to an original coordinate system. At that point, this transformation prevents to read directional stresses of a laminate in composite analysis if MSC Patran interface is used. So, for this reason "op2" output is preferred in the progressive failure analysis study.

Important settings for implicit nonlinear solution SOL600 take place in "Subcase Parameters" interface. As it can be seen from Figure B6, selections about geometric nonlinear effects and solution process are made from this interface.

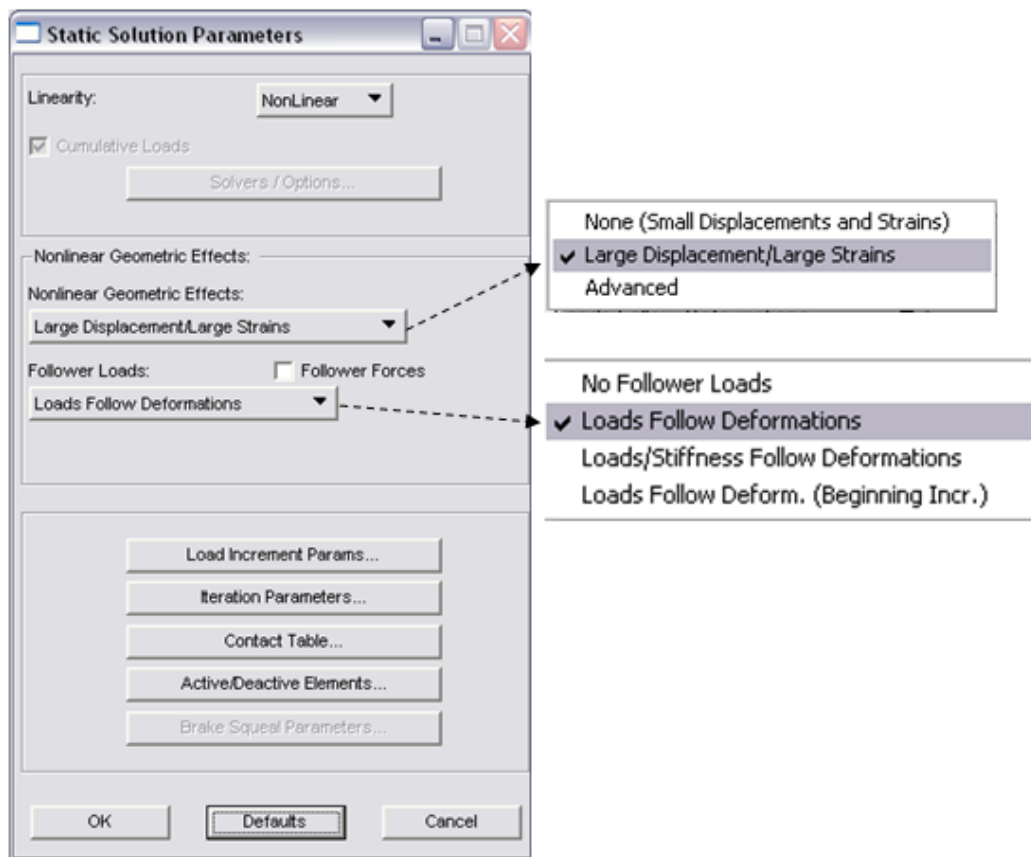


Figure B6: SOL600 subcase parameters

For the problems which contain large displacement and strain, SOL600 solution can be employed by selecting nonlinear geometric effects option as "Large Displacement/Large Strains". Also, follower force effect can be included to the analysis by using this interface. But in the terminology of SOL600, follower loads mean pressure type loads and follower forces mean point forces. Since in this study, pressure loads follow deformations and point forces as tension or compression loads stay fixed in direction, "Follower Forces" option is not selected. In addition, "Loads Follow Deformations" option is also selected from the "Follower Loads" section. Bulk data file entry which defines follower loads is "MRFOLLOW1" and follower forces are "MRFOLLOW4". For the follower load selection and no follower force selection, MRFOLLOW1 is equal to "1" and "MRFOLLOW4" is equal to "0". Since these settings are default, they are not written into bulk data file as "PARAM" entry. The detailed information about other selections can be obtained from implicit nonlinear user's guide [25].

There are three types of load increment schemes in the SOL600. These are fixed, adaptive and adaptive with arc length method. In earlier versions of MSC Nastran, these parameters are written in "NLPARAM" and "NLSTRAT" entries. If adaptive increment type is selected, the interface which is shown in Figure B7 needs to be filled. Generally, the default settings defined in the interface should not be changed, since they are obtained from various numerical experimental and theoretical studies. But, for problems require an additional adjustment, the definition of the parameters is explained as shown in Figure B7. Same situation is valid for fixed type increment which is shown in Figure B8. The default options are used for the purpose of performing implicit nonlinear analysis. In this study, fixed type increment is used based on the experiences and previous works in the literature.

Defines the initial time step size. Default is 1% of Total Time if left blank.

Indicates load will be allowed to be scaled up by 20% each increment if possible. Default is 1.2.

Indicates the smallest time step that can be used. Default is Trial Time Step / 1000 if left blank.

Indicates the largest time step that can be used. Default is Total Time / 2 if left blank.

Defines the maximum number of time steps. It can be left blank which will default to the Initial Step Size divided by the Total Time.

This is the total time of the analysis for a particular step. It defaults to one (1) if left blank for static load cases. For time dependent load cases, the total time is the length of time between distinct time points if left blank. Otherwise the actual value is used (not recommended because it can't be variable).

Indicates that this many increments evenly spaced in time will be placed in the output file. Default is 0 if left blank. Which means all converged increments will be output (SOL 600 only).

Figure B7: SOL600 adaptive increment type [25]

For Statics and Creep this is the number of increments specified in the **NLAUTO** option. Or for Transient Dynamics defines the number of steps to use throughout the analysis for fixed time step type. Default is 10.

This is the total time of the analysis for a particular step. It defaults to one (1) if left blank for static load cases

Applies to nonlinear statics only. It is ON by default. If an increment does not converge, it allows for a restart from the last increment cuts the increment size in half.

This is associated with Automatic Cutback. This parameter determines how many times a cutback is allowed.

Figure B8: SOL600 fixed increment type [25]

In Figure B9, an example for implicit nonlinear analysis bulk data file is shown. As it can be noticed, there are Marc entries such as "MARCPRNH", "MARCND99", "MARCOTIM" and "MARCSLHT". Here "MARCPRNH" controls the printing of nodal stress and strain outputs in Marc "out" file. If it is equal to "1" then these results are written to the output file. If "MARCND99" is equal to "-1", a set named ND999999 will be generated to output all nodes for at least one type of nodal output. "MARCOTIM" determines if Marc is to be processed at selective or at all output times. If it is equal to "2", Marc output will be generated only at times around 1.0, 2.0 etc. similar to "INTOUT" control in "NLPARM". "MARCSLHT" defines the number of layers through the shell thickness for output. For SOL600 it should be greater than "5". Furthermore, "NLSTRAT" controls the solution strategy according to the convergence type defined as "AIMAXINC 10" which means that maximum increment number "10".

```

$ NASTRAN input file created by the Patran 2008r2 input file translator
$ on April 19, 2011 at 20:49:37.
$ Direct Text Input for Nastran System Cell Section
$ Direct Text Input for File Management Section
$ Direct Text Input for Executive Control
$ Implicit Nonlinear Analysis
SOL 600,NLSTATIC OTR=op2
CEND
$ Direct Text Input for Global Case Control Data
TITLE = MSC.Nastran job created on 19-Apr-11 at 20:43:47
SUBCASE 1
  TITLE=This is a default subcase.
  NLPARM = 1
  SPC = 2
  LOAD = 2
  DISPLACEMENT(PLOT, SORT1, REAL)=ALL
  SPCFORCES(PLOT, SORT1, REAL)=ALL
  STRESS(PLOT, SORT1, REAL, VONMISES, BILIN)=ALL
$ Direct Text Input for this Subcase
BEGIN BULK
$ Direct Text Input for Bulk Data
PARAM POST -1
PARAM, NOCOMPS, 0
PARAM PRTMAXIM YES
PARAM MARCPRNH 1
PARAM MARCND99 -1
PARAM LGDISP 1
PARAM MARCOTIM 2
PARAM MARCSLHT 8
NLPARM 1 10 ITER 1 25 P YES
NLSTRAT 1 AIMAXINC 10
$ Elements and Element Properties for region : prop
$ Composite Property Record created from P3/PATRAN composite material
$ record : pcomp.2
$ Composite Material Description :
PCOMP 1 0. 0.
1 .1308 0. YES 1 .1308 90. YES
1 .1308 45. YES 1 .1308 -45. YES
1 .1308 -45. YES 1 .1308 45. YES
1 .1308 90. YES 1 .1308 0. YES

```

Figure B9: SOL600 bulk data example

APPENDIX C

MESH SENSITIVITY STUDY

In this section, for finite element model which have different number of elements, mesh sensitivity study is performed. Here, instead of using progressive failure analysis and comparing first ply and ultimate failure loads for different mesh alternatives, stress results of the elements around hole are compared. For this comparison, individual implicit nonlinear solutions have been employed for combined pressure and tension case by using ten different mesh sizes contain "100" through "1200" number of elements.

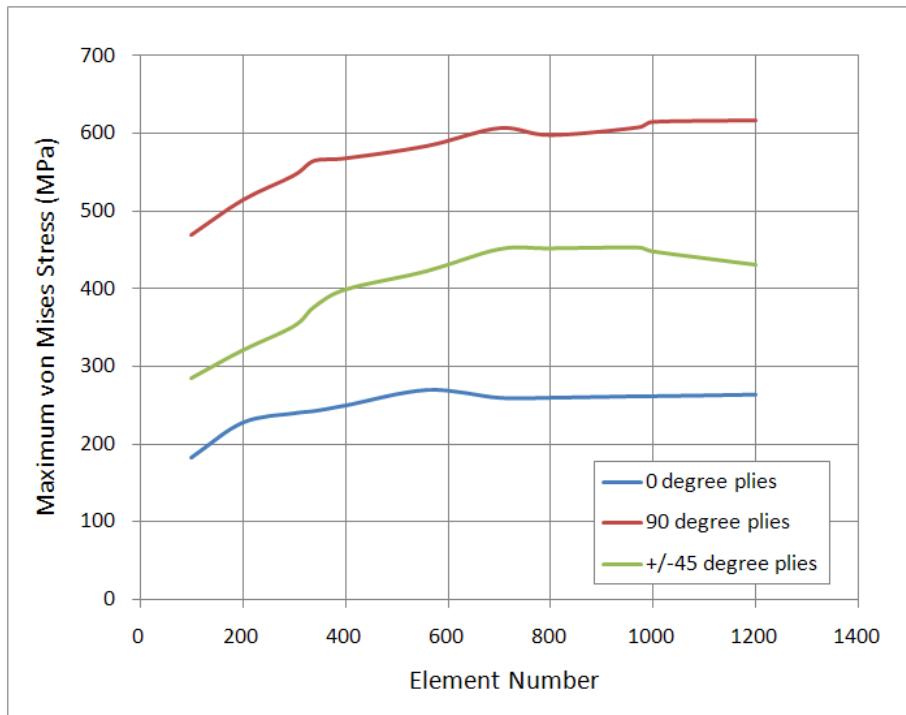


Figure C1: Stress results of different mesh sizes

In Figure C1, the convergence of stress results for different mesh sizes is shown. For different ply angles, stress results of elements around hole converges after a certain element number and this level can be named as optimum mesh size. As it can be seen from the figure, according to the results of this study, optimum mesh size for this problem is around "600" elements. However, as mentioned in Section 5.4, computational difficulties and solution times should be taken into consideration while selecting appropriate mesh size. In this study, the mesh configuration which has "340" elements has been used by considering those issues and the required accuracy in the results.

CURRICULUM VITAE

MURAT GUNEL

Address: Fethiye Mahallesi Havacılık Bulvarı

TAI Lojmanları B10/9 06980 Akıncı/Kazan/ANKARA

Mobile: (+90) 506 510 11 27

E-mail: gunelmu@yahoo.com

EDUCATION

2007 - 2011 **MIDDLE EAST TECHNICAL UNIVERSITY (METU), ANKARA**

MS, Aerospace Engineering (C.GPA: 3.45/4.00)

Specialist Subjects: Progressive Failure Analysis, Linear/Non-Linear Mechanics of Composite Materials, Finite Element Applications for Advanced Engineering Problems

Final Year Project: Progressive Failure Analysis of Laminated Composite Materials by using Patran Command Language (PCL)

2003 - 2007 **ISTANBUL TECHNICAL UNIVERSITY (ITU), ISTANBUL**

BS, Aeronautical Engineering (C.GPA: 2.75/4.00)

Specialist Subjects: Stress and Design of Aircraft Structures.

Final Year Subjects: Preliminary UAV Design, Mechanics of Composites.

Final Year Project: Parametric Design Tool Development for A400M Wing Spar in MSC.Patran by using PCL (TAI cooperative)

EXPERIENCE

September 2007- present

TAI , ANKARA

Senior Stress Engineer

HURKUS Project Front-Center Fuselage System Installation Stress Responsible. Detailed Static and Dynamic Analysis of Metallic and Composite Parts by Using Hand Calculations Bruhn,Niu,ESDU,etc.), Developed Analysis Tools (Excel,Mathcad,PCL) and FEM (MSC.Patran/Nastran/Mentat/Marc).

December 2006-September 2007

MSC SOFTWARE TURKEY/BIAS , ISTANBUL

Intern Project Engineer

Played active role at providing consultancy service and developing analysis tools. Worked as trainer of MSC.Software products in the universities.

INTERNATIONAL CONFERENCE PAPERS AND PRESENTATIONS

Günel, M., Kayran, A., ‘Comparative Study of Linear and Non-Linear Progressive Failure Analysis of Composite Aerospace Structures’, ICCS 16, 16th International Conference on Composite Structures, Porto, Portugal, 28-30 June 2011 (in CD-ROM).

Günel, M., Kayran, A., ‘Non-Linear Progressive Failure Analysis of Composite Aerospace Structures’, ICCM 18, 18th International Conference on Composite Materials, Jeju Island, Korea, 21-26 August 2011 (in stick harddisk).